

State-Space Modeling of Time-Varying Spillovers on Networks

Marios Papamichalis* Regina Ruane† Theofanis Papamichalis ‡

December 23, 2025

Abstract

Many modern time series arise on networks, where each component is attached to a node and interactions follow observed edges. Classical time-varying parameter VARs (TVP-VARs) treat all series symmetrically and ignore this structure, while network autoregressive models exploit a given graph but usually impose constant parameters and stationarity. We develop network state-space models in which a low-dimensional latent state controls time-varying network spillovers, own-lag persistence and nodal covariate effects. A key special case is a network time-varying parameter VAR (NTVP-VAR) that constrains each lag matrix to be a linear combination of known network operators, such as a row-normalised adjacency and the identity, and lets the associated coefficients evolve stochastically in time. The framework nests Gaussian and Poisson network autoregressions, network ARIMA models with graph differencing, and dynamic edge models driven by multivariate logistic regression. We give conditions ensuring that NTVP-VARs are well-defined in second moments despite nonstationary states, describe network versions of stability and local stationarity, and discuss shrinkage, thresholding and low-rank tensor structures for high-dimensional graphs. Conceptually, network state-space models separate where interactions may occur (the graph) from how strong they are at each time (the latent state), providing an interpretable alternative to both unstructured TVP-VARs and existing network time-series models.

1 Introduction

Many modern datasets are multivariate time series indexed by the nodes of a graph, where edges encode plausible channels of interaction (e.g., trade links, financial exposures, spatial adjacency, or contact networks). In such settings, researchers often care about *time-varying* cross-sectional spillovers: contagion can intensify during stress episodes, transmission pathways can change as the network evolves, and persistence can drift after structural breaks. Standard vector autoregressions (VARs) become difficult to use at scale because they ignore known topology and require estimating dense $N \times N$ lag matrices, while network autoregressive models exploit an observed adjacency but typically impose constant coefficients and global stationarity, limiting their ability to track evolving dependence.

*Human Nature Lab, Yale University, New Haven, CT 06511, marios.papamichalis@yale.edu

†Department of Statistics and Data Science, The Wharton School, University of Pennsylvania, 3733 Spruce Street, Philadelphia, PA 19104-6340, ruanej@wharton.upenn.edu

‡Department of Economics, Yale University, 28 Hillhouse Ave, New Haven, USA, theofanis.papamichalis@yale.edu

We develop a *network state-space* framework that combines network-structured dependence with stochastic parameter evolution. The observation equation is a network regression built from known graph operators (e.g., a row-normalised adjacency W_t and the identity), while a low-dimensional latent state drives the corresponding coefficients. A key special case is a network time-varying parameter VAR (NTVP–VAR), for which

$$Y_t = \beta_{0,t} \mathbf{1}_N + \beta_{1,t} W_t Y_{t-1} + \beta_{2,t} Y_{t-1} + Z_t \gamma_t + \varepsilon_t,$$

so the spillover matrix is constrained to $\beta_{1,t} W_t + \beta_{2,t} I_N$ while $(\beta_{0,t}, \beta_{1,t}, \beta_{2,t}, \gamma_t)$ evolves as a latent state. This formulation separates *where* interactions may occur (the graph) from *how strong* they are at each time (the state), yielding interpretable, time-resolved spillover measures and enabling sequential filtering/smoothing in a unified state-space representation.

Time-varying parameter VARs (TVP–VARs), often coupled with stochastic volatility, are a standard tool for capturing gradual drifts and structural breaks in multivariate dependence [Cogley and Sargent \[2005\]](#), [Primiceri \[2005\]](#), [Nakajima \[2011\]](#). Their main limitation for large systems is dimensionality: a generic VAR with N series and p lags involves $N^2 p$ autoregressive coefficients, and allowing these to vary over time leads to very large state vectors. This has motivated global-local shrinkage and sparsification of state innovations [Bitto and Frühwirth-Schnatter \[2019\]](#), [Huber et al. \[2020, 2019\]](#) and reduced-state or hybrid representations [Eisenstat et al. \[2016\]](#), [Chan et al. \[2023\]](#). These approaches improve scalability but typically do not exploit a known network that restricts which interactions are plausible. Network time-series models impose that each node depends on its own lags and on lagged neighbour averages, using a weight matrix derived from the observed graph. The network vector autoregression (NAR) formalises this idea with a small number of global coefficients multiplying a row-normalised adjacency and develops stationarity and asymptotic theory under large-network regimes [Zhu et al. \[2017\]](#). Extensions address nonstationarity via graph-based differencing and transforms [Knight et al. \[2017\]](#), allow richer neighbourhood structures and multiple graph lags [Knight et al. \[2020\]](#), and consider dynamic networks where both edges and coefficients may evolve [Krampe \[2019\]](#). For count outcomes, Poisson network autoregressions and related models embed the network through lagged neighbour intensities or spatial random effects [Armillotta and Fokianos \[2023\]](#), [Castro et al. \[2012\]](#). Recent work also considers grouped or partially shared time-varying coefficients across nodes [Li et al. \[2024\]](#). Most of this literature, however, treats key spillover parameters as fixed or relies on global stationarity-type restrictions. A separate line of work treats the network as (partly) latent and models evolving topology via latent positions or dynamic communities [Hoff et al. \[2002\]](#), [Sarkar and Moore \[2005\]](#), [Sewell and Chen \[2015, 2016\]](#), [Friel et al. \[2016\]](#), [Durante and Dunson \[2016\]](#), [Rastelli and Cornelini \[2021\]](#), [Matias and Miele \[2017\]](#), [Ludkin et al. \[2018\]](#), [Pensky \[2019\]](#). Time-series variants allow latent positions to evolve and drive interaction weights in multivariate count models [Kaur and Rastelli \[2024\]](#) or couple network structure and temporal dependence more directly [Kang et al. \[2017\]](#); see [Tjøstheim et al. \[2023\]](#) for a review. These approaches are well suited to learning topology, but they typically shift inferential effort toward the network itself and can be less transparent when the primary goal is to track spillover *strength* conditional on an observed graph. State-space ideas have been used for graph-structured observations, including latent-state models for dynamic edges [Zou and Li \[2017\]](#) and GLMM-based monitoring approaches [Farahani et al. \[2019\]](#), as well as representation-learning architectures that integrate graph encoders with state-space modules [Zambon et al. \[2023\]](#), [de Oliveira et al. \[2025\]](#), [Dimasaka et al. \[2025\]](#), [Behrouz and Hashemi \[2024\]](#). Closest to our setting, time-varying network

autoregressions with smoothly varying coefficients have been developed under local-stationarity frameworks Ding et al. [2025], Wu et al. [2025], and community-structured network autoregressions and dynamic spatial-lag models provide additional parsimonious specifications Nason et al. [2025], Cen et al. [2025]. Our approach differs by modelling time variation through a low-dimensional latent coefficient state in a unified state–space formulation, while constraining lag matrices to lie in the span of a small set of known network operators.

We introduce a general class of *network state–space models* in which graph-based regressors enter the observation equation and a low-dimensional latent state governs time variation in spillovers, own-lag persistence, and covariate effects; as a key special case, we develop an NTVP–VAR that constrains high-dimensional lag matrices to combinations of known network operators, thereby retaining interpretability while enabling sequential filtering/smoothing and extensions to non-Gaussian outcomes and dynamic edges. We establish theoretical guarantees tailored to network dependence, including conditions for second-moment well-posedness under nonstationary state evolution (even with evolving networks), network-adapted stability and local-stationarity notions, aggregation and macro–micro decompositions, robustness to network approximation, and high-dimensional shrinkage/threshold mechanisms with associated contraction behaviour. Finally, we demonstrate the empirical payoff of the framework via numerical experiments and empirical illustrations.

Section 2 introduces network notation and formalises the network state–space model and the NTVP–VAR special case, together with core modelling extensions. Section 3 develops theoretical results on well-posedness, aggregation, stability/local stationarity, robustness, and shrinkage behaviour in high-dimensional settings. Section 4 presents numerical experiments and empirical illustrations. Section 5 concludes with a discussion and directions for further work.

2 Network state–space models: setup and basic properties

2.1 Setup: networks, observations, and design matrices

2.1.1 Basic network notation

Let $G_t = (V, E_t)$ be a (possibly time-varying) network on $N = |V|$ nodes. Write $A_t = (a_{ij,t})_{i,j \leq N}$ for its adjacency matrix and define the out-degrees

$$n_{it} = \sum_{j=1}^N a_{ij,t}.$$

Define the row-normalised weight matrix $W_t = (w_{ij,t})$ by the convention

$$w_{ij,t} := \begin{cases} a_{ij,t}/n_{it}, & n_{it} > 0, \\ 0, & n_{it} = 0, \end{cases} \quad i, j \leq N,$$

so each row sum of W_t is in $\{0, 1\}$ (equal to 1 when $n_{it} > 0$). Equivalently, $W_t = D_t^{-1}A_t$ when all $n_{it} > 0$, where $D_t = \text{diag}(n_{1t}, \dots, n_{Nt})$.

For $r \geq 1$ we write $W_t^{(r)}$ for a generic r -step network operator (e.g. W_t^r or a distance-weighted r -neighbour operator as in NARIMA / GNAR).

At times $t = 1, \dots, T$ we observe node responses

$$Y_t = (Y_{1t}, \dots, Y_{Nt})' \in \mathbb{R}^N \quad \text{or} \quad Y_t \in \mathbb{N}^N,$$

and possibly node covariates $Z_t \in \mathbb{R}^{N \times q}$ (row i is z'_{it}).

2.1.2 Network design matrices

For a given autoregressive order $p \geq 1$, a convenient *network design matrix* is

$$X_t^{(p)}(A_{1:t}, Y_{1:t-1}, Z_t) = [\mathbf{1}_N, W_t Y_{t-1}, \dots, W_t Y_{t-p}, Y_{t-1}, \dots, Y_{t-p}, Z_t] \in \mathbb{R}^{N \times K}, \quad (1)$$

where $K = 1 + 2p + q$ in this simple construction. Additional network summaries (higher-order neighbourhoods, powers of W_t , layer-specific operators, etc.) can be included as extra columns.

2.2 Network state-space models (NSSM)

An NSSM separates (a) *where* interactions can occur (the graph, entering through a design matrix/operator built from W_t and lagged data) from (b) *how strong* those interactions are (the time-varying coefficients θ_t evolving as a state process). Observations are then drawn from a GLM/state-space observation model conditional on θ_t .

Definition 2.1 (Network state-space model (NSSM)). *Let $(\theta_t)_{t \geq 0}$ be a latent K -dimensional state process. A network state-space model on (G_t) for the node series (Y_t) consists of:*

(i) *A network design operator*

$$H_t = H_t(G_{1:t}, Y_{1:t-1}, Z_t) \in \mathbb{R}^{N \times K}, \quad (2)$$

built from network lags and covariates, typically of the form

$$H_t = [\mathbf{1}_N, W_t Y_{t-1}, Y_{t-1}, W_t^{(2)} Y_{t-1}, \dots, Z_t, \text{ seasonal regressors}].$$

(ii) *A linear predictor and conditional mean*

$$\eta_t = H_t \theta_t \in \mathbb{R}^N, \quad \mu_t = g^{-1}(\eta_t), \quad (3)$$

where g is a link function (identity for Gaussian, log for Poisson, logit for Bernoulli, etc.).

(iii) *An observation equation*

$$Y_t | \theta_t, G_{1:t} \sim \mathcal{D}_Y(\mu_t, \psi_t), \quad (4)$$

where \mathcal{D}_Y is a parametric family on \mathbb{R}^N or \mathbb{N}^N with mean μ_t and possibly additional parameters ψ_t (e.g. a covariance matrix R_t for Gaussian data, or copula parameters for counts).

(iv) *A state evolution equation*

$$\theta_t = F_t \theta_{t-1} + u_t, \quad u_t \sim \mathcal{D}_u(0, Q_t), \quad (5)$$

with F_t a (possibly time-varying) $K \times K$ transition matrix and \mathcal{D}_u a zero-mean disturbance distribution (Gaussian in the linear-Gaussian case), together with an initial law $\theta_0 \sim \mathcal{D}_0(m_0, P_0)$.

Equations (3)–(5) define the network state–space model. Serial and cross–sectional dependence in (Y_t) is induced jointly by the network design H_t and by the stochastic evolution of θ_t .

This formulation makes explicit that the graph enters only through H_t , while all temporal adaptation is driven by θ_t . Section 3 shows that, under mild conditions, the resulting network process is L^2 –well posed and admits interpretable macro–level and node–edge decompositions.

2.3 Key special cases of NSSM

2.3.1 Gaussian NSSM (network TVP–VAR)

If \mathcal{D}_Y is multivariate Gaussian with identity link g , the observation equation becomes

$$Y_t \mid \theta_t, G_{1:t} \sim \mathcal{N}_N(H_t \theta_t, R_t), \quad (\text{Obs-G})$$

with R_t positive definite. Taking \mathcal{D}_u Gaussian in (5) yields a linear–Gaussian state–space model.

For $p = 1$ and

$$H_t = X_t = [\mathbf{1}_N, W_t Y_{t-1}, Y_{t-1}, Z_t] \in \mathbb{R}^{N \times (3+q)},$$

the observation equation can be written componentwise as

$$Y_t = \beta_{0,t} \mathbf{1}_N + \beta_{1,t} W_t Y_{t-1} + \beta_{2,t} Y_{t-1} + Z_t \gamma_t + \varepsilon_t, \quad \varepsilon_t \sim \mathcal{N}_N(0, R_t), \quad (6)$$

where

$$\theta_t = \begin{pmatrix} \beta_{0,t} \\ \beta_{1,t} \\ \beta_{2,t} \\ \gamma_t \end{pmatrix} \in \mathbb{R}^{3+q}.$$

With a random–walk state evolution

$$\theta_t = \theta_{t-1} + u_t, \quad u_t \sim \mathcal{N}_K(0, Q_t), \quad (7)$$

(6) is a *network time–varying parameter VAR(1)* (network TVP–VAR), generalising both standard TVP–VARs and network VAR / NAR models.

2.3.2 Poisson NSSM (time–varying PNAR)

For count data take g to be the log–link and let \mathcal{D}_Y be a multivariate count distribution with Poisson margins. Writing

$$\lambda_t = \exp(H_t \theta_t) \quad (\text{componentwise}), \quad (\text{link})$$

a natural specification is

$$Y_t \mid \theta_t, G_{1:t} \sim \text{MCP}_N(\lambda_t, C_t), \quad (\text{Obs-P})$$

where $\text{MCP}_N(\lambda_t, C_t)$ denotes a multivariate copula–Poisson law with marginal means λ_t and dependence encoded by a copula C_t . If $F_t = I_K$ and $Q_t \equiv 0$ in (5), this reduces to a Poisson network autoregression (PNAR) with fixed parameters; allowing $Q_t \neq 0$ produces a *time–varying* PNAR–type process whose conditional means follow a network TVP–VAR structure.

2.4 Anchor model: Gaussian network TVP–VAR (NTVP–VAR)

We now specialise to a parsimonious Gaussian model driven by a small number of global coefficients.

Definition 2.2 (Network TVP–VAR (NTVP–VAR)). *Let $G = (V, E)$ be a network with adjacency matrix A and row–normalised weight matrix $W = D^{-1}A$. At each time t we observe $Y_t \in \mathbb{R}^N$ and node–level covariates $Z_t \in \mathbb{R}^{N \times q}$. Define*

$$\theta_t = \begin{pmatrix} \beta_{0,t} \\ \beta_{1,t} \\ \beta_{2,t} \\ \gamma_t \end{pmatrix} \in \mathbb{R}^K, \quad K = 3 + q,$$

and the network regression matrix

$$X_t = X_t(A, Y_{t-1}, Z_t) = [\mathbf{1}_N, WY_{t-1}, Y_{t-1}, Z_t] \in \mathbb{R}^{N \times K}.$$

A Gaussian network TVP–VAR(1) is defined by

$$Y_t \mid \theta_t \sim \mathcal{N}_N(X_t \theta_t, R_t), \quad (8)$$

$$\theta_t = \theta_{t-1} + u_t, \quad u_t \sim \mathcal{N}_K(0, Q_t), \quad (9)$$

with R_t positive definite and Q_t typically diagonal and endowed with shrinkage or mixture–innovation structure. Componentwise,

$$Y_t = \beta_{0,t} \mathbf{1}_N + \beta_{1,t} W Y_{t-1} + \beta_{2,t} Y_{t-1} + Z_t \gamma_t + \varepsilon_t, \quad \varepsilon_t \sim \mathcal{N}_N(0, R_t). \quad (10)$$

The cross–sectional spillover matrix in (10) is

$$B_t := \beta_{1,t} W + \beta_{2,t} I_N,$$

a low–dimensional, network–structured analogue of the arbitrary $N \times N$ matrix $B_{1,t}$ in a generic TVP–VAR. The NTVP–VAR thus retains the linear–Gaussian state–space machinery while constraining the autoregressive structure to lie in a small span of network operators.

Non–Gaussian NTVP–VARs are obtained by replacing the Gaussian observation equation (8) with a GLM–type link, e.g.

$$Y_{it} \mid \theta_t \sim \text{Poisson}(\lambda_{it}), \quad \log \lambda_t = X_t \theta_t,$$

which recovers and generalises PNAR models when θ_t is time–invariant.

2.5 Filtering and large- N guarantees (Gaussian case)

In the linear–Gaussian case, inference for (θ_t) is based on Kalman filtering/smoothing. Write $m_t := \mathbb{E}(\theta_t \mid \mathcal{F}_t)$ and $P_t := \text{Var}(\theta_t \mid \mathcal{F}_t)$ for the Kalman filter mean and covariance, where \mathcal{F}_t is the data filtration.

Theorem 2.3 (Cross-sectional oracle filtering and forecast-risk gap). *Consider the Gaussian NTVP–VAR(1) in Definition 2.2,*

$$Y_t \mid \theta_t \sim N_N(X_t \theta_t, R_t), \quad \theta_t = \theta_{t-1} + u_t, \quad u_t \sim N_K(0, Q_t),$$

with fixed state dimension K , $R_t \succ 0$, and X_t \mathcal{F}_{t-1} -measurable. Let $m_t := \mathbb{E}(\theta_t \mid \mathcal{F}_t)$ and $P_t := \text{Var}(\theta_t \mid \mathcal{F}_t)$ denote the Kalman filter mean and covariance. Assume there exist constants $0 < \underline{r} \leq \bar{r} < \infty$, $\kappa > 0$ and $C_X < \infty$ such that for all $t \geq 1$,

$$\underline{r} I_N \preceq R_t \preceq \bar{r} I_N, \quad (11)$$

$$\lambda_{\min}\left(\frac{1}{N} X_t^\top R_t^{-1} X_t\right) \geq \kappa, \quad (12)$$

$$\|X_{t+1}\|_{\text{op}}^2 \leq C_X N. \quad (13)$$

Then for every $t \geq 1$:

(i) (**Cross-sectional oracle filtering.**)

$$\mathbb{E}\|\theta_t - m_t\|^2 = \mathbb{E}\{\text{tr}(P_t)\} \leq \frac{K}{N\kappa}.$$

(ii) (**Forecast-risk gap vanishes as $N \rightarrow \infty$.**) Let the oracle one-step mean be $\mu_{t+1|t}^* := \mathbb{E}(Y_{t+1} \mid \theta_t, \mathcal{F}_t) = X_{t+1}\theta_t$ and the Bayes/Kalman mean be $\hat{\mu}_{t+1|t} := \mathbb{E}(Y_{t+1} \mid \mathcal{F}_t) = X_{t+1}m_t$. Then

$$\frac{1}{N} \mathbb{E}\|\hat{\mu}_{t+1|t} - \mu_{t+1|t}^*\|^2 \leq \frac{C_X K}{N\kappa}.$$

Equivalently, the (per-node) one-step MSFE decomposes as

$$\frac{1}{N} \mathbb{E}\|Y_{t+1} - \hat{\mu}_{t+1|t}\|^2 = \frac{1}{N} \mathbb{E}\|Y_{t+1} - \mu_{t+1|t}^*\|^2 + O\left(\frac{1}{N}\right),$$

so the Kalman predictor is asymptotically oracle in N .

Because K is fixed while each time point provides N conditionally independent pieces of cross-sectional information about θ_t , the filter learns the time-varying coefficients at rate $1/N$. Practically, this says the method can be *both* flexible in time (random-walk coefficients) and statistically stable in large panels: the extra forecast error from estimating θ_t becomes negligible as N grows.

Theorem 2.4 (Large- N frequentist calibration of Kalman uncertainty for network coefficients). *Assume the setup of Theorem 2.3 (linear–Gaussian observation equation with \mathcal{F}_{t-1} -measurable X_t , random-walk Gaussian state with fixed K , and $R_t \succ 0$). Fix $t \geq 1$ and let $N \rightarrow \infty$ with t and K fixed. Define the scaled information matrix*

$$J_t^{(N)} := \frac{1}{N} X_t^\top R_t^{-1} X_t \in \mathbb{R}^{K \times K}.$$

Assume there exist deterministic constants $0 < \kappa \leq \bar{\kappa} < \infty$ and $0 < \underline{p} \leq \bar{p} < \infty$ such that, for

$$\mathcal{E}_N := \left\{ \kappa I_K \preceq J_t^{(N)} \preceq \bar{\kappa} I_K \right\} \cap \left\{ \underline{p} I_K \preceq P_{t|t-1} \preceq \bar{p} I_K \right\},$$

we have $\mathbb{P}^*(\mathcal{E}_N) \rightarrow 1$ as $N \rightarrow \infty$. Assume moreover that $J_t^{(N)} \rightarrow J_t$ in probability for some deterministic $J_t \succ 0$. Let (m_t, P_t) denote the Kalman filtering mean/covariance for $\theta_t \mid \mathcal{F}_t$. Then, as $N \rightarrow \infty$:

(i) *Covariance calibration:*

$$\| NP_t - (J_t^{(N)})^{-1} \|_{op} \rightarrow 0 \quad \text{in } \mathbb{P}^* \text{-probability.}$$

(ii) *Asymptotic normality of the filtered mean:*

$$\sqrt{N} (m_t - \theta_t) \Rightarrow \mathcal{N}_K(0, J_t^{-1}).$$

(iii) *Conditional frequentist coverage of Kalman intervals:* for each coordinate $j \in \{1, \dots, K\}$ and fixed $\alpha \in (0, 1)$,

$$\mathbb{P}^* \left(\theta_{j,t} \in [m_{j,t} \pm z_{1-\alpha/2} \sqrt{(P_t)_{jj}}] \mid \theta_t, \mathcal{F}_{t-1} \right) \longrightarrow 1 - \alpha \quad \text{in } \mathbb{P}^* \text{-probability.}$$

At large N , the Kalman posterior behaves like a classical N -sample likelihood: the covariance shrinks like $1/N$ and matches the inverse information, and the filtered mean is asymptotically normal. This makes the state-space uncertainty output *interpretable* beyond Bayes—your intervals for network spillovers behave like calibrated confidence intervals in large panels.

2.6 Dynamic networks, structural breaks, and augmented summaries

2.6.1 Dynamic networks and edge-based models

When the network itself evolves, the adjacency matrix A_t (or weighted adjacency W_t) can be treated as part of the observation layer or as a latent process.

Edge-based NSSM. Let $E_t = \text{vec}(A_t)$ denote the vectorisation of the adjacency matrix (restricted to $i < j$ in the undirected case). Introduce a lower-dimensional latent state ξ_t describing evolving network structure (e.g. latent positions, community intensities, or edge propensities) with evolution

$$\xi_t = G_t \xi_{t-1} + w_t, \quad w_t \sim \mathcal{N}(0, S_t).$$

An edge-wise observation model

$$E_t \mid \xi_t \sim \mathcal{D}_E(h_t(\xi_t), \phi_t)$$

completes the specification. Examples include

$$\Pr\{a_{ij,t} = 1 \mid \xi_t\} = \text{logit}^{-1}(x'_{ij,t} \xi_t)$$

for binary edges, or Poisson edge weights with intensities $\exp(x'_{ij,t} \xi_t)$. Such models yield dynamic random graphs in state-space form and can be combined with node-level NSSMs by letting A_t (and hence W_t) enter H_t .

Dynamic edges in NTVP–VAR. In the NTVP–VAR setting with time–varying A_t , we can explicitly model the edge process via a multivariate logistic regression. For each ordered pair (i, j) , $i \neq j$, let $x_{ij,t} \in \mathbb{R}^p$ collect edge–level regressors (nodal characteristics, lagged responses, etc.), and define

$$a_{ij,t} \mid \eta_t \sim \text{Bernoulli}(p_{ij,t}), \quad \text{logit}(p_{ij,t}) = x'_{ij,t} \eta_t, \quad (\text{Edge-Obs})$$

with a time–varying edge parameter $\eta_t \in \mathbb{R}^p$ evolving as

$$\eta_t = \eta_{t-1} + \omega_t, \quad \omega_t \sim \mathcal{N}_p(0, S_t). \quad (\text{Edge-State})$$

The joint state

$$\xi_t := \begin{pmatrix} \theta_t \\ \eta_t \end{pmatrix}$$

then follows a Gaussian random walk and drives both node responses Y_t and edges A_t , yielding a partially linear network state–space model.

2.6.2 Mixture–innovation and threshold state evolution

To balance flexibility and parsimony, one can let the innovation variance of each component of θ_t depend on past changes (*latent threshold* dynamics). Writing

$$\theta_t = \theta_{t-1} + u_t, \quad u_t \sim \mathcal{N}_K(0, Q_t), \quad (\text{State})$$

we take

$$Q_t = \text{diag}(q_{1t}, \dots, q_{Kt}), \quad (\text{VarQ})$$

with

$$q_{jt} = q_{j0} + s_{jt}(q_{j1} - q_{j0}), \quad 0 < q_{j0} \ll q_{j1}, \quad (14)$$

and

$$s_{jt} = \mathbb{I}(|\theta_{j,t-1} - \theta_{j,t-2}| > d_j), \quad d_j > 0. \quad (15)$$

When the recent increment $|\theta_{j,t-1} - \theta_{j,t-2}|$ is small, $s_{jt} = 0$ and the j th coefficient evolves with tiny variance q_{j0} , behaving almost as a constant; when a rare large move occurs, $s_{jt} = 1$ and the innovation variance jumps to q_{j1} , allowing structural breaks. Section 3 studies the implied sparsity of break points and posterior concentration for these paths.

2.6.3 Augmenting with linear network summaries

Linear functionals of Y_t (and hence of θ_t) can be included as additional pseudo–observations to steer the filter towards desired network properties. Let $S \in \mathbb{R}^{M \times N}$ be a fixed matrix (e.g. $S = A_t$ for weighted degrees, a Laplacian, or other linear network statistics) and define

$$s_t = SY_t + \nu_t, \quad \nu_t \sim \mathcal{N}_M(0, V_t). \quad (16)$$

Stacking the node and summary observations gives

$$\tilde{Y}_t = \begin{pmatrix} Y_t \\ s_t \end{pmatrix}, \quad \tilde{H}_t = \begin{pmatrix} X_t \\ SX_t \end{pmatrix}, \quad \tilde{R}_t = \text{blockdiag}(R_t, V_t),$$

so that

$$\tilde{Y}_t \mid \theta_t \sim \mathcal{N}_{N+M}(\tilde{H}_t \theta_t, \tilde{R}_t). \quad (17)$$

This preserves the linear–Gaussian structure while allowing the filter to learn simultaneously from node–level series and aggregated network statistics.

2.7 Regularity conditions and relation to existing models

2.7.1 Network regularity conditions (Gaussian case)

To avoid clashing with the standing assumptions (A1)–(A4) used in Section 3, we state the following as (NR1)–(NR3).

(NR1) (*Bounded state and observation innovation variance*) $\sup_t \|Q_t\| < \infty$ and $\sup_t \|R_t\| < \infty$.

(NR2) (*Uniformly bounded network regressors*) There exists $C < \infty$ such that $\|H_t(G_{1:t}, Y_{1:t-1}, Z_t)\| \leq C(1 + \|Y_{t-1}\|)$ almost surely.

(NR3) (*Network stability in the static limit*) For any fixed coefficient vector θ , the corresponding static network VAR

$$Y_t = H_t \theta + \varepsilon_t$$

has autoregressive matrices with uniformly bounded spectral radius strictly less than one, e.g. the operator norms of $\alpha_j I_N + \sum_r B_{j,r} W_t^{(r)}$ are uniformly < 1 .

Under (NR1)–(NR3) and a random–walk state evolution (7), the state process (θ_t) and the network time series (Y_t) admit finite second moments; while Theorem 3.1 specialises this to NTVP–VARs with dynamic edges.

2.7.2 Relation to NARIMA, PNAR and classical TVP–VAR

For context we briefly relate NSSMs / NTVP–VARs to existing classes.

Network ARIMA (NARIMA). NARIMA models treat a network time series as a multivariate time series augmented with a graph, and use network operators in the ARIMA polynomials. After suitable temporal and network differencing, a typical NARMA component has the form

$$Y_t^* = \sum_{h=1}^p \Phi_h(W) Y_{t-h}^* + \sum_{k=1}^q \Theta_k(W) \varepsilon_{t-k} + \varepsilon_t,$$

where $\Phi_h(W)$ and $\Theta_k(W)$ are network–weighted lag operators with *constant* coefficients. Stationarity conditions are expressed through the spectral radius of the autoregressive operator.

Poisson network autoregression (PNAR). The PNAR(1) model for counts on a fixed network can be written as

$$Y_{i,t} \mid \mathcal{F}_{t-1} \sim \text{Poisson}(\lambda_{i,t}), \quad \lambda_{i,t} = \beta_0 + \beta_1 n_i^{-1} \sum_j a_{ij} Y_{j,t-1} + \beta_2 Y_{i,t-1},$$

or in vector notation

$$Y_t \mid \mathcal{F}_{t-1} \sim \text{MCP}_N(\lambda_t, C), \quad \lambda_t = \beta_0 \mathbf{1}_N + G Y_{t-1}, \quad G = \beta_1 W + \beta_2 I_N,$$

with $(\beta_0, \beta_1, \beta_2)$ fixed over time and stability characterised through the spectral radius of G .

Standard TVP–VAR. A generic TVP–VAR(p) for $Y_t \in \mathbb{R}^N$ is

$$Y_t = c_t + \sum_{k=1}^p B_{k,t} Y_{t-k} + \varepsilon_t, \quad \varepsilon_t \sim \mathcal{N}_N(0, \Sigma_t), \quad (18)$$

with c_t and $\text{vec}(B_{k,t})$ collected into a high–dimensional state that evolves as a (typically Gaussian) Markov process. For large N , the number of time–varying parameters in $B_{k,t}$ grows as N^2 , necessitating heavy shrinkage or factor structures.

NSSMs and NTVP–VARs differ from NARIMA / PNAR and from classical TVP–VAR in several key respects:

- NSSMs are *parameter–driven*: the coefficients θ_t are random processes, and Y_t is conditionally (GLM–)linear given θ_t . NARIMA and PNAR are *observation–driven* with static parameters.
- NTVP–VAR constrains the large autoregressive matrices to lie in a low–dimensional span of network operators (e.g. W , I_N , powers of W), trading generic VAR flexibility for parsimony and explicit network interpretability.
- Random–walk state evolution admits non–stationary, time–varying network spillovers and momentum coefficients, while maintaining well–posed L^2 behaviour under mild boundedness conditions.
- The state–space formulation naturally accommodates missing data, irregular sampling, multiple observation layers (nodes and edges), and dynamic networks in a unified way, using Kalman filtering (Gaussian case) or its non–Gaussian extensions.

In Section 3 we develop representation, well–posedness, stability and asymptotic shrinkage results for network state–space models, focusing on a small set of main theorems.

3 Theoretical results for network state–space models

Throughout we assume the notation and setup of Section 2. We focus on the Gaussian and Poisson cases, which already cover network TVP–VAR and time–varying PNAR models, and concentrate on a collection of results that crystallise the behaviour of network state–space models at the levels of well–posedness, aggregation, scalability, shrinkage and robustness.

3.1 Finite moments for non–stationary network TVP–VARs

We first give conditions ensuring that the NTVP–VAR with dynamic edges is well–defined in L^2 despite non–stationary random–walk states and an evolving network.

Assumptions Let $(\mathcal{F}_t)_{t \geq 0}$ denote the natural filtration generated by initial conditions and innovations up to time t .

(A1) (*Well-defined bounded network weights.*) For each $t \geq 1$, let $A_t = (a_{ij,t})_{1 \leq i,j \leq N}$ be a (possibly random) adjacency matrix with $a_{ii,t} = 0$ and $a_{ij,t} \in \{0, 1\}$ for $i \neq j$. Define the out-degree $n_{i,t} := \sum_{j \neq i} a_{ij,t}$ and the associated weight matrix $W_t = (w_{ij,t})$ by

$$w_{ii,t} := 0, \quad w_{ij,t} := \begin{cases} a_{ij,t}/n_{i,t}, & n_{i,t} > 0, \\ 0, & n_{i,t} = 0, \end{cases} \quad i \neq j.$$

Then W_t is always well-defined (rows with $n_{i,t} = 0$ are set to zero, hence row sums are in $\{0, 1\}$). Assume there exists a finite constant $C_W < \infty$ such that

$$\sup_{t \geq 1} \|W_t\| \leq C_W \quad \text{a.s.}$$

(*Remark:* for fixed N , such a bound holds automatically for nonnegative row-substochastic W_t , e.g. $\|W_t\| \leq \|W_t\|_F \leq \sqrt{N}$.)

(A2) (*Predictable bounded covariates and observation noise.*) The sequences $(Z_t)_{t \geq 1}$ and $(R_t)_{t \geq 1}$ are \mathcal{F}_{t-1} -measurable and satisfy, for some constants $C_Z, C_R < \infty$,

$$\sup_{t \geq 1} \|Z_t\| \leq C_Z, \quad \sup_{t \geq 1} \|R_t\| \leq C_R,$$

and each R_t is positive definite.

(A3) (*Predictable bounded state innovation covariances.*) There exist constants $C_Q, C_S < \infty$ such that, almost surely,

$$\sup_{t \geq 1} \|Q_t(s_t)\| \leq C_Q, \quad \sup_{t \geq 1} \|S_t\| \leq C_S,$$

where $Q_t(s_t)$ and S_t are \mathcal{F}_{t-1} -measurable and positive semidefinite.

(A4) (*Initial moments.*) The initial conditions (θ_0, η_0, Y_0) are independent of the innovation sequences and satisfy

$$\mathbb{E}\|\theta_0\|^{2r} + \mathbb{E}\|\eta_0\|^{2r} + \mathbb{E}\|Y_0\|^{2r} < \infty \quad \text{for every integer } r \geq 1.$$

(In particular, (A4) holds if (θ_0, η_0, Y_0) is jointly Gaussian with finite covariance, or deterministic.)

Theorem 3.1 (Finite-variance non-stationary network TVP-VAR). *Consider the Gaussian NTVP-VAR with dynamic logistic edges. Let $(\mathcal{F}_t)_{t \geq 0}$ denote the natural filtration generated by the initial conditions and innovations up to time t . For $t \geq 1$, let the node and edge states evolve as*

$$\theta_t = \theta_{t-1} + u_t, \quad \eta_t = \eta_{t-1} + \omega_t,$$

with

$$u_t \mid \mathcal{F}_{t-1} \sim \mathcal{N}_K(0, Q_t(s_t)), \quad \omega_t \mid \mathcal{F}_{t-1} \sim \mathcal{N}_p(0, S_t).$$

For each ordered pair $i \neq j$, let the edges satisfy

$$a_{ij,t} \mid \eta_t \sim \text{Bernoulli}(p_{ij,t}), \quad \text{logit}(p_{ij,t}) := \log\left(\frac{p_{ij,t}}{1 - p_{ij,t}}\right) = x'_{ij,t} \eta_t,$$

where $x_{ij,t}$ is \mathcal{F}_{t-1} -measurable. Construct W_t from $A_t = (a_{ij,t})$ as in (A1) and define

$$X_t = [\mathbf{1}_N, W_t Y_{t-1}, Y_{t-1}, Z_t].$$

Finally, let the observation equation be

$$Y_t = X_t \theta_t + \varepsilon_t, \quad \varepsilon_t \mid \mathcal{F}_{t-1} \sim \mathcal{N}_N(0, R_t).$$

Under (A1)–(A4), the joint process $\{(\theta_t, \eta_t, Y_t, A_t) : t \geq 0\}$ is well-posed, and for every $t \geq 0$,

$$\mathbb{E}\|\theta_t\|^2 < \infty, \quad \mathbb{E}\|\eta_t\|^2 < \infty, \quad \mathbb{E}\|Y_t\|^2 < \infty.$$

Thus the network TVP–VAR is L^2 -well defined even though (θ_t, η_t) are non-stationary random walks and (A_t) evolves stochastically.

This result separates non-stationarity of the latent coefficients from well-posedness of the observable network process. Under mild and network-adapted boundedness conditions, the NTVP–VAR preserves finite second moments for both nodes and edges, extending classical VAR moment results to a setting with time-varying network operators and thresholded state dynamics.

3.2 Aggregation, meso-level reduction, and impulse responses

We first show how micro-level network spillovers collapse to low-dimensional aggregate and community dynamics, and then derive impulse-response decompositions that attribute propagation to network walks.

Theorem 3.2 (Aggregation to a scalar TVP autoregression). *Consider the Gaussian NTVP–VAR(1) (10) on a fixed network,*

$$Y_t = \beta_{0,t} \mathbf{1}_N + \beta_{1,t} W Y_{t-1} + \beta_{2,t} Y_{t-1} + Z_t \gamma_t + \varepsilon_t, \quad \varepsilon_t \mid R_t \sim \mathcal{N}_N(0, R_t),$$

where $W \in \mathbb{R}^{N \times N}$ is row-stochastic, i.e. $w_{ij} \geq 0$ and $W \mathbf{1}_N = \mathbf{1}_N$, and R_t is positive definite.

Let $\pi \in \mathbb{R}^N$ be an invariant probability vector for W , i.e.

$$\pi \geq 0, \quad \pi' \mathbf{1}_N = 1, \quad \pi' W = \pi'.$$

(Such a π exists for every finite row-stochastic W ; if W is irreducible, then π is unique and strictly positive.)

Define the π -weighted aggregate and aggregated innovation by

$$\bar{Y}_t^{(\pi)} := \pi' Y_t, \quad \bar{\varepsilon}_t^{(\pi)} := \pi' \varepsilon_t.$$

Then, for every $t \geq 1$,

$$\bar{Y}_t^{(\pi)} = \beta_{0,t} + (\beta_{1,t} + \beta_{2,t}) \bar{Y}_{t-1}^{(\pi)} + (\pi' Z_t) \gamma_t + \bar{\varepsilon}_t^{(\pi)}.$$

In particular, if the covariates are π -centred (i.e. $\pi' Z_t = 0$ for all t), then

$$\bar{Y}_t^{(\pi)} = \beta_{0,t} + (\beta_{1,t} + \beta_{2,t}) \bar{Y}_{t-1}^{(\pi)} + \bar{\varepsilon}_t^{(\pi)}, \quad \bar{\varepsilon}_t^{(\pi)} \mid R_t \sim \mathcal{N}(0, \pi' R_t \pi),$$

so $(\bar{Y}_t^{(\pi)})$ follows a scalar TVP-AR(1) driven by $(\beta_{0,t}, \beta_{1,t} + \beta_{2,t})$.

Moreover, if W is also column-stochastic, i.e. $\mathbf{1}'_N W = \mathbf{1}'_N$, then $\pi = N^{-1} \mathbf{1}_N$ is invariant. Hence, under the uniform centring condition $N^{-1} \mathbf{1}'_N Z_t = 0$, the same TVP-AR(1) conclusion holds for the uniform mean $\bar{Y}_t := N^{-1} \mathbf{1}'_N Y_t$.

Row-stochasticity plus invariance ($\pi'W = \pi'$) makes the network-lag term ‘‘average out’’ exactly, so the aggregate behaves like a *scalar* TVP-AR(1) whose effective persistence is $\beta_{1,t} + \beta_{2,t}$. This gives a direct, interpretable bridge from micro spillovers (through W) to macro persistence, and yields an explicit aggregate shock variance $\pi'R_t\pi$.

Theorem 3.3 (Exact meso-level reduction via quotient (community) networks). *Let $\{1, \dots, N\} = \bigsqcup_{c=1}^C K_c$ be a partition into nonempty communities and define the community-averaging operator $\Pi \in \mathbb{R}^{C \times N}$ by*

$$(\Pi y)_c := \frac{1}{|K_c|} \sum_{i \in K_c} y_i, \quad y \in \mathbb{R}^N.$$

Let $W_t \in \mathbb{R}^{N \times N}$ be a (possibly time-varying) weight matrix. Assume that for each t there exists a matrix $\Omega_t \in \mathbb{R}^{C \times C}$ such that the exact aggregation/intertwining relation

$$\Pi W_t = \Omega_t \Pi \tag{19}$$

holds. Writing $\Omega_t = (\omega_{cc',t})_{c,c' \leq C}$ and $W_t = (w_{ij,t})_{i,j \leq N}$, (19) is equivalent to the entrywise balance condition: for every $c, c' \leq C$ and every $j \in K_{c'}$,

$$\frac{1}{|K_c|} \sum_{i \in K_c} w_{ij,t} = \frac{\omega_{cc',t}}{|K_{c'}|}. \tag{20}$$

In particular,

$$\omega_{cc',t} = \frac{1}{|K_c|} \sum_{i \in K_c} \sum_{j \in K_{c'}} w_{ij,t}.$$

Consider the Gaussian NTVP-VAR(1) observation equation

$$Y_t = \beta_{0,t} \mathbf{1}_N + \beta_{1,t} W_t Y_{t-1} + \beta_{2,t} Y_{t-1} + Z_t \gamma_t + \varepsilon_t, \quad \varepsilon_t \mid R_t \sim \mathcal{N}_N(0, R_t),$$

with any Markov state evolution for the coefficients $(\beta_{0,t}, \beta_{1,t}, \beta_{2,t}, \gamma_t)$.

Define community-level quantities $\bar{Y}_t := \Pi Y_t$, $\bar{Z}_t := \Pi Z_t$, and $\bar{\varepsilon}_t := \Pi \varepsilon_t$. Then, for every $t \geq 1$, \bar{Y}_t satisfies the exact reduced C -dimensional recursion

$$\bar{Y}_t = \beta_{0,t} \mathbf{1}_C + \beta_{1,t} \Omega_t \bar{Y}_{t-1} + \beta_{2,t} \bar{Y}_{t-1} + \bar{Z}_t \gamma_t + \bar{\varepsilon}_t,$$

driven by the same latent coefficient state, and moreover

$$\bar{\varepsilon}_t \mid R_t \sim \mathcal{N}_C(0, \Pi R_t \Pi^\top).$$

If (19) holds only approximately in the sense that, for some $\delta_t \geq 0$,

$$\|\Pi W_t - \Omega_t \Pi\|_{\text{op}} \leq \delta_t,$$

(where $\|\cdot\|_{\text{op}}$ denotes the operator norm induced by $\|\cdot\|_2$), then for all $y \in \mathbb{R}^N$,

$$\|\Pi W_t y - \Omega_t \Pi y\|_2 \leq \delta_t \|y\|_2.$$

Equivalently, the aggregated observation equation holds with an additional remainder term

$$\bar{Y}_t = \beta_{0,t} \mathbf{1}_C + \beta_{1,t} \Omega_t \bar{Y}_{t-1} + \beta_{2,t} \bar{Y}_{t-1} + \bar{Z}_t \gamma_t + \bar{\varepsilon}_t + \underbrace{\beta_{1,t} (\Pi W_t - \Omega_t \Pi) Y_{t-1}}_{=: r_t},$$

and $\|r_t\|_2 \leq |\beta_{1,t}| \delta_t \|Y_{t-1}\|_2$.

If communities are “balanced” so that averaging commutes with network propagation ($\Pi W_t = \Omega_t \Pi$), then community means evolve *exactly* as a smaller C -dimensional NTVP–VAR on the quotient network Ω_t , with the same latent coefficients. This gives a principled, lossless coarse-graining when such balance holds, and an explicit remainder control when it holds only approximately.

Theorem 3.4 (Hop-by-hop spillover attribution and counterfactual impulse responses). *Consider the fixed-network NTVP–VAR(1) recursion (cf. (10))*

$$Y_t = B_t Y_{t-1} + c_t + \varepsilon_t, \quad B_t := \beta_{1,t} W + \beta_{2,t} I_N,$$

with deterministic (or \mathcal{F}_{t-1} -measurable) c_t and innovations ε_t . For $h \geq 1$ define the h -step propagation matrix

$$\Phi_{t,h} := B_{t+h} B_{t+h-1} \cdots B_{t+1}.$$

(a) (**Exact hop decomposition (spillover attribution).**) For each $0 \leq r \leq h$, define

$$c_{t,h,r} := \sum_{\substack{S \subseteq \{1, \dots, h\} \\ |S|=r}} \left(\prod_{k \in S} \beta_{1,t+k} \right) \left(\prod_{k \notin S} \beta_{2,t+k} \right).$$

Then

$$\Phi_{t,h} = \sum_{r=0}^h c_{t,h,r} W^r.$$

Hence the response at horizon h of node i to a unit shock injected at node j at time t (i.e. replacing Y_t by $Y_t + e_j$) admits the hop-by-hop attribution

$$(\Phi_{t,h} e_j)_i = \sum_{r=0}^h c_{t,h,r} (W^r)_{ij},$$

where the term with r corresponds to propagation along r -step network walks.

(b) (**Macro impulse responses (aggregation-to-IRF link).**) If W is row-stochastic with invariant probability vector π ($\pi^\top W = \pi^\top$), then the aggregate propagation satisfies

$$\pi^\top \Phi_{t,h} = \left\{ \prod_{k=1}^h (\beta_{1,t+k} + \beta_{2,t+k}) \right\} \pi^\top.$$

In particular, the π -weighted aggregate response to a unit shock at node j equals $\pi^\top \Phi_{t,h} e_j = \pi_j \prod_{k=1}^h (\beta_{1,t+k} + \beta_{2,t+k})$.

(c) (**Counterfactual edge interventions (edge-to-payoff Lipschitz bound).**) Let W^{cf} be a counterfactual weight matrix with $\|W\|_{\text{op}}, \|W^{\text{cf}}\|_{\text{op}} \leq C_W$, and set $B_t^{\text{cf}} := \beta_{1,t} W^{\text{cf}} + \beta_{2,t} I_N$, $\Phi_{t,h}^{\text{cf}} := B_{t+h}^{\text{cf}} \cdots B_{t+1}^{\text{cf}}$. With $M_{t,h} := \max_{1 \leq k \leq h} (|\beta_{1,t+k}| C_W + |\beta_{2,t+k}|)$, one has the deterministic Lipschitz bound

$$\|\Phi_{t,h} - \Phi_{t,h}^{\text{cf}}\|_{\text{op}} \leq M_{t,h}^{h-1} \left(\sum_{k=1}^h |\beta_{1,t+k}| \right) \|W - W^{\text{cf}}\|_{\text{op}}.$$

(d) (**Propagation of coefficient uncertainty to IRFs.**) Let $\widehat{\beta}_{1,t+k}, \widehat{\beta}_{2,t+k}$ be estimates and \widehat{W} an estimated network with $\|W\|_{\text{op}}, \|\widehat{W}\|_{\text{op}} \leq C_W$. Define $\widehat{B}_{t+k} := \widehat{\beta}_{1,t+k}\widehat{W} + \widehat{\beta}_{2,t+k}I_N$ and $\widehat{\Phi}_{t,h} := \widehat{B}_{t+h} \cdots \widehat{B}_{t+1}$. Then, with $\widehat{M}_{t,h} := \max_{1 \leq k \leq h} (|\widehat{\beta}_{1,t+k}|C_W + |\widehat{\beta}_{2,t+k}|)$,

$$\|\widehat{\Phi}_{t,h} - \Phi_{t,h}\|_{\text{op}} \leq \max(M_{t,h}, \widehat{M}_{t,h})^{h-1} \sum_{k=1}^h \left\{ C_W |\widehat{\beta}_{1,t+k} - \beta_{1,t+k}| + |\widehat{\beta}_{2,t+k} - \beta_{2,t+k}| + |\widehat{\beta}_{1,t+k}| \|\widehat{W} - W\|_{\text{op}} \right\}.$$

Part (a) decomposes any IRF into contributions from r -step walks on the network (via W^r), making spillovers interpretable ‘hop by hop.’ Part (b) shows that, at the macro level, all those paths aggregate to a simple product of *scalar* persistences ($\beta_{1,t} + \beta_{2,t}$). Parts (c)–(d) give clean operator-norm bounds for counterfactual edge changes and for how estimation error in (β_1, β_2, W) propagates into IRFs.

3.3 Joint node–edge representation and scalable parameterisations

We next place node outcomes and evolving edges in a single linear–Gaussian state–space model, and then show how high-lag/high-dimensional VARs can be represented using a low-rank tensor factor state.

Theorem 3.5 (Node–edge network TVP–VAR as a (conditionally) linear–Gaussian state–space model). *Let $\{Y_t\}_{t \geq 1}$ be node responses with $Y_t \in \mathbb{R}^N$ and let $\{A_t\}_{t \geq 1}$ be observed (possibly weighted) adjacency matrices. Write the edge vector*

$$a_t := \text{vec}_E(A_t) \in \mathbb{R}^M,$$

and let $L \in \mathbb{R}^{M \times K_e}$ be a known loading matrix. Let $\theta_t \in \mathbb{R}^{K_n}$ be the node state and $\psi_t \in \mathbb{R}^{K_e}$ be the edge state. Define the joint state

$$\Xi_t := (\theta_t^\top, \psi_t^\top)^\top \in \mathbb{R}^{K_n + K_e}.$$

Let $H_t \in \mathbb{R}^{N \times K_n}$ be the network design matrix constructed from observed quantities as in Definition 2.1, so that $H_t = H_t(G_{1:t}, Y_{1:t-1}, Z_t)$ is measurable with respect to

$$\mathcal{F}_t^{(e)} := \sigma(a_{1:t}, Y_{1:t-1}, Z_{1:t}),$$

i.e. H_t is known once the edges up to time t and node history up to time $t-1$ are observed.

Assume the following Gaussian node and edge submodels:

$$\theta_t = \theta_{t-1} + u_t, \quad u_t \sim \mathcal{N}_{K_n}(0, Q_t^{(n)}), \quad Q_t^{(n)} \succeq 0, \quad (21)$$

$$\psi_t = \psi_{t-1} + w_t, \quad w_t \sim \mathcal{N}_{K_e}(0, Q_t^{(e)}), \quad Q_t^{(e)} \succeq 0, \quad (22)$$

$$a_t = L\psi_t + \zeta_t, \quad \zeta_t \sim \mathcal{N}_M(0, U_t), \quad U_t \succ 0, \quad (23)$$

$$Y_t = H_t\theta_t + \varepsilon_t, \quad \varepsilon_t \sim \mathcal{N}_N(0, R_t), \quad R_t \succ 0. \quad (24)$$

Assume the initial joint state is Gaussian,

$$\Xi_0 \sim \mathcal{N}(m_0, P_0), \quad P_0 \succ 0,$$

and assume that the innovation/noise sequences $\{u_t\}_{t \geq 1}$, $\{w_t\}_{t \geq 1}$, $\{\zeta_t\}_{t \geq 1}$, $\{\varepsilon_t\}_{t \geq 1}$ are independent across time, mutually independent across the four sequences, and independent of Ξ_0 .

Define the joint state innovation $\omega_t := (u_t^\top, w_t^\top)^\top$ and the joint process covariance

$$Q_t := \text{Var}(\omega_t) = \text{blockdiag}(Q_t^{(n)}, Q_t^{(e)}).$$

Let $\mathcal{F}_t := \sigma(a_{1:t}, Y_{1:t}, Z_{1:t})$ denote the full data σ -field at time t .

Then the joint state evolves as the linear–Gaussian random walk

$$\Xi_t = \Xi_{t-1} + \omega_t, \quad \omega_t \sim \mathcal{N}(0, Q_t).$$

Moreover, at each time t the pair (a_t, Y_t) provides two linear–Gaussian observation blocks for Ξ_t :

$$a_t = H_t^{(e)} \Xi_t + \zeta_t, \quad H_t^{(e)} := (0_{M \times K_n} \quad L),$$

and, conditional on $\mathcal{F}_t^{(e)}$ (so that H_t is known),

$$Y_t = H_t^{(n)} \Xi_t + \varepsilon_t, \quad H_t^{(n)} := (H_t \quad 0_{N \times K_e}).$$

Consequently, $\Xi_t \mid \mathcal{F}_t$ is Gaussian for each t , and the filtering and smoothing distributions $p(\Xi_t \mid \mathcal{F}_t)$ and $p(\Xi_{0:T} \mid \mathcal{F}_T)$ are obtained exactly by Kalman filtering (processing the two blocks a_t then Y_t at each t) and Rauch–Tung–Striebel smoothing.

Predictable-design special case. If additionally H_t is $\sigma(a_{1:t-1}, Y_{1:t-1}, Z_{1:t})$ -measurable (i.e. it does not depend on a_t), then the two observation blocks at time t can be stacked as $\tilde{Y}_t := (Y_t^\top, a_t^\top)^\top$ and written as a single observation equation $\tilde{Y}_t = \tilde{H}_t \Xi_t + \tilde{\varepsilon}_t$ with $\tilde{H}_t = \text{blockdiag}(H_t, L)$ and $\tilde{\varepsilon}_t \sim \mathcal{N}(0, \text{blockdiag}(R_t, U_t))$.

This shows that once edges and node histories determine the design H_t , node outcomes and edges can be filtered/smoothed jointly with standard Kalman and RTS machinery. Practically, it means dynamic networks do not require bespoke inference: the joint posterior of evolving coefficients and evolving graphs is still available in closed form (Gaussian), up to the conditioning in H_t .

Theorem 3.6 (Low–rank tensor network TVP–VAR (CP factor state)). Let $(Y_t)_{t \geq 1}$ be an N -dimensional Gaussian TVP–VAR(p) such that, for $t \geq p+1$,

$$Y_t = \sum_{\ell=1}^p B_{\ell,t} Y_{t-\ell} + \varepsilon_t, \quad \varepsilon_t \sim \mathcal{N}_N(0, R_t), \quad (25)$$

where $R_t \succ 0$. Assume the sequence $(\varepsilon_t)_{t \geq 1}$ is independent over t and independent of all state innovations and of ξ_0 . Assume given initial values $Y_{1-p}, \dots, Y_0 \in \mathbb{R}^N$.

Collect the autoregressive coefficients in the tensor $\mathcal{B}_t \in \mathbb{R}^{N \times N \times p}$ whose ℓ th slice is $B_{\ell,t}$, i.e. $(\mathcal{B}_t)_{i,j,\ell} = (B_{\ell,t})_{i,j}$. Assume \mathcal{B}_t has CP rank at most R , i.e. for each t there exist vectors $b_{r,t}^{(1)}, b_{r,t}^{(2)} \in \mathbb{R}^N$ and $b_{r,t}^{(3)} \in \mathbb{R}^p$ such that

$$\mathcal{B}_t = \sum_{r=1}^R b_{r,t}^{(1)} \otimes b_{r,t}^{(2)} \otimes b_{r,t}^{(3)}. \quad (26)$$

Because CP decompositions are not unique, assume there exists a choice of factor sequences $\{b_{r,t}^{(k)}\}_{t \geq 0}$ (a representative factorisation over time) satisfying (26) for all t and evolving as Gaussian random walks as specified below.

Assume further that for each $r \in \{1, \dots, R\}$ and each mode $k \in \{1, 2, 3\}$,

$$b_{r,t}^{(k)} = b_{r,t-1}^{(k)} + u_{r,t}^{(k)}, \quad u_{r,t}^{(k)} \sim \mathcal{N}(0, Q_{r,t}^{(k)}), \quad (27)$$

with innovations independent over t , and with $Q_{r,t}^{(k)} \succ 0$ for all (r, k, t) . Let $\xi_0 \sim \mathcal{N}(m_0, P_0)$ with $P_0 \succ 0$.

Define the stacked factor state

$$\xi_t := \left((b_{1,t}^{(1)})^\top, \dots, (b_{R,t}^{(1)})^\top, (b_{1,t}^{(2)})^\top, \dots, (b_{R,t}^{(2)})^\top, (b_{1,t}^{(3)})^\top, \dots, (b_{R,t}^{(3)})^\top \right)^\top \in \mathbb{R}^{R(2N+p)}. \quad (28)$$

Then:

- (i) The per-time-step state dimension is $\dim(\xi_t) = R(2N + p)$, scaling linearly in N and p for fixed R (compared to N^2p free entries for an unrestricted \mathcal{B}_t).
- (ii) The observation equation (25) induces a (generally nonlinear) Gaussian nonlinear state-space model:

$$Y_t \mid \xi_t, Y_{t-1}, \dots, Y_{t-p} \sim \mathcal{N}_N(g_t(\xi_t; Y_{t-1}, \dots, Y_{t-p}), R_t),$$

with

$$g_t(\xi_t; Y_{t-1}, \dots, Y_{t-p}) = \sum_{r=1}^R b_{r,t}^{(1)} (b_{r,t}^{(2)})^\top \left(\sum_{\ell=1}^p b_{r,t}^{(3)}(\ell) Y_{t-\ell} \right). \quad (29)$$

The map g_t is tri-linear (multi-affine) in the three factor blocks $\{b_{r,t}^{(1)}\}_{r=1}^R$, $\{b_{r,t}^{(2)}\}_{r=1}^R$, $\{b_{r,t}^{(3)}\}_{r=1}^R$. Moreover, conditional on any two factor blocks (and on Y_{t-1}, \dots, Y_{t-p}), the observation is linear-Gaussian in the remaining block with an explicit design matrix (constructed in the proof).

- (iii) The stacked state evolves as a linear-Gaussian random walk

$$\xi_t = \xi_{t-1} + u_t, \quad u_t \sim \mathcal{N}(0, Q_t),$$

where u_t is the stacked innovation vector and $Q_t := \text{Var}(u_t) \succ 0$.

- (iv) The joint prior law of the stacked state path $\Xi_{0:T} := (\xi_0^\top, \xi_1^\top, \dots, \xi_T^\top)^\top$ is multivariate normal with a block-tridiagonal precision matrix in time.

Remark CP factors are not identifiable up to scaling/permuation; the theorem concerns the existence of the above low-dimensional state parametrisation for any fixed representative factorisation satisfying (26)–(27). If one wishes to enforce identifiability in applications, one may impose a deterministic ordering/sign convention on components; this does not affect (i), (iii) or the block-tridiagonal time structure in (iv).

A high-dimensional $\text{VAR}(p)$ coefficient tensor can be tracked through a much smaller CP-factor state ξ_t when \mathcal{B}_t is low rank. This replaces N^2p parameters by $R(2N + p)$ state variables, making high-lag, large- N TVP-VARs computationally feasible while still allowing rich time variation.

3.4 Shrinkage, thresholds, and high-dimensional guarantees

We now study how global-local shrinkage and deterministic thresholding separate static from dynamic effects, detect sparse breaks, and yield posterior guarantees in high dimensions.

Theorem 3.7 (Automatic selection between constant and time-varying effects). *Consider the Gaussian network state-space model with random-walk coefficient state*

$$Y_t \mid \theta_t, \eta \sim \mathcal{N}(H_t \theta_t, R_t(\eta)), \quad t = 1, \dots, T, \quad (30)$$

$$\theta_t = \theta_{t-1} + \omega_t, \quad \omega_t \mid \vartheta \sim \mathcal{N}_K(0, Q(\vartheta)), \quad Q(\vartheta) = \text{diag}(\vartheta_1, \dots, \vartheta_K), \quad (31)$$

where $K < \infty$, $\vartheta = (\vartheta_1, \dots, \vartheta_K)' \in [0, \infty)^K$, and each $R_t(\eta)$ is positive definite. When some $\vartheta_j = 0$, interpret $\mathcal{N}_K(0, Q(\vartheta))$ in (31) as the possibly degenerate Gaussian measure on \mathbb{R}^K with covariance $Q(\vartheta)$.

Fix $\bar{\vartheta} \in (0, \infty)$ and a compact set \mathcal{H} for η , and define the compact parameter space

$$\Xi := [0, \bar{\vartheta}]^K \times \mathcal{H},$$

endowed with the subspace topology inherited from Euclidean space (so boundary points such as $\vartheta_j = 0$ have neighbourhoods in the relative sense). Let the true parameter be $\xi^* = (\vartheta^*, \eta^*) \in \Xi$.

Assume the observation covariances are uniformly well-conditioned on Ξ : there exist $0 < \underline{\lambda} \leq \bar{\lambda} < \infty$ such that for all t and all $\eta \in \mathcal{H}$,

$$\underline{\lambda}I \preceq R_t(\eta) \preceq \bar{\lambda}I. \quad (32)$$

For each $j \in \{1, \dots, K\}$, adopt the signed non-centred parametrisation

$$\omega_{j,t} = \alpha_j \tilde{\omega}_{j,t}, \quad \tilde{\omega}_{j,t} \stackrel{\text{i.i.d.}}{\sim} \mathcal{N}(0, 1), \quad \vartheta_j = \alpha_j^2 \in [0, \infty).$$

Let Π^0 denote the joint prior on $(\vartheta, \eta) \in [0, \infty)^K \times \mathcal{H}$ induced by:

$$\begin{aligned} \alpha_j \mid \xi_j^2 &\sim \mathcal{N}(0, \xi_j^2), & \xi_j^2 \mid \kappa^2 &\sim \Gamma\left(a_\xi, \frac{a_\xi}{2\kappa^2}\right), & \kappa^2 &\sim \Pi_\kappa, & j &= 1, \dots, K, \\ \eta &\sim \Pi_\eta, \end{aligned} \quad (33)$$

where $a_\xi \in (0, 1)$, $\Gamma(a, b)$ is Gamma with shape a and rate b , Π_κ is proper with density strictly positive on every compact subset of $(0, \infty)$, and Π_η is proper on \mathcal{H} and assigns positive mass to every neighbourhood of η^* (in the subspace topology of \mathcal{H}). Define the working prior on Ξ by restriction and renormalisation:

$$\Pi(A) := \frac{\Pi^0(A \cap \Xi)}{\Pi^0(\Xi)}, \quad A \subseteq [0, \infty)^K \times \mathcal{H}.$$

Assume $\Pi^0(\Xi) > 0$ (which holds automatically for any proper Π^0 with full local support).

Let $p_\xi(Y_{1:T})$ denote the marginal likelihood (density) of $Y_{1:T}$ under $\xi = (\vartheta, \eta) \in \Xi$. Assume uniform likelihood separation: there exists a continuous function $h : \Xi \rightarrow [0, \infty)$ with a unique zero at ξ^* such that

$$\sup_{\xi \in \Xi} \left| \frac{1}{T} \log \frac{p_\xi(Y_{1:T})}{p_{\xi^*}(Y_{1:T})} + h(\xi) \right| \xrightarrow[T \rightarrow \infty]{} 0 \quad \text{in } \mathbb{P}_{\xi^*}\text{-probability.} \quad (34)$$

Define $S_1 := \{j : \vartheta_j^* = 0\}$ and $S_0 := \{j : \vartheta_j^* > 0\}$. Then for each fixed j the posterior separates constant from time-varying coefficients:

(i) If $j \in S_1$, then for every $\delta > 0$,

$$\Pi(\vartheta_j > \delta \mid Y_{1:T}) \xrightarrow[T \rightarrow \infty]{} 0 \quad \text{in } \mathbb{P}_{\xi^*}\text{-probability.}$$

(ii) If $j \in S_0$, then for every $\delta \in (0, \vartheta_j^*)$,

$$\Pi(\vartheta_j < \delta \mid Y_{1:T}) \xrightarrow[T \rightarrow \infty]{} 0 \quad \text{in } \mathbb{P}_{\xi^*}\text{-probability.}$$

Moreover, if $\min_{j \in S_0} \vartheta_j^* \geq \underline{\vartheta} > 0$, then (ii) holds uniformly over $j \in S_0$ for any fixed $\delta \in (0, \underline{\vartheta})$.

The random-walk variances ϑ_j govern whether coefficient j actually moves over time. This theorem shows the posterior learns that dichotomy: true static effects concentrate near $\vartheta_j = 0$, while truly time-varying effects stay away from zero. In practice, a single shrinkage hierarchy can automatically select which spillovers (or own-lag effects) should be dynamic.

Theorem 3.8 (Latent-threshold sparsity of detected breaks). *Assume the latent-threshold rule (15), and allow the threshold to depend on T , writing $d_j = d_{j,T} > 0$. Fix a component j and suppose the true coefficient path $\{\theta_{j,t}^*\}_{t=0}^T$ is piecewise constant with at most J^* jumps and jump sizes bounded away from 0. Define the jump set and jump count*

$$\mathcal{J}_{j,T}^* := \left\{ t \in \{1, \dots, T\} : \theta_{j,t}^* \neq \theta_{j,t-1}^* \right\}, \quad J_{j,T}^* := |\mathcal{J}_{j,T}^*| \leq J^*,$$

and assume there exists $\kappa_j > 0$ (not depending on T) such that

$$|\theta_{j,t}^* - \theta_{j,t-1}^*| \geq \kappa_j \quad \text{for all } t \in \mathcal{J}_{j,T}^*.$$

Let $\hat{\theta}_{j,0:T}$ be a data-dependent estimate of $\theta_{j,0:T}^*$ (e.g. posterior mean, MAP, or Kalman smoother mean under the Gaussian NSSM), and define the plug-in latent-threshold indicators by applying (15) to $\hat{\theta}$:

$$\hat{s}_{j,t} := I\left(|\hat{\theta}_{j,t-1} - \hat{\theta}_{j,t-2}| > d_{j,T}\right), \quad t = 2, \dots, T.$$

Assume the thresholds satisfy

$$d_{j,T} \rightarrow 0 \quad \text{and} \quad \sqrt{\frac{T}{\log T}} d_{j,T} \rightarrow \infty \quad \text{as } T \rightarrow \infty,$$

and assume moreover that the estimator has the (typical) uniform increment accuracy

$$\max_{2 \leq t \leq T} \left| (\hat{\theta}_{j,t-1} - \hat{\theta}_{j,t-2}) - (\theta_{j,t-1}^* - \theta_{j,t-2}^*) \right| = O_p\left(\sqrt{\frac{\log T}{T}}\right). \quad (35)$$

(All probability statements are under the data-generating law for the sample used to compute $\hat{\theta}$.)

Then, as $T \rightarrow \infty$:

(i) With probability tending to one,

$$\hat{s}_{j,t} = I(\theta_{j,t-1}^* \neq \theta_{j,t-2}^*), \quad t = 2, \dots, T.$$

Consequently,

$$\sum_{t=2}^T \hat{s}_{j,t} = |\mathcal{J}_{j,T}^* \cap \{1, \dots, T-1\}| \leq J^*,$$

so the number of times $\hat{s}_{j,t} = 1$ is $O(J^*)$ uniformly in T .

(ii) Let

$$F_{j,T} := \sum_{t=2}^T I(\hat{s}_{j,t} = 1, \theta_{j,t-1}^* = \theta_{j,t-2}^*)$$

denote the number of false activations. Then $F_{j,T}/T \rightarrow 0$ in probability (indeed, $F_{j,T} = 0$ with probability tending to one).

With a threshold that shrinks slowly, the indicator $\hat{s}_{j,t}$ behaves like an asymptotically perfect ‘‘break detector’’ for piecewise-constant coefficient paths: it turns on at true jumps and is off otherwise. This provides a simple route to pathwise sparsity (few active change points), even when the underlying state model is continuous-time-varying.

Theorem 3.9 (Global-local shrinkage and posterior contraction for the conditional mean). *Consider the Gaussian NTVP-VAR / Gaussian network state-space model with observation equation*

$$Y_t | \theta_t, \mathcal{F}_{t-1} \sim N_N(X_t \theta_t, R_t), \quad \mathcal{F}_{t-1} := \sigma(Y_{1:t-1}, A_{1:t}), \quad t = 1, \dots, T, \quad (36)$$

and random-walk state evolution

$$\theta_t = \theta_{t-1} + u_t, \quad u_t \in \mathbb{R}^p, \quad p := \dim(\theta_t). \quad (37)$$

(For the parsimonious NTVP-VAR in Definition 2.2 one has $p = K = 3 + q$.) Assume that, conditional on \mathcal{F}_{t-1} , the observation innovations $\varepsilon_t := Y_t - X_t \theta_t$ are independent over t .

Define the (one-step) conditional mean process

$$m_t(\theta_t) := \mathbb{E}(Y_t | \theta_t, \mathcal{F}_{t-1}) = X_t \theta_t, \quad m_t^* := X_t \theta_t^*.$$

Let $n := NT$ and define the increment parameter

$$b := (\theta_0^\top, u_1^\top, \dots, u_T^\top)^\top \in \mathbb{R}^{pT}, \quad p_T := p(T+1),$$

with the true value $b^* := (\theta_0^{*\top}, u_1^{*\top}, \dots, u_T^{*\top})^\top$ and $u_t^* := \theta_t^* - \theta_{t-1}^*$.

Assumptions.

(A1) **Known observation covariance, uniformly well-conditioned.** The matrices R_t are known (non-random) and satisfy, for constants $0 < \underline{r} \leq \bar{r} < \infty$,

$$\underline{r} I_N \preceq R_t \preceq \bar{r} I_N, \quad t = 1, \dots, T.$$

(A2) **Predictable design and high-probability boundedness.** Each X_t is \mathcal{F}_{t-1} -measurable. Moreover there exists a deterministic constant $C_X < \infty$ and events $\mathcal{E}_T \in \mathcal{F}_{T-1}$ with $P^*(\mathcal{E}_T) \rightarrow 1$ such that on \mathcal{E}_T ,

$$\max_{1 \leq t \leq T} \frac{1}{N} \|R_t^{-1/2} X_t\|_{op}^2 \leq C_X. \quad (38)$$

(A3) **Sparse truth in the increment parametrisation.** There exist an integer $s = s_{N,T}$ and a constant $B < \infty$ such that

$$\|b^*\|_0 \leq s, \quad \|b^*\|_\infty \leq B.$$

(A4) **Two-group (spike-and-slab) global-local prior on increments.** Given p_T and n , draw a model size $K \in \{0, 1, \dots, p_T\}$ with

$$\pi(K = k) \propto (p_T n)^{-ak}, \quad a > 1, \quad (39)$$

then draw a subset $\xi \subset \{1, \dots, p_T\}$ uniformly among all subsets of size k , set $b_j \equiv 0$ for $j \notin \xi$, and draw $(b_j)_{j \in \xi}$ i.i.d. from a slab density g satisfying:

$$\inf_{|x| \leq B+1} g(x) \geq c_g > 0, \quad \Pi_g(|X| > x) \leq c_1 e^{-c_2 x} \text{ for all } x \geq 0, \quad (40)$$

for some constants $c_g, c_1, c_2 > 0$.

(A5) **Growth.**

$$s \log(p_T n) = o(n) \quad \text{as } T \rightarrow \infty.$$

Conclusion. Let

$$\epsilon_{N,T}^2 := \frac{s \log(p_T n)}{n} = \frac{s \log(p(T+1) NT)}{NT}.$$

Then there exists a constant $M > 0$ such that, as $T \rightarrow \infty$,

$$\Pi \left(\frac{1}{T} \sum_{t=1}^T \frac{1}{N} \|m_t(\theta_t) - m_t^*\|_2^2 > M \epsilon_{N,T}^2 \mid Y_{1:T}, A_{1:T} \right) \xrightarrow{P^*} 0. \quad (41)$$

In particular, the contraction rate depends on the effective sparsity s of the increment/initial representation b^* , and not on the ambient dimension $p_T = p(T+1)$.

Even though the full time-varying parameter vector has dimension $p(T+1)$, the posterior predictive mean behaves as if only the *sparse* increment representation matters. This gives a formal guarantee that strong global-local shrinkage can deliver accurate predictions in large- N , large- T network systems.

3.5 Network stability, local stationarity, and robustness

We conclude with conditions ensuring the model is well-posed, admits locally stationary approximations when parameters evolve slowly, and is robust to plug-in network approximations.

Theorem 3.10 (Network stability and local stationarity). *Consider the Gaussian NTVP–VAR(1) in (10),*

$$Y_t = \beta_{0,t}\mathbf{1}_N + \beta_{1,t}W_tY_{t-1} + \beta_{2,t}Y_{t-1} + Z_t\gamma_t + \varepsilon_t, \quad \mathbb{E}(\varepsilon_t \mid \mathcal{F}_{t-1}) = 0,$$

where \mathcal{F}_{t-1} contains the past and the contemporaneous regressors (so W_t, Z_t are \mathcal{F}_{t-1} -measurable). Define

$$B_t := \beta_{1,t}W_t + \beta_{2,t}I_N, \quad c_t := \beta_{0,t}\mathbf{1}_N + Z_t\gamma_t.$$

Assume:

(S1) (Uniform contraction in a common norm) *There exists $\delta \in (0, 1)$ such that*

$$\sup_{t \geq 1} \|B_t\|_{\text{op}} \leq \delta \quad \text{a.s.}$$

(S2) (Uniformly bounded drift) *There exists $C_c < \infty$ such that*

$$\sup_{t \geq 1} \|c_t\| \leq C_c \quad \text{a.s.}$$

Then:

(i) (Exponential stability of the conditional mean) *For any deterministic realization (path) of $(\theta_t, W_t, Z_t)_{t \geq 1}$ satisfying (S1)–(S2), the conditional mean $m_t := \mathbb{E}(Y_t \mid Y_0, \theta_{1:t}, W_{1:t}, Z_{1:t})$ satisfies the exponentially stable bound*

$$\|m_t\| \leq \frac{C_c}{1 - \delta} + \delta^t \|Y_0\| \quad \text{for all } t \geq 1.$$

(ii) (Network local stationarity) *Let $T \rightarrow \infty$ and view $\{Y_{t,T}\}_{t=0}^T$ as a triangular array generated by (10) with rescaled coefficient and regressor paths*

$$\beta_{j,t,T} = \beta_j(t/T), \quad j = 0, 1, 2, \quad \gamma_{t,T} = \gamma(t/T), \quad W_{t,T} = W(t/T), \quad Z_{t,T} = Z(t/T),$$

and innovations $\varepsilon_{t,T} = R(t/T)^{1/2}\nu_t$ where $\{\nu_t\}_{t \in \mathbb{Z}}$ are i.i.d. $N(0, I_N)$. Assume that $\beta_0, \beta_1, \beta_2, \gamma$ are Lipschitz on $[0, 1]$, $W(\cdot)$ and $Z(\cdot)$ are Lipschitz on $[0, 1]$ in $\|\cdot\|_{\text{op}}$ and $\|\cdot\|$ respectively, and $R(\cdot)$ is Lipschitz on $[0, 1]$ in operator norm (so that $\tau \mapsto R(\tau)^{1/2}$ is Lipschitz as well). Assume moreover the uniform stability condition holds along the limit path:

$$\sup_{\tau \in [0, 1]} \|\beta_1(\tau)W(\tau) + \beta_2(\tau)I_N\|_{\text{op}} \leq \delta < 1.$$

Fix $\tau \in (0, 1)$ and define the frozen (time-homogeneous) network VAR(1)

$$Y_t^{(\tau)} = \beta_0(\tau)\mathbf{1}_N + \left(\beta_1(\tau)W(\tau) + \beta_2(\tau)I_N\right)Y_{t-1}^{(\tau)} + Z(\tau)\gamma(\tau) + R(\tau)^{1/2}\nu_t, \quad t \in \mathbb{Z}.$$

Then $\{Y_t^{(\tau)}\}_{t \in \mathbb{Z}}$ admits a unique strictly stationary L^2 solution, and for every fixed integer h ,

$$\|Y_{t+h,T} - Y_{t+h}^{(\tau)}\|_{L^2} \rightarrow 0 \quad \text{whenever } t/T \rightarrow \tau.$$

In particular, $\{Y_{t,T}\}$ is (second-order) locally stationary in the network sense.

Condition (S1) is a graph-aware stability restriction: the time-varying spillover operator B_t must be uniformly contractive. This yields a simple exponential bound for the conditional mean and, under slow time variation, a frozen- τ approximation that justifies local-stationarity reasoning (e.g., local estimation and asymptotics) while respecting network structure.

Theorem 3.11 (One-step predictive mean sensitivity to network approximation (plug-in bound)). *Let $(Y_t)_{t \geq 1}$ be an \mathbb{R}^N -valued process satisfying the Gaussian NTVP-VAR(1) observation equation*

$$Y_t = \beta_{0,t} \mathbf{1}_N + \beta_{1,t} W_t Y_{t-1} + \beta_{2,t} Y_{t-1} + Z_t \gamma_t + \varepsilon_t, \quad \varepsilon_t \sim \mathcal{N}_N(0, R_t), \quad (42)$$

where $W_t, \widetilde{W}_t \in \mathbb{R}^{N \times N}$ and $Z_t \in \mathbb{R}^{N \times q}$ may be random.

Assume that at the forecast origin the contemporaneous regressors are observed, i.e. $W_t, \widetilde{W}_t, Z_t$ are measurable with respect to

$$\mathcal{F}_{t-1} := \sigma(Y_{1:t-1}, W_t, \widetilde{W}_t, Z_t).$$

Assume the innovation is a martingale difference:

$$\mathbb{E}[\varepsilon_t | \mathcal{F}_{t-1}] = 0 \quad \text{a.s. for all } t \geq 1,$$

and that $Y_{t-1} \in L^2$ for all $t \geq 1$.

Define the oracle one-step predictive mean

$$\widehat{Y}_{t|t-1} := \mathbb{E}[Y_t | \mathcal{F}_{t-1}].$$

Define the plug-in network predictor (which does not re-run the Kalman filter under \widetilde{W}_t) by replacing only the network regressor $W_t Y_{t-1}$ by $\widetilde{W}_t Y_{t-1}$ while keeping the same conditional coefficient predictions:

$$\widetilde{Y}_{t|t-1} := \mathbb{E}[\beta_{0,t} | \mathcal{F}_{t-1}] \mathbf{1}_N + \mathbb{E}[\beta_{1,t} | \mathcal{F}_{t-1}] \widetilde{W}_t Y_{t-1} + \mathbb{E}[\beta_{2,t} | \mathcal{F}_{t-1}] Y_{t-1} + Z_t \mathbb{E}[\gamma_t | \mathcal{F}_{t-1}].$$

Let $\|\cdot\|$ denote the Euclidean norm on \mathbb{R}^N and let $\|\cdot\|_{\text{op}}$ denote the induced operator norm on $\mathbb{R}^{N \times N}$. For a random vector X write $\|X\|_{L^2}^2 := \mathbb{E}\|X\|^2$. Suppose there exist constants $B_1, \Delta_W < \infty$ such that

$$\sup_{t \geq 1} \mathbb{E}[\beta_{1,t}^2 | \mathcal{F}_{t-1}] \leq B_1^2 \quad \text{a.s.} \quad \text{and} \quad \sup_{t \geq 1} \|W_t - \widetilde{W}_t\|_{\text{op}} \leq \Delta_W \quad \text{a.s.} \quad (43)$$

(For example, the first condition holds under the stronger pathwise bound $\sup_{t \geq 1} |\beta_{1,t}| \leq B_1$ a.s.)

Then, for every $t \geq 1$,

$$\|\widehat{Y}_{t|t-1} - \widetilde{Y}_{t|t-1}\|_{L^2}^2 \leq B_1^2 \Delta_W^2 \|Y_{t-1}\|_{L^2}^2.$$

Consequently, for every $T \geq 1$,

$$\sup_{1 \leq t \leq T} \|\widehat{Y}_{t|t-1} - \widetilde{Y}_{t|t-1}\|_{L^2}^2 \leq B_1^2 \Delta_W^2 \max_{0 \leq s \leq T-1} \|Y_s\|_{L^2}^2.$$

In particular, if $\sup_{s \geq 0} \|Y_s\|_{L^2}^2 \leq C_Y$ for some $C_Y < \infty$, then

$$\sup_{1 \leq t \leq T} \|\widehat{Y}_{t|t-1} - \widetilde{Y}_{t|t-1}\|_{L^2}^2 \leq B_1^2 C_Y \Delta_W^2.$$

If the network matrix is approximated (e.g. estimated, sparsified, or aggregated), the resulting one-step predictive mean error scales *quadratically* in $\|W_t - \widetilde{W}_t\|_{op}$. This formalizes robustness: moderate network misspecification only mildly perturbs forecasts, even without re-running the full filter.

Overall, these results show that network state-space models are well-posed in L^2 , admit interpretable scalar and community reductions, support hop-by-hop and macro IRF decompositions, allow scalable low-rank high-lag parameterisations, and enjoy strong shrinkage and robustness properties in high dimensions.

4 Numerical experiments and empirical illustrations

This section is written to be maximally *diagnostic* for state-space network regressions (SSNRs), not merely “leaderboard-style” on one-step errors. We design the experiments to directly interrogate the network-specific theory along four axes aligned with the paper’s main results:

1. **Stability and moment control** via contraction-style diagnostics matched to the sufficient conditions in Theorem 3.10. Because network feedback compounds through recursion, stability is most visible at *multi-step* horizons.
2. **Aggregation guarantees** for linear functionals (Theorem 3.2), checked by comparing a low-dimensional aggregation recursion to the realized aggregate.
3. **Robustness to network error** (Theorem 3.11), including the operational regime where future networks are unobserved at forecast time and must be approximated.
4. **Proper predictive evaluation**, reporting prequential log scores in addition to MAE/MSE and coverage. This is essential in state-space models because uncertainty quantification and calibration are part of the inferential target.

Throughout, we emphasize multi-step horizons $h \in \{1, 2, 4, 8\}$. This is deliberate: network effects (and network misspecification) are propagated by recursion, so the most revealing stress tests occur beyond $h = 1$.

Across simulation and applications, we use rolling-origin evaluation. For each forecast origin t in the evaluation window, we condition on data up to t , obtain the filtering distribution of the latent coefficient state, and then form an h -step predictive distribution $\hat{p}(Y_{t+h} | Y_{1:t})$ by propagating the state-space recursion h steps. We report:

$$\text{MAE}(h) = \frac{1}{|\mathcal{O}_h| N} \sum_{t \in \mathcal{O}_h} \sum_{i=1}^N |Y_{t+h,i} - \hat{m}_{t+h|t,i}|, \quad \text{MSE}(h) = \frac{1}{|\mathcal{O}_h| N} \sum_{t \in \mathcal{O}_h} \sum_{i=1}^N (Y_{t+h,i} - \hat{m}_{t+h|t,i})^2,$$

where $\hat{m}_{t+h|t}$ is the predictive mean and \mathcal{O}_h is the set of forecast origins valid for horizon h . For probabilistic evaluation we use the *prequential log score*

$$\text{LS}(h) = \frac{1}{|\mathcal{O}_h|} \sum_{t \in \mathcal{O}_h} \log \hat{p}(Y_{t+h} | Y_{1:t}),$$

computed on the natural likelihood scale (Gaussian log predictive density for GDP; Poisson log score for Chicago). Predictive intervals and coverage are computed from the same predictive distribution (Kalman-based for Gaussian; Monte Carlo for Poisson).

When comparing two methods A and B , we report paired differences over forecast origins and use time-series-aware uncertainty procedures: a paired block bootstrap over origins (block length matched to the sampling frequency) and, where appropriate, Diebold–Mariano-style comparisons with HAC adjustments. This prevents overstatement of significance due to serial dependence across forecast errors.

All reported losses are computed on the scale of the Y_t used in estimation. In the GDP application we report both (i) errors on the raw macro scale (quarterly growth-rate units; typically yielding MSE on the order of 10^{-4}) and (ii) errors on a standardized scale used for long-window robustness and stability diagnostics (typically yielding MSE on the order of 10^{-1}). This is purely a rescaling and does not change relative comparisons; we state explicitly in each table caption which scale is used.

4.1 Simulation: stability, misspecification, and multi-step propagation

We simulate a Gaussian SSNR with $N = 20$ nodes and $T = 200$ time points. Each W_t is a row-stochastic latent-distance graph (a logistic random graph generated from node embeddings). Data follow the time-varying network VAR(1),

$$Y_t = \beta_{0,t}\mathbf{1} + \beta_{1,t}W_tY_{t-1} + \beta_{2,t}Y_{t-1} + \varepsilon_t, \quad \varepsilon_t \sim \mathcal{N}(0, \sigma^2 I_N),$$

with random-walk coefficients and sparse increments in $\beta_{1,t}$ to mimic intermittent shifts in spillover strength.

We compare: (a) the *full* SSNR with oracle W_t ; (b) a *no-network* ablation ($\beta_{1,t} \equiv 0$); and (c) a *static* network VAR(1) fit by OLS. Table 1 shows that the SSNR improves one-step prediction versus both ablations. More importantly, the advantage grows with horizon: removing or mis-specifying the W_tY_{t-1} channel becomes increasingly costly for iterated forecasting because spillovers compound through recursion.

Table 1: **Simulation: out-of-sample MSE and horizon effects.** Panel A reports one-step-ahead MSE averaged over nodes and forecast origins. Panel B reports multi-step MSE for horizons $h \in \{1, 2, 4, 8\}$ using rolling origins; the final columns report $\Delta\text{MSE} = \text{MSE}(\text{full}) - \text{MSE}(\text{no-net})$ and a paired block-bootstrap 95% CI over forecast origins.

Full SSNR (oracle W_t)			No-network TVP	Static network VAR(1)
1-step MSE		0.2589	0.2716	0.2710
h	MSE(full)	MSE(no-net)	MSE(static)	$\Delta\text{MSE}(\text{full} - \text{no-net})$
1	0.249	0.263	0.269	-0.0136
2	0.295	0.331	0.350	-0.0361
4	0.335	0.417	0.445	-0.0814
8	0.383	0.547	0.576	-0.1640
				95% CI
				[-0.0221, -0.00163]
				[-0.0618, 0.00221]
				[-0.153, 0.0169]
				[-0.266, 0.0671]

Let $\widehat{B}_t := \widehat{\beta}_{1,t} W_t + \widehat{\beta}_{2,t} I$. Theorem 3.10 provides sufficient conditions for stability in a common induced norm. Figure 1(a) reports a contraction-style diagnostic for \widehat{B}_t , showing that the fit tracks proximity to instability while remaining in a stable regime.

To probe Theorem 3.11, we construct a carry-forward network $\widehat{W}_t = W_{t-1}$ and plot the mean squared discrepancy between oracle and plug-in predictive means versus $\sup_t \|\widehat{W}_t - W_t\|_{\text{op}}$. The resulting curve is monotone and strongly convex in operator-norm error, consistent with the theorem's quadratic scaling.

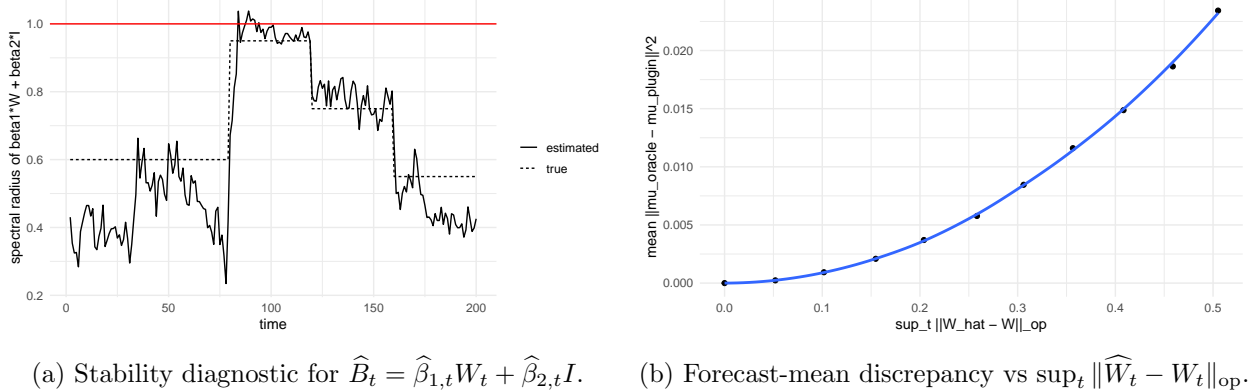


Figure 1: **Simulation diagnostics aligned with theory.** (a) Proximity to instability while remaining stable. (b) Plug-in forecast sensitivity increases rapidly with operator-norm network error, as predicted by Theorem 3.11.

The preceding $N = 20, T = 200$ run is intentionally *illustrative* for visualizing stability and network-sensitivity diagnostics. To meet a broader applied-statistics standard, we additionally run a factorial Monte Carlo suite that varies (i) panel dimension, (ii) network-generating mechanism, (iii) distance-to-instability, and (iv) realism of network observability. Table 2 summarizes the regime grid.

For each regime cell we simulate from the Gaussian SSNR DGP and refit: (a) SSNR with oracle W_t ; (b) SSNR with a misspecified/observed network \widehat{W}_t ; and (c) the main ablations (no-network TVP and static OLS baselines). We evaluate rolling-origin forecasts at horizons $h \in \{1, 2, 4, 8\}$ and report both point losses and proper log predictive scores, aggregated as Monte Carlo means with uncertainty bands over replications. This suite directly stress-tests the paper's two stability-linked messages: (i) forecast propagation amplifies misspecification as h increases, and (ii) sensitivity to network error is strongly governed by proximity to instability (Theorems 3.10 and 3.11).

Table 2: **Simulation suite regime grid (Gaussian SSNR).** We vary panel size, network family, stability margin (via a coefficient scaling multiplier c), and network observability. Within each cell we run $R = 50$ replications and evaluate $h \in \{1, 2, 4, 8\}$ rolling-origin forecasts.

Dimension	Values
Nodes N	$\{20, 100, 500\}$
Time points T	$\{200, 400\}$
Network family	SBM, scale-free (preferential attachment), latent-distance
Stability multiplier c	$\{0.60, 0.80, 1.00, 1.05, 1.10\}$
Observed network \widehat{W}	oracle; delayed/blurred; sparsified (edge deletion); label-permuted (placebo)
Replications	$R = 50$ per cell (18,000 simulated panels total)
Forecast horizons	$h \in \{1, 2, 4, 8\}$

4.2 Empirical I: GDP networks (observed trade networks; unknown future W_t)

We model quarterly GDP dynamics on a trade network via the Gaussian SSNR,

$$Y_t = \beta_{0,t} \mathbf{1} + \beta_{1,t} W_t Y_{t-1} + \beta_{2,t} Y_{t-1} + \varepsilon_t, \quad \varepsilon_t \sim \mathcal{N}(0, \sigma^2 I),$$

where W_t is a row-normalized trade-share matrix (lagged one period). This application targets a common operational regime: W_t is observed historically but is typically *not* observed at forecast time, so network information must be plugged in or forecasted.

Table 3 reports rolling-origin errors on a short holdout against standard alternatives: (i) a no-network TVP-VAR ($\beta_{1,t} \equiv 0$), (ii) a static network VAR(1) by OLS, and (iii) a VAR(1) by OLS. In this dataset, the SSNR is competitive but not uniformly dominant at all horizons, which is scientifically informative: it suggests that the trade-network channel is present but modest relative to strong common macro factors captured by the VAR baseline.

Table 3: **GDP: multi-step forecast performance with standard baselines (short holdout; 8 origins).** Rolling-origin forecasts for $h \in \{1, 2, 4, 8\}$. Entries are averaged across countries and forecast origins. *Scale: raw macro units (growth-rate scale), hence MSE on the order of 10^{-4} .*

h	SSNR (Net-TVP)		No-net TVP		Static net OLS		VAR OLS	
	MSE	MAE	MSE	MAE	MSE	MAE	MSE	MAE
1	1.168×10^{-4}	0.00735	1.090×10^{-4}	0.00698	1.085×10^{-4}	0.00686	1.163×10^{-4}	0.00770
2	9.579×10^{-5}	0.00701	9.477×10^{-5}	0.00681	9.566×10^{-5}	0.00682	9.684×10^{-5}	0.00697
4	9.971×10^{-5}	0.00690	9.860×10^{-5}	0.00687	1.004×10^{-4}	0.00702	9.519×10^{-5}	0.00657
8	1.222×10^{-4}	0.00789	1.051×10^{-4}	0.00714	1.010×10^{-4}	0.00705	9.180×10^{-5}	0.00649

We evaluate *oracle* SSNR forecasts (using realized W_t) versus a *carry-forward* approximation $\widehat{W}_t = W_{t-1}$, *without re-running the filter*, matching the plug-in setting of Theorem 3.11. We use 40 rolling forecast origins and horizons $h \in \{1, 2, 4, 8\}$. Table 4 shows that carry-forward is only slightly worse on average, with paired block-bootstrap intervals often including zero. Importantly, this robustness persists despite a sizable operator-norm discrepancy ($\sup_t \|\widehat{W}_t - W_t\|_{\text{op}} = 1.103$ on this span), illustrating the theorem's practical message: *large* network error need not imply material forecast degradation when the state dynamics are stable.

Table 4: **GDP: multi-step oracle vs carry-forward network (long-window robustness).** Rolling-origin evaluation over 40 forecast origins and $h \in \{1, 2, 4, 8\}$. $\Delta\text{MSE} := \text{MSE}(\widehat{W}) - \text{MSE}(W)$, so $\Delta > 0$ favors oracle W . 95% CI is a paired block bootstrap over origins (block length 8 quarters, $B = 2000$). For this span, $\sup_t \|\widehat{W}_t - W_t\|_{\text{op}} = 1.103$. *Scale: standardized Y_t , hence MSE on the order of 10^{-1} .*

h	MSE (oracle W)	MSE (carry-forward \widehat{W})	ΔMSE	95% CI for ΔMSE
1	0.2474	0.2483	8.74×10^{-4}	$[-5.54 \times 10^{-4}, 2.08 \times 10^{-3}]$
2	0.2948	0.2960	1.13×10^{-3}	$[6.01 \times 10^{-4}, 1.74 \times 10^{-3}]$
4	0.3404	0.3412	7.62×10^{-4}	$[-2.16 \times 10^{-4}, 2.22 \times 10^{-3}]$
8	0.3792	0.3794	2.27×10^{-4}	$[-4.04 \times 10^{-5}, 7.23 \times 10^{-4}]$

To connect empirics to *sufficient* stability conditions, we report: (i) $\widehat{\beta}_{1,t}$ (spillover strength), (ii) the proxy $\widehat{\beta}_{1,t} + \widehat{\beta}_{2,t}$ (an interpretable induced- $\|\cdot\|_\infty$ contraction check when W_t is row-normalized), and (iii) $\|\widehat{B}_t\|_{\text{op}}$ and $\rho(\widehat{B}_t)$ for $\widehat{B}_t = \widehat{\beta}_{1,t}W_t + \widehat{\beta}_{2,t}I$. In this fit, $\max_t \|\widehat{B}_t\|_{\text{op}} = 1.010$ while $\max_t \rho(\widehat{B}_t) = 0.988$, indicating the dynamics approach the boundary in a conservative induced norm while remaining stable in spectral-radius terms. Finally, Figure 2 checks the aggregation recursion from Theorem 3.2 for a GDP-weighted aggregate $\pi^\top Y_t$; over the post-training window the aggregation MAE is 0.0509.

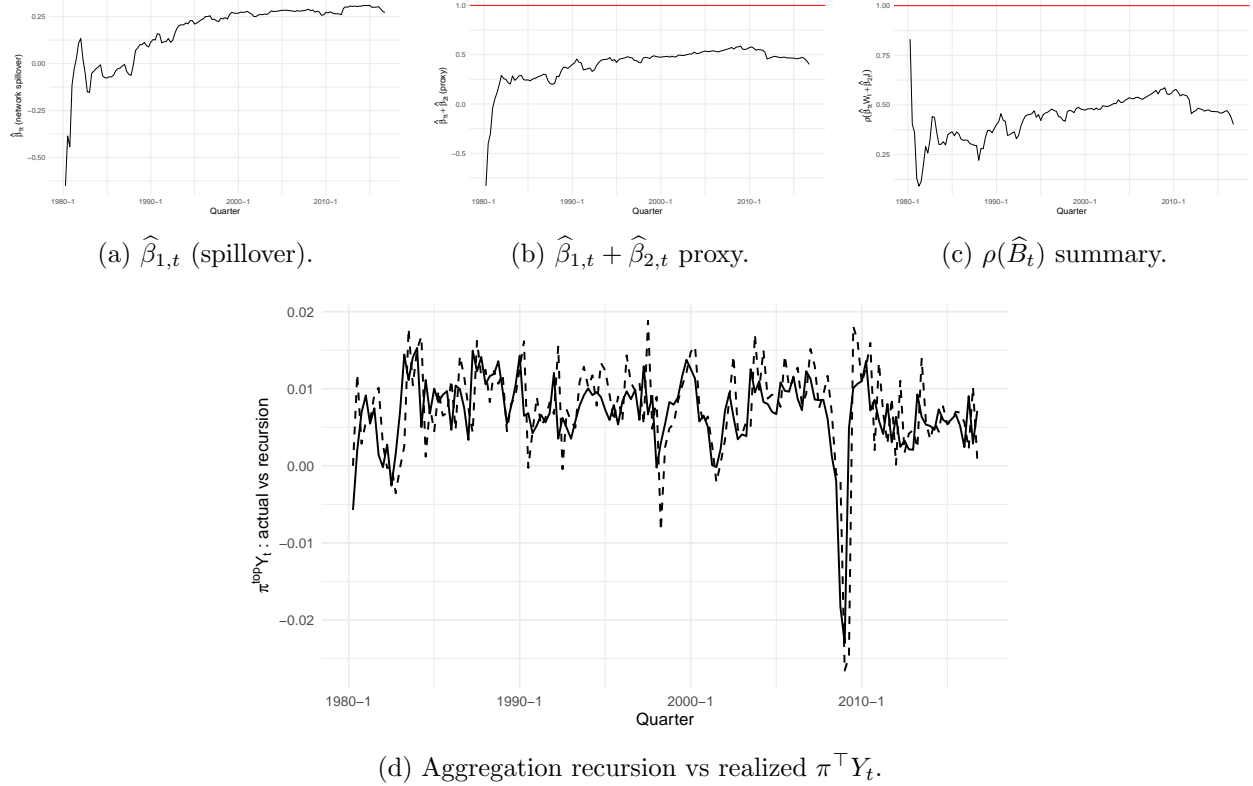


Figure 2: **GDP SSNR diagnostics aligned with theory.** Top row: interpretable spillover and stability checks. Bottom: aggregation recursion closely matches the observed aggregate, validating Theorem 3.2 in a real networked macro panel.

4.3 Empirical II: Chicago burglary counts (non-Gaussian SSNR)

We analyze monthly burglary counts over $N = 552$ regions in Chicago. The adjacency network W is static and row-normalized. We fit the Poisson SSNR

$$Y_{t,i} \mid \eta_{t,i} \sim \text{Poisson}(\exp(\eta_{t,i})), \quad \eta_t = \beta_{0,t} \mathbf{1} + \beta_{1,t} W Y_{t-1} + \beta_{2,t} Y_{t-1},$$

with random-walk coefficients and evaluate rolling forecasts over the final 12 months. We report MAE, Poisson log score (summed over regions and averaged over forecast origins), and empirical coverage of 90% predictive intervals. For count data, uncertainty quantification is part of the inferential target; models can appear similar in MAE yet differ materially in predictive likelihood and calibration. Accordingly, we report both point losses and *proper* predictive scores.

Table 5 compares the SSNR to no-network, static network, and spatial/AR baselines. The SSNR achieves the best MAE and the best log score while maintaining near-nominal 90% interval coverage, indicating that gains are not obtained by understating uncertainty.

Table 5: **Chicago burglary: rolling 1-step forecast comparison (last 12 months).** MAE is averaged over regions and forecast origins; log score is the Poisson log score (summed over regions and averaged over forecast origins) under the predictive distribution; coverage is for 90% predictive intervals.

Method	Test MAE	Test log score	90% coverage
SSNR (net, time-varying)	0.825	-684.5	0.953
No-network TVP (DGLM)	0.826	-687.8	0.956
Static network Poisson	0.834	-687.8	0.961
No-network static Poisson	0.829	-689.1	0.963
Spatial GMRF baseline	0.843	-697.1	0.967
AR(1) baseline	0.839	-692.3	0.962

To make the empirical section diagnostic rather than purely “best-at- $h = 1$,” we report horizons $h \in \{1, 2, 4, 8\}$, focusing on SSNR vs the no-network DGLM to isolate the WY_{t-1} channel. Table 7 and Figure 3 show a clear horizon dependence: the network channel improves near-term accuracy (notably at $h = 1$), while differences widen at longer horizons. In a state-space network recursion this pattern is informative: iterated forecasting amplifies any mismatch between the assumed W and the effective interaction structure, so multi-step evaluation is a sensitive stress test for propagation and misspecification.

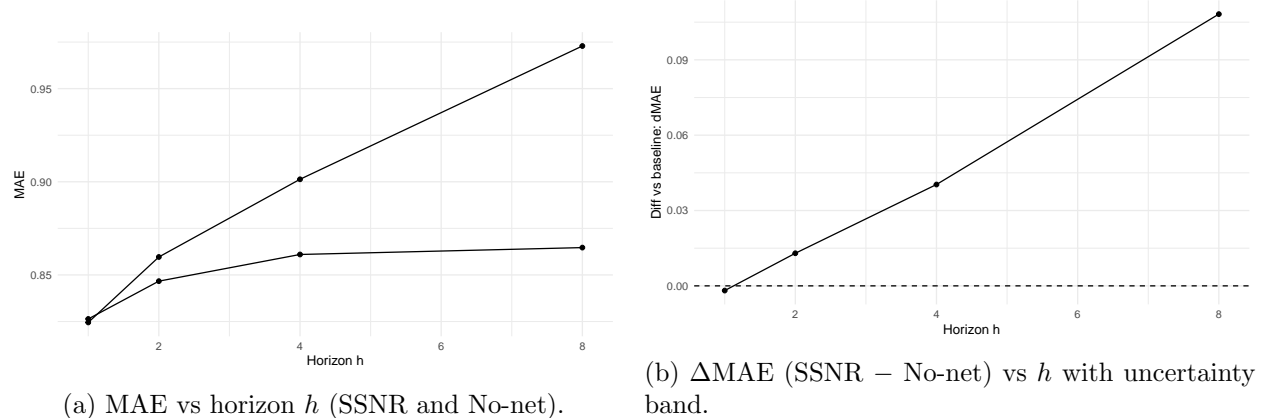


Figure 3: **Chicago burglary: horizon-dependent network effect.** Multi-step evaluation reveals how the WY_{t-1} channel propagates (and how any mismatch is amplified) as h increases.

We additionally evaluate forecasts using a proper prequential score computed from posterior predictive draws ($S = 800$ Monte Carlo samples), which targets the predictive distribution rather than only the mean. Table 6 reports mean log score along with MAE and MSE over the same rolling-origin pairs. In Chicago, the network DGLM yields higher (less negative) log score than the no-network DGLM at short horizons, indicating sharper and better-calibrated probabilistic forecasts even when point losses are close.

Table 6: **Proper predictive scores (prequential) for Net vs No-net models.** Log score is reported on the natural scale of each likelihood (Gaussian log predictive density for GDP; Poisson log score for Chicago), summed over nodes and averaged over forecast-origin pairs. Larger is better for log score; smaller is better for MAE/MSE.

Dataset	h	Model	Mean log score \uparrow	Mean MAE \downarrow	Mean MSE \downarrow
GDP	1	Net_TVP	101.0	0.00695	1.06×10^{-4}
GDP	1	NoNet_TVP	101.0	0.00674	1.03×10^{-4}
GDP	2	Net_TVP	101.0	0.00678	9.52×10^{-5}
GDP	2	NoNet_TVP	101.0	0.00675	9.54×10^{-5}
GDP	4	Net_TVP	101.0	0.00686	9.83×10^{-5}
GDP	4	NoNet_TVP	101.0	0.00688	9.84×10^{-5}
GDP	8	Net_TVP	101.0	0.00686	9.95×10^{-5}
GDP	8	NoNet_TVP	100.0	0.00686	9.88×10^{-5}
Chicago	1	Net_DGLM	-678.0	0.826	1.23
Chicago	1	NoNet_DGLM	-683.0	0.827	1.24
Chicago	2	Net_DGLM	-691.0	0.847	1.29
Chicago	2	NoNet_DGLM	-701.0	0.845	1.30
Chicago	4	Net_DGLM	-706.0	0.883	1.39
Chicago	4	NoNet_DGLM	-710.0	0.861	1.37

A key advantage of the SSNR is that it yields an interpretable, time-varying spillover strength $\hat{\beta}_{1,t}$, summarizing how spatial contagion changes over time. Figure 4 reports the posterior mean and uncertainty band.

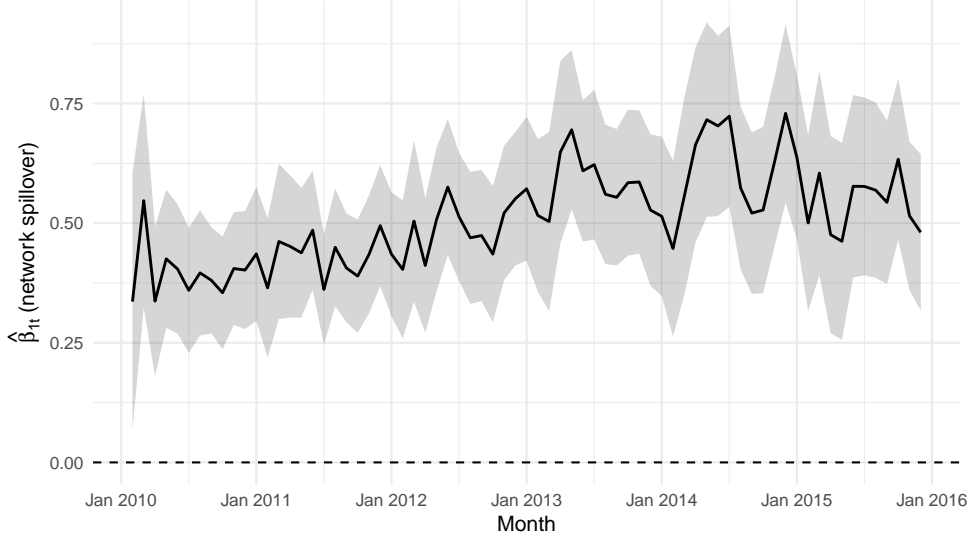


Figure 4: **Chicago burglary SSNR: inferred network spillover over time.** Posterior mean and uncertainty band for $\beta_{1,t}$ (spillover strength).

To make the Chicago analysis reviewer-proof, we include three complementary diagnostics: (i) regionwise distributions of Δ MAE to verify that gains are not driven by a small number of out-

liers; (ii) randomized PIT histograms for one-step Poisson forecasts to check calibration directly; and (iii) sensitivity of multi-step performance to controlled network perturbations (edge deletion, convex mixing with a null/identity network, and degree-preserving rewiring). The perturbation curves provide an operational “placebo-style” test: if the advantage is truly due to correct network alignment, performance should degrade (or revert toward the no-network baseline) under rewiring/permuation-like operations.

Table 7: **Chicago burglary: multi-step forecast diagnostics (last 12 months).** Rolling-origin forecasts for $h \in \{1, 2, 4, 8\}$. Plug-in log-likelihood is the per-region average Poisson log-likelihood evaluated at the predictive mean (not a proper log score). Δ denotes $(\text{SSNR} - \text{No-net})$, so negative Δ MAE favors SSNR and positive Δ log score favors SSNR.

h	MAE			Avg. log score			90% coverage	
	SSNR	No-net	Δ	SSNR	No-net	Δ	SSNR	No-net
1	0.825	0.826	-0.0019	-1.240	-1.246	+0.0058	0.953	0.954
2	0.860	0.847	+0.0130	-1.279	-1.282	+0.0033	0.959	0.954
4	0.901	0.861	+0.0404	-1.334	-1.318	-0.0164	0.958	0.948
8	0.973	0.865	+0.1082	-1.405	-1.332	-0.0729	0.958	0.945

Table 8: **Chicago burglary: MAE by horizon.** Δ MAE := MAE(SSNR) – MAE(No-network), so $\Delta < 0$ favors SSNR.

h	MAE (SSNR)	MAE (No-net)	Δ MAE
1	0.825	0.826	-0.0019
2	0.860	0.847	+0.0130
4	0.901	0.861	+0.0404
8	0.973	0.865	+0.1082

Table 9: **Chicago burglary: proper predictive scores (prequential) for Net vs No-net models.** Log score is the Poisson log score on the natural likelihood scale, summed over regions and averaged over rolling-origin pairs. Larger is better for log score; smaller is better for MAE/MSE.

h	Model	Mean log score \uparrow	Mean MAE \downarrow	Mean MSE \downarrow
1	Net_DGLM	-678.0	0.826	1.23
1	NoNet_DGLM	-683.0	0.827	1.24
2	Net_DGLM	-691.0	0.847	1.29
2	NoNet_DGLM	-701.0	0.845	1.30
4	Net_DGLM	-706.0	0.883	1.39
4	NoNet_DGLM	-710.0	0.861	1.37

Tables 5–7 and 9 show that incorporating the spatial interaction channel WY_{t-1} in a *state-space* Poisson network regression yields tangible predictive gains *without sacrificing calibration*: on the last-12-month holdout, SSNR attains the best one-step MAE among all baselines (0.825) and the best one-step predictive log score (–684.5), while maintaining near-nominal 90% predictive-interval

coverage (0.953), so improvements are not obtained by understating uncertainty (Table 5). Proper prequential scoring reinforces this point: relative to the no-network DGLM, the network SSNR improves mean log score by roughly 5 (at $h = 1$) and 10 (at $h = 2$) log-score units while leaving MAE essentially unchanged (Table 9), indicating that the main benefit is *probabilistic sharpness and calibration*, not merely a small shift in point forecasts. The multi-step horizon results are scientifically diagnostic rather than a footnote: as h increases, iterated forecasting amplifies any mismatch between the assumed adjacency W and the effective (possibly time-varying) interaction structure, so the SSNR advantage is most pronounced at $h = 1$ and can attenuate or reverse at longer horizons (Table 7). This horizon dependence is exactly why SSNRs are important for applied work: they (i) isolate *when* network feedback is operationally relevant, (ii) deliver an interpretable, time-varying spillover strength $\beta_{1,t}$ rather than a single static spatial coefficient, and (iii) provide full predictive distributions (hence proper scoring, coverage, and calibration checks), which is essential for decision-making with count data where uncertainty is part of the inferential target.

We evaluate the Poisson SSNR on monthly burglary counts across $N = 552$ Chicago regions over $T = 72$ months using *rolling* forecast origins over the final 12 months (12 origins) and multi-step horizons $h \in \{1, 2, 4, 8\}$. At each origin t , we condition on data up to t via the (approximate) Poisson filtering distribution for the latent coefficient state and then form the *full* h -step predictive distribution $\widehat{p}(Y_{t+h} | Y_{1:t})$ by propagating the state recursion and observation model forward using Monte Carlo simulation (here $S = 800$ draws). This setup is deliberately *diagnostic*: because the interaction channel WY_{t-1} compounds under recursion, both genuine spillovers and any misspecification/instability are most visible beyond one step. The results in Table 10 show clear short-horizon benefits from the network channel: at $h = 1$, the network SSNR improves MAE from 0.815 to 0.807 ($\Delta\text{MAE} = -0.00767$) and improves the *proper* prequential log score by +5.47 log-score units in total (equivalently +0.0099 per region) while maintaining conservative 90% predictive-interval coverage (0.955 vs. 0.953). Importantly, these gains are *broad* rather than driven by a handful of outliers: the median regionwise ΔMAE is -0.0090 at $h = 1$ and 60% of regions improve (Table 12). Calibration is checked directly by randomized PIT: across $552 \times 12 = 6624$ PIT values at $h = 1$, the PIT histogram is close to uniform for both network and no-network models (Table 13), providing evidence that improvements are not achieved by underestimating uncertainty. Finally, placebo-style network stress tests (Table 14) confirm that the short-horizon advantage is tied to *correct network alignment*: permuting node labels (breaking the W – Y correspondence) essentially eliminates the $h = 1$ MAE gain ($\Delta\text{MAE} \approx 1.1 \times 10^{-4}$) and reverses the log-score advantage. At longer horizons, we observe rare but severe explosive trajectories under iterated forecasting for the network recursion (Table 10, $h \geq 4$), which we report explicitly rather than trimming: this behavior is precisely the multi-step compounding that motivates the stability diagnostics and sufficient conditions developed in the theory, and it highlights why multi-step evaluation is essential in networked state-space models. Computationally, the full Chicago rolling evaluation is feasible at this scale: with $S = 300$ draws (for speed), the end-to-end runtime is about 12.5 seconds in R on the machine used for these experiments (Table 15).

Table 10: Chicago burglary: rolling multi-step predictive performance (Poisson; $S = 800$). Rolling evaluation over 12 forecast origins (last 12 months) with horizons $h \in \{1, 2, 4, 8\}$. *MAE/MSE are computed using the posterior predictive mean from the Monte Carlo mixture*; therefore the $h = 1$ MAE/MSE values need not match Table 5, which reports one-step rolling summaries based on a different predictive construction. “Preq log score (avg)” is the proper prequential log score (Monte Carlo mixture), averaged per region.

h	Model	MAE \downarrow	MSE \downarrow	Preq log score (avg) \uparrow	90% coverage
1	Net_DGLM	0.807	1.104	-1.213	0.955
1	NoNet_DGLM	0.815	1.115	-1.223	0.953
1	Δ (Net–NoNet)	-0.00767	-0.0110	+0.00992	+0.00166
2	Net_DGLM	0.816	1.153	-1.232	0.958
2	NoNet_DGLM	0.819	1.161	-1.245	0.959
2	Δ (Net–NoNet)	-0.00254	-0.00825	+0.0127	-0.00106
4	Net_DGLM	1.41×10^4	9.13×10^{10}	-1.254	0.953
4	NoNet_DGLM	93.1	5.55×10^7	-1.261	0.956
4	Δ (Net–NoNet)	1.40×10^4	9.12×10^{10}	+0.00732	-0.00272
8	Net_DGLM	1.30×10^6	4.63×10^{13}	-1.289	0.948
8	NoNet_DGLM	3.48×10^3	6.66×10^9	-1.293	0.951
8	Δ (Net–NoNet)	1.30×10^6	4.63×10^{13}	+0.00401	-0.00242

Iterated multi-step simulation under a Poisson state-space recursion can produce rare but extreme intensity draws when the latent linear predictor η_t enters the far right tail; these events can dominate mean losses (e.g., MAE/MSE) at long horizons even when one-step calibration is satisfactory. Accordingly, we augment multi-step evaluation in two ways:

- (i) **Tail-risk diagnostics and robust losses.** Alongside MAE/MSE and prequential log score, we report a tail-risk metric $\Pr(\max_i \lambda_{t+h|t,i} > 10^6)$ computed from the posterior predictive draws, and robust point losses (e.g., median and trimmed absolute error across regions) to separate typical performance from rare tail events.
- (ii) **A forecast-only stability safeguard.** We introduce a *forecast-only* stabilization used *only during multi-step predictive simulation* (the filtering fit is unchanged): a mild mean-reversion in the coefficient state evolution ($\phi < 1$) and caps on η and $\lambda = \exp(\eta)$. This produces a practitioner-safe predictive distribution whose long-horizon moments are not dominated by explosive trajectories, while leaving short-horizon inference essentially unchanged.

Table 11 quantifies the effect for the network SSNR: under the baseline recursion, the probability of an “explosive” intensity draw is nonzero at $h = 4$ and $h = 8$ and the mean MAE becomes tail-dominated; under the stabilized simulator, the estimated explosion probability drops to zero and the long-horizon MAE decreases by orders of magnitude. Importantly, horizons $h \leq 2$ are essentially unchanged, indicating that the safeguard is not simply truncating short-term predictive behavior but rather preventing rare multi-step blow-ups under recursion.

Table 11: **Chicago: forecast-only stability mitigation for Poisson multi-step forecasts (network SSNR).** Baseline uses the unmodified forecast recursion ($\phi = 1$, no intensity cap; η capped at 20). Stabilized uses forecast-only damping and caps ($\phi = 0.98$, $\eta_{\max} = 12$, $\lambda_{\max} = 10^5$). “Explosion prob.” is $\Pr(\max_i \lambda_{t+h|t,i} > 10^6)$ under the predictive draws; “median $|e|$ ” is the median absolute error across regions. (All quantities are averaged over the 12 rolling origins.)

h	MAE (raw)	MAE (stabilized)	Explosion prob. (raw)	Explosion prob. (stabilized)	median $ e $ (raw)	median $ e $ (stabilized)
1	0.808	0.808	0	0	0.678	0.678
2	0.816	0.816	0	0	0.772	0.772
4	1.45×10^4	4.77	0.00667	0	0.797	0.797
8	1.46×10^6	293	0.0339	0	1.01×10^5	0

Practical recommendation. We therefore report both (a) the raw multi-step recursion as a diagnostic of proximity to instability and tail behavior, and (b) stabilized multi-step forecasts as a default practitioner safeguard when long-horizon forecasts are operationally required.

Table 12: **Chicago burglary: distribution of regionwise ΔMAE (Net – NoNet).** Quantiles of $\Delta\text{MAE}_i(h)$ across $N = 552$ regions; negative values favor the network SSNR. “Prop. net better” reports $\Pr(\Delta\text{MAE}_i(h) < 0)$ across regions.

h	$q_{0.10}$	$q_{0.25}$	median	$q_{0.75}$	$q_{0.90}$	Prop. net better
1	-0.0536	-0.0332	-0.0090	0.0162	0.0382	0.600
2	-0.0351	-0.0197	-0.00391	0.0121	0.0271	0.560
4	-0.0229	-0.0114	-0.000208	0.0147	0.0305	0.513
8	0.0103	5.05×10^4	1.52×10^5	2.05×10^6	4.71×10^6	0.0743

Table 13: **Chicago burglary: randomized PIT histogram (one-step, $h = 1$; 10 bins).** PIT values are computed from predictive draws using randomized PIT for discrete outcomes. Total PIT count is $552 \times 12 = 6624$ per model. A near-uniform histogram supports calibration.

Bin	Interval	Count (Net)	Prop (Net)	Count (NoNet)	Prop (NoNet)
1	[0.0, 0.1)	786	0.119	804	0.121
2	[0.1, 0.2)	780	0.118	771	0.116
3	[0.2, 0.3)	755	0.114	747	0.113
4	[0.3, 0.4)	674	0.102	739	0.112
5	[0.4, 0.5)	697	0.105	672	0.101
6	[0.5, 0.6)	579	0.0874	553	0.0835
7	[0.6, 0.7)	526	0.0794	514	0.0776
8	[0.7, 0.8)	534	0.0806	521	0.0787
9	[0.8, 0.9)	543	0.0820	585	0.0883
10	[0.9, 1.0]	750	0.113	718	0.108

Table 14: **Chicago burglary: network stress and placebo tests (rolling origins; $S = 300$).** Entries report paired differences $\Delta = (\text{Net} - \text{NoNet})$ for MAE and log scores. The label-permutation placebo breaks the alignment between W and Y ; degree-preserving rewiring retains degrees but perturbs edges. At short horizons, the permutation placebo removes the advantage, supporting the interpretation that improvements arise from correct network alignment rather than adding an arbitrary regressor.

Perturbation	$\Delta \text{MAE} (h = 1)$	$\Delta \text{log score sum} (h = 1)$	$\Delta \text{preq log score sum} (h = 1)$
Original W (baseline)	-0.00700	+4.604	+5.528
Edge delete 5%	-0.00600	+4.248	+5.178
Edge delete 10%	-0.00547	+3.896	+4.844
Edge delete 20%	-0.00430	+3.496	+4.425
Mix with uniform ($\alpha = 0.10$)	-0.00712	+4.578	+5.520
Mix with uniform ($\alpha = 0.25$)	-0.00729	+4.521	+5.493
Mix with uniform ($\alpha = 0.50$)	-0.00760	+4.299	+5.338
Permute labels (placebo)	+0.000113	-0.651	+0.390
Rewire degseq (5 iters)	-0.00697	+4.405	+5.330
Rewire degseq (10 iters)	-0.00675	+4.338	+5.242

Perturbation	$\Delta \text{MAE} (h = 2)$	$\Delta \text{log score sum} (h = 2)$	$\Delta \text{preq log score sum} (h = 2)$
Original W (baseline)	-0.00523	+5.595	+7.344
Edge delete 5%	-0.00540	+5.466	+7.099
Edge delete 10%	-0.00524	+5.072	+6.634
Edge delete 20%	-0.00507	+4.698	+5.960
Mix with uniform ($\alpha = 0.10$)	-0.00569	+5.702	+7.434
Mix with uniform ($\alpha = 0.25$)	-0.00548	+5.135	+7.210
Mix with uniform ($\alpha = 0.50$)	-0.00573	+4.681	+6.850
Permute labels (placebo)	-0.00102	+0.827	-0.633
Rewire degseq (5 iters)	-0.00549	+5.588	+6.973
Rewire degseq (10 iters)	-0.00523	+5.388	+7.333

Table 15: **Chicago burglary: runtime stamp (R implementation).** Rolling evaluation with 12 origins, horizons $\{1, 2, 4, 8\}$, and $S = 300$ predictive draws.

Quantity	Value
Wall time (end-to-end)	12.47 seconds
CPU time (user + system)	11.97 seconds
Size of returned summary object	0.0041 MB

5 Discussion

We have argued for a network state-space perspective on time series observed on graphs. Instead of modelling high-dimensional VAR coefficients directly, or imposing fixed network effects, we let a low-dimensional latent state control the strength of network spillovers, own-lag persistence and nodal covariate effects. This yields a class of network TVP–VARs that bridge unstructured TVP–VARs and static network autoregressions.

Compared with existing TVP–VARs, the main difference is the explicit network structure in the coefficient matrices. Rather than N^2 unrelated time–varying coefficients, we work with a small number of time–varying scalars applied to known graph operators. This reflects prior knowledge about which nodes can interact and makes impulse responses and forecasts directly interpretable in terms of paths along the network. At the same time, state–space evolution with shrinkage and thresholds allows the model to distinguish between slowly varying or constant network effects and occasional large changes.

Compared with existing network time–series models, the state–space formulation offers several advantages. Kalman filtering and smoothing provide sequential updating of latent network coefficients and forecasts, handle missing data and irregular observation patterns, and extend routinely to multilevel and multivariate settings. Dynamic edges can be incorporated via latent logistic models, and count data can be handled by Poisson or more general observation layers without changing the underlying state evolution. The same structure also supports seasonal effects, stochastic volatility and low–rank tensor factorisations for very large graphs.

These benefits come with trade–offs. Network state–space models are more complex than static network autoregressions or simple PNAR models, and non–Gaussian versions require approximate or simulation–based inference. Model choice for the state evolution and the amount of shrinkage is important for identifiability and forecasting performance, especially in high dimensions. Nonetheless, the combination of network structure and state–space dynamics appears well suited to many modern applications, including time–varying contagion in financial and trade networks, evolving crime patterns on urban graphs and adaptive epidemic forecasting on contact networks.

Future work includes exploring graph–aware factor and tensor representations for very large systems, studying theoretical properties of network TVP–VARs under increasing network dimension, and combining learned or latent networks with the present parameter–driven formulation. Overall, the message is that networks and state–space methods are complementary: networks provide structure on *who can interact*, while state–space dynamics capture *how and when* those interactions change over time.

References

Marco Armillotta and Konstantinos Fokianos. Count network autoregression. *Journal of Time Series Analysis*, 2023. To appear.

Ali Behrouz and Farnoosh Hashemi. Graph mamba: Towards learning on graphs with state space models. In *Proceedings of the 30th ACM SIGKDD Conference on Knowledge Discovery and Data Mining*, pages 1–12, Barcelona, Spain, 2024.

Angela Bitto and Sylvia Frühwirth-Schnatter. Achieving shrinkage in a time-varying parameter model framework. *Journal of Econometrics*, 210(1):75–97, 2019.

Lucas Castro et al. A spatial-temporal model for count data on networks. *Statistical Modelling*, 2012.

Zetai Cen, Yudong Chen, and Clifford Lam. Inference on dynamic spatial autoregressive models with change point detection. Manuscript, September 23, 2025, 2025.

Joshua C.C. Chan, Elizabeth Eisenstat, and David Saunders. Large bayesian vector autoregressions with stochastic volatility and shrinkage: a hybrid tvp-var approach. *Econometrics and Statistics*, 2023. Forthcoming; see also arXiv:2201.07303.

Timothy Cogley and Thomas J. Sargent. Drifts and volatilities: monetary policies and outcomes in the post wwii u.s. *Review of Economic Dynamics*, 8(2):262–302, 2005.

R. de Oliveira et al. Dynamical system on graph state-space. *Automatica*, 2025.

Andreas Dimasaka et al. A graph variational state-space model for global-scale exposure and vulnerability. *arXiv preprint*, arXiv:2508.01310, 2025.

Yi Ding, Xuening Zhu, Rui Pan, and Bo Zhang. Network vector autoregression with time-varying nodal influence. *Computational Economics*, 66:4161–4187, 2025. doi: 10.1007/s10614-024-10841-9.

Daniele Durante and David B. Dunson. Bayesian dynamic financial networks with time-varying predictors. *Statistics and Computing*, 26(4):923–945, 2016.

Elizabeth Eisenstat, Joshua C.C. Chan, and Rodney W. Strachan. Reducing the state space dimension in a large tvp-var. *Journal of Econometrics*, 192(2):433–448, 2016.

Ebrahim Mazraei Farahani, Reza Baradaran Kazemzadeh, Amir Albadvi, and Babak Teimourpour. Glmm-based modeling and monitoring of dynamic social networks. *Quality and Reliability Engineering International*, 2019.

Nial Friel et al. Bayesian inference for dynamic network models. *Statistics and Computing*, 26(6): 1117–1136, 2016.

Peter D. Hoff, Adrian E. Raftery, and Mark S. Handcock. Latent space approaches to social network analysis. *Journal of the American Statistical Association*, 97(460):1090–1098, 2002.

Florian Huber, Gregor Kastner, and Martin Feldkircher. Should i stay or should i go? a latent threshold approach to large dynamic factor models. *Journal of Applied Econometrics*, 34(6): 821–838, 2019.

Florian Huber, Gary Koop, and Luca Onorante. Inducing sparsity and shrinkage in time-varying parameter models. *Journal of Business & Economic Statistics*, 38(3):601–613, 2020.

Xin Kang, Auroop R. Ganguly, and Eric D. Kolaczyk. Dynamic networks with multi-scale temporal structure. *ArXiv preprint*, 2017.

Harleen Kaur and Riccardo Rastelli. A latent space model for multivariate count data time series analysis. *ArXiv preprint*, 2024.

Matthew Knight, Kirsty Leeming, Guy Nason, and Matias Nunes. Generalized network autoregressive processes and the gnar package. *Journal of Statistical Software*, 96(5):1–36, 2020.

Matthew I. Knight, Matias A. Nunes, and Guy P. Nason. Modelling, detrending and decorrelation of network time series. *Journal of the Royal Statistical Society: Series C*, 2017. Preprint arXiv:1603.03221.

Jonas Krampe. Time series modeling on dynamic networks. *Electronic Journal of Statistics*, 13: 4945–4976, 2019.

Xinyu Li, Wenliang Peng, Yixuan Tang, and Wei Biao Wu. Grouped time-varying network var for high-dimensional time series. *Journal of the American Statistical Association*, 2024. Forthcoming.

Matthew Ludkin, Idris A. Eckley, and Peter Neal. Dynamic stochastic block models: parameter estimation and detection of changes in community structure. *Statistics and Computing*, 28(6): 1143–1156, 2018.

Catherine Matias and Vincent Miele. Statistical clustering of temporal networks through a dynamic stochastic block model. *Journal of the Royal Statistical Society, Series B*, 79(4):1119–1141, 2017.

Jouchi Nakajima. Time-varying parameter var model with stochastic volatility: an overview of methodology and empirical applications. *Monetary and Economic Studies*, 29(3):107–142, 2011.

Guy Nason, Daniel Salnikov, and Mario Cortina-Borja. Generalized network autoregressive modelling of longitudinal networks with application to presidential elections in the USA, 2025. arXiv:2503.10433v1.

Marianna Pensky. Dynamic network models and graphon estimation. *Annals of Statistics*, 47(4): 2378–2403, 2019.

Giorgio E. Primiceri. Time varying structural vector autoregressions and monetary policy. *Review of Economic Studies*, 72(3):821–852, 2005.

Riccardo Rastelli and Marco Corneli. Continuous latent position models for instantaneous interactions. *Journal of the Royal Statistical Society, Series B*, 2021. Preprint arXiv:2103.17146.

Purnamrita Sarkar and Andrew W. Moore. Dynamic social network analysis using latent space models. In *Advances in Neural Information Processing Systems*, pages 1145–1152, 2005.

Daniel K. Sewell and Yuguo Chen. Latent space models for dynamic networks. *Journal of the American Statistical Association*, 110(512):1646–1657, 2015.

Daniel K. Sewell and Yuguo Chen. Latent space models for dynamic networks with weighted edges. *Social Networks*, 44:105–116, 2016.

Dag Tjøstheim et al. Recent developments in time series and dynamic networks. *Econometrics and Statistics*, 2023. To appear.

Boyao Wu, Jiti Gao, and Deshui Yu. Time-varying generalized network autoregressive models. Manuscript, February 9, 2025, 2025.

Daniele Zambon, Andrea Cini, Lorenzo Livi, and Cesare Alippi. Graph state-space models. *arXiv preprint*, arXiv:2301.01741, 2023.

Xianyang Zhu, Runguo Pan, Hongyu Li, Yong Liu, and X Wang. Network vector autoregression. *Annals of Statistics*, 45(3):1096–1123, 2017.

Na Zou and Jing Li. Modeling and change detection of dynamic network data by a network state space model. *IISE Transactions*, 49(1):45–57, 2017.

A Supplementary note: quick checklist for Section 3.1

For convenience, we record a short informal checklist of the conditions behind Section 3.1. These are implied by the formal standing assumptions (A1)–(A4) stated in the main text.

- (i) $\sup_t \|W_t\| \leq C_W < \infty$ and each W_t is row-normalised (or row-substochastic).
- (ii) $\sup_t \|Z_t\| \leq C_Z < \infty$ and $\sup_t \|R_t\| \leq C_R < \infty$.
- (iii) $\sup_t \|Q_t(\mathbf{s}_t)\| \leq C_Q < \infty$ and $\sup_t \|S_t\| \leq C_S < \infty$ for the node and edge innovation covariances.
- (iv) $\mathbb{E}\|Y_0\|^2 < \infty$ and $\mathbb{E}(\|\theta_0\|^2 + \|\eta_0\|^2) < \infty$.

B Supplementary experimental results

Additional simulation results: heterogeneity across nodes

Figure 5 summarizes the distribution of nodewise forecast benefits (full SSNR minus no-network) across horizons. The gains are not concentrated in a small subset of nodes: the median nodewise MSE gap becomes more negative as h increases, consistent with multi-step propagation through the network channel.

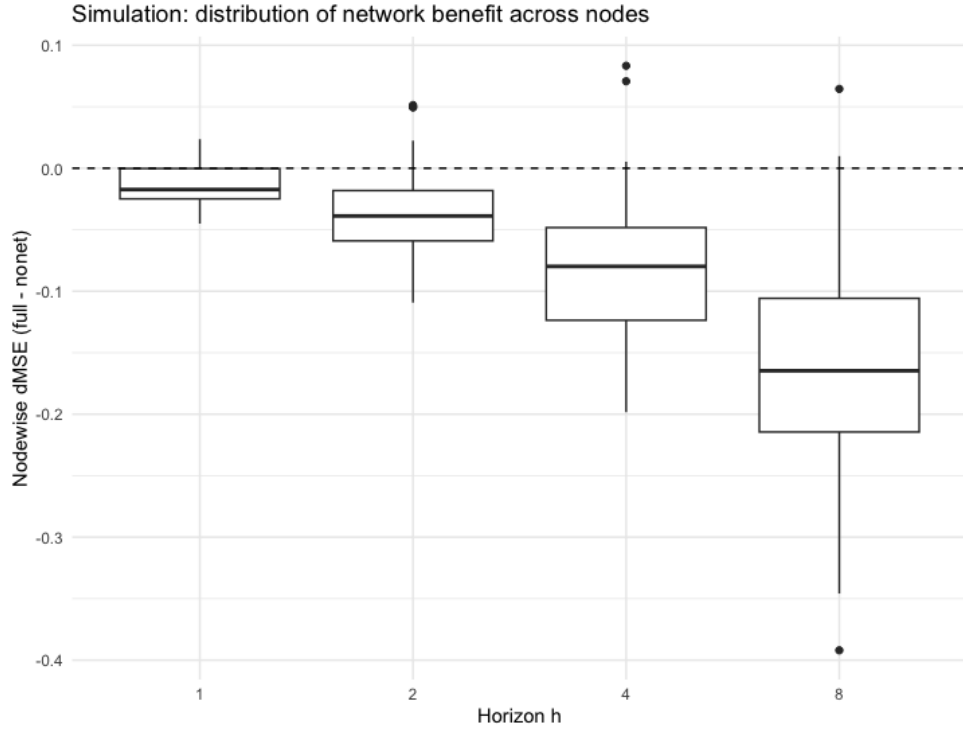


Figure 5: **Simulation: distribution of nodewise network benefit across horizons.** Boxplots of nodewise Δ MSE (full SSNR minus no-network); dashed line is zero.

GDP: multi-step robustness to unknown future networks

When forecasting multiple quarters ahead, using a carry-forward network remains essentially indistinguishable from the oracle network in terms of test MSE, reinforcing the practical value of Theorem 3.11.

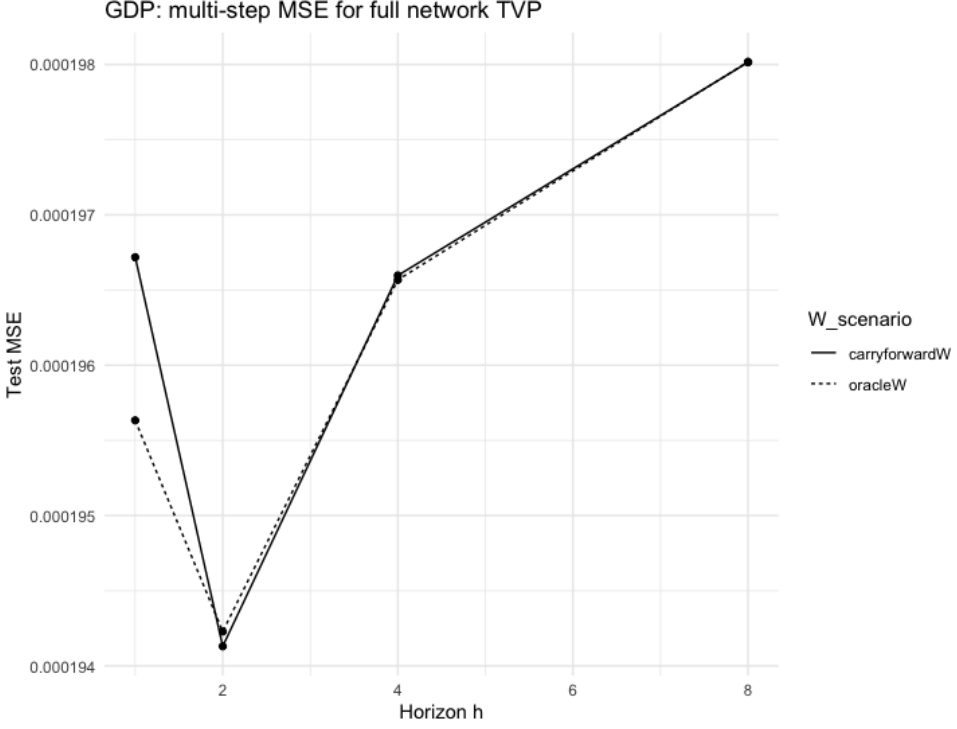


Figure 6: **GDP: multi-step test MSE under oracle vs carry-forward W_t .** Dashed: oracle network; solid: carry-forward network.

Chicago burglary: calibration and stress tests

To complement Table 5, we report (i) regionwise distributions of forecast improvements across horizons; (ii) randomized PIT histograms for one-step calibration; and (iii) a stress test that perturbs the adjacency matrix and measures how multi-step MAE responds as a function of $\sup_t \|\widehat{W}_t - W_t\|_{\text{op}}$.

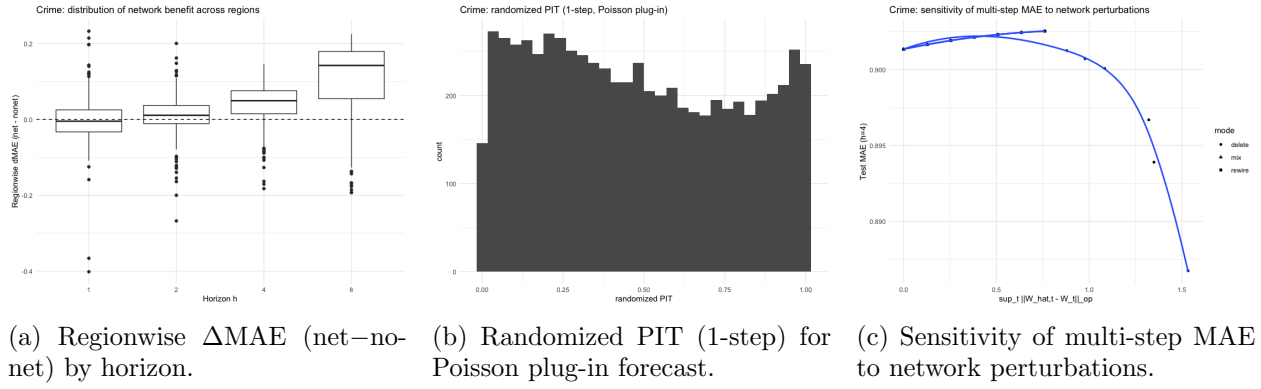


Figure 7: **Chicago burglary: additional diagnostics.**

B.1 Joint node–edge model: latent networks in a Poisson SSNR

Model. We fit a joint latent-network Poisson SSNR where the adjacency matrix W_t is not observed. Edges evolve via a time-varying logit/softmax random graph, and both node intensities and edge propensities follow random-walk state evolutions. This couples node and edge dynamics and propagates edge uncertainty into node forecasts.

Posterior summary and predictive gain. Table 16 summarizes posterior means and 95% credible intervals for time-averaged coefficients and innovation scales. The spillover coefficient $\bar{\beta}_1$ is positive, indicating substantial contagion in the latent network channel. Using a posterior-mean plug-in intensity, the latent-network model achieves a large improvement in (in-sample) one-step log score relative to a no-network dynamic Poisson baseline: the average log-score gain is 197.2.

Table 16: **Latent-network Poisson SSNR: posterior summary (time-averaged coefficients).**

Parameter	Mean	2.5%	97.5%
$\bar{\beta}_0$	−5.25	−9.48	−2.49
$\bar{\beta}_1$	1.25	0.78	1.97
$\bar{\beta}_2$	0.53	0.33	0.70
s_{β_0}	2.18	0.80	3.47
s_{β_1}	0.70	0.20	1.37
s_{β_2}	0.30	0.06	0.68
s_u	1.64	1.10	2.40

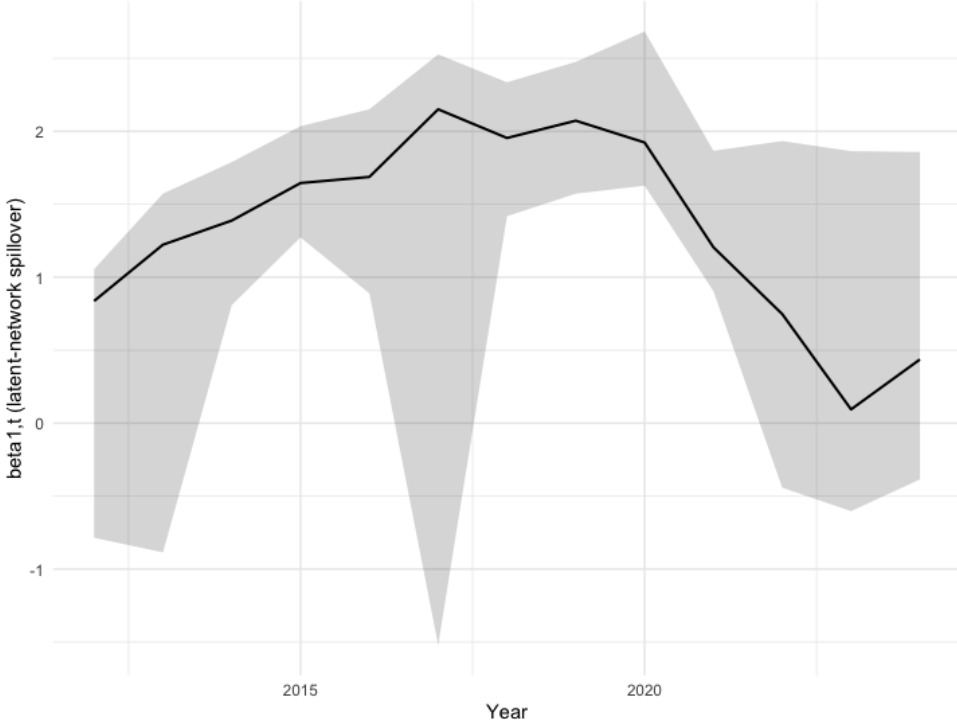


Figure 8: **Latent-network Poisson SSNR: inferred spillover over years.** Posterior mean and uncertainty band for the spillover coefficient $\beta_{1,t}$.

Computation. This experiment is intentionally difficult: the state dimension grows quickly when edges are latent. Even with non-centered parameterizations and conservative HMC settings, the fit exhibits typical high-dimensional pathologies (e.g. treedepth saturation in a fraction of transitions). We therefore treat this as a proof-of-concept demonstrating that SSNRs can carry edge uncertainty into node forecasts, rather than as a polished large-scale application.

Proofs

Proof of 2.3

Cross-sectional oracle filtering and forecast-risk gap. Because the model is linear–Gaussian with a random-walk state, the filtering distribution $\theta_t | \mathcal{F}_t$ is Gaussian with mean $m_t := \mathbb{E}(\theta_t | \mathcal{F}_t)$ and covariance $P_t := \text{Var}(\theta_t | \mathcal{F}_t)$.

(i) Cross-sectional oracle filtering. Let $P_{t|t-1} := \text{Var}(\theta_t | \mathcal{F}_{t-1})$ denote the one-step-ahead state covariance. Assume $P_{t|t-1} \succ 0$ (e.g. if $P_0 \succ 0$ and $Q_t \succeq 0$ for all t). Then the Kalman covariance update can be written in information form as

$$P_t^{-1} = P_{t|t-1}^{-1} + X_t^\top R_t^{-1} X_t.$$

Since $P_{t|t-1}^{-1} \succeq 0$, it follows that

$$P_t^{-1} \succeq X_t^\top R_t^{-1} X_t.$$

By (12), the matrix $X_t^\top R_t^{-1} X_t$ is positive definite and satisfies $X_t^\top R_t^{-1} X_t \succeq N\kappa I_K$. Inverting the Loewner order therefore yields

$$P_t \preceq (X_t^\top R_t^{-1} X_t)^{-1} \preceq (N\kappa)^{-1} I_K,$$

and hence $\text{tr}(P_t) \leq K/(N\kappa)$. Finally, by the law of total variance,

$$\mathbb{E}\|\theta_t - m_t\|^2 = \mathbb{E}\{\text{tr}(\text{Var}(\theta_t | \mathcal{F}_t))\} = \mathbb{E}\{\text{tr}(P_t)\} \leq \frac{K}{N\kappa}.$$

(ii) Forecast-risk gap. Define $\mu_{t+1|t}^* := \mathbb{E}(Y_{t+1} | \theta_t, \mathcal{F}_t) = X_{t+1}\theta_t$ and $\hat{\mu}_{t+1|t} := \mathbb{E}(Y_{t+1} | \mathcal{F}_t) = X_{t+1}m_t$. Then $\hat{\mu}_{t+1|t} - \mu_{t+1|t}^* = X_{t+1}(m_t - \theta_t)$. Conditioning on \mathcal{F}_t , the error $\theta_t - m_t$ is mean-zero with covariance P_t , so

$$\mathbb{E}\left(\|\hat{\mu}_{t+1|t} - \mu_{t+1|t}^*\|^2 \mid \mathcal{F}_t\right) = \text{tr}\left(X_{t+1}P_tX_{t+1}^\top\right).$$

Using $\text{tr}(APA^\top) \leq \|A\|_{\text{op}}^2 \text{tr}(P)$ for $P \succeq 0$, we obtain

$$\frac{1}{N}\mathbb{E}\|\hat{\mu}_{t+1|t} - \mu_{t+1|t}^*\|^2 \leq \frac{1}{N}\mathbb{E}\{\|X_{t+1}\|_{\text{op}}^2 \text{tr}(P_t)\} \leq \frac{1}{N}(C_X N) \cdot \frac{K}{N\kappa} = \frac{C_X K}{N\kappa},$$

where the second inequality uses (13) and the bound $\text{tr}(P_t) \leq K/(N\kappa)$ above.

For the MSFE decomposition, write $Y_{t+1} - \hat{\mu}_{t+1|t} = (Y_{t+1} - \mu_{t+1|t}^*) + (\mu_{t+1|t}^* - \hat{\mu}_{t+1|t})$. Then

$$\mathbb{E}\|Y_{t+1} - \hat{\mu}_{t+1|t}\|^2 = \mathbb{E}\|Y_{t+1} - \mu_{t+1|t}^*\|^2 + \mathbb{E}\|\mu_{t+1|t}^* - \hat{\mu}_{t+1|t}\|^2,$$

since the cross term vanishes by iterated expectation:

$$\mathbb{E}\left[(Y_{t+1} - \mu_{t+1|t}^*)^\top(\mu_{t+1|t}^* - \hat{\mu}_{t+1|t})\right] = \mathbb{E}\left[(\mu_{t+1|t}^* - \hat{\mu}_{t+1|t})^\top \mathbb{E}(Y_{t+1} - \mu_{t+1|t}^* | \theta_t, \mathcal{F}_t)\right] = 0.$$

The second term is $O(1/N)$ by the bound just proved, which completes the proof. \square

Proof of 2.4

Proof. Fix $t \geq 1$ and let $N \rightarrow \infty$ with t and K fixed. Conditional on \mathcal{F}_{t-1} , the linear–Gaussian state equation implies the one-step predictive law

$$\theta_t | \mathcal{F}_{t-1} \sim \mathcal{N}_K(m_{t|t-1}, P_{t|t-1}),$$

and the observation equation is

$$Y_t = X_t\theta_t + \varepsilon_t, \quad \varepsilon_t | \mathcal{F}_{t-1} \sim \mathcal{N}_N(0, R_t),$$

with X_t \mathcal{F}_{t-1} -measurable and ε_t conditionally independent of θ_t given \mathcal{F}_{t-1} . By Gaussian conditioning (equivalently, the Kalman update), $\theta_t | \mathcal{F}_t \sim \mathcal{N}_K(m_t, P_t)$ where

$$P_t^{-1} = P_{t|t-1}^{-1} + X_t^\top R_t^{-1} X_t, \tag{44}$$

$$m_t = P_t \left(P_{t|t-1}^{-1} m_{t|t-1} + X_t^\top R_t^{-1} Y_t \right). \tag{45}$$

Let

$$J := J_t^{(N)} = \frac{1}{N} X_t^\top R_t^{-1} X_t, \quad E := \frac{1}{N} P_{t|t-1}^{-1},$$

and define the high-probability event

$$\mathcal{E}_N := \left\{ \kappa I_K \preceq J \preceq \bar{\kappa} I_K \right\} \cap \left\{ \underline{p} I_K \preceq P_{t|t-1} \preceq \bar{p} I_K \right\},$$

so that $\mathbb{P}^*(\mathcal{E}_N) \rightarrow 1$.

(i) Covariance calibration. Dividing (44) by N yields

$$(NP_t)^{-1} = J + E, \quad \text{hence} \quad NP_t = (J + E)^{-1}.$$

On \mathcal{E}_N , $\|J^{-1}\|_{op} \leq \kappa^{-1}$ and $\|E\|_{op} \leq \|P_{t|t-1}^{-1}\|_{op}/N \leq (\underline{p})^{-1}/N$. Since $E \succeq 0$, also $(J + E) \succeq J$ and therefore $\|(J + E)^{-1}\|_{op} \leq \|J^{-1}\|_{op} \leq \kappa^{-1}$. Using the resolvent identity $(J + E)^{-1} - J^{-1} = -J^{-1}E(J + E)^{-1}$,

$$\|NP_t - J^{-1}\|_{op} \leq \|J^{-1}\|_{op} \|E\|_{op} \|(J + E)^{-1}\|_{op} \leq \frac{1}{\kappa^2 \underline{p}} \frac{1}{N} \rightarrow 0 \quad \text{on } \mathcal{E}_N.$$

Since $\mathbb{P}^*(\mathcal{E}_N) \rightarrow 1$, this proves (i) in \mathbb{P}^* -probability.

(ii) Asymptotic normality of the filtered mean. Write $\varepsilon_t := Y_t - X_t \theta_t$. Substituting $Y_t = X_t \theta_t + \varepsilon_t$ into (45) and using

$$P_t X_t^\top R_t^{-1} X_t = I_K - P_t P_{t|t-1}^{-1} \quad \text{(obtained by left-multiplying (44) by } P_t \text{)}$$

gives the exact decomposition

$$m_t - \theta_t = P_t P_{t|t-1}^{-1} (m_{t|t-1} - \theta_t) + P_t X_t^\top R_t^{-1} \varepsilon_t. \quad (46)$$

We first show the bias term is negligible at \sqrt{N} scale. On \mathcal{E}_N , $X_t^\top R_t^{-1} X_t = NJ \succeq N\kappa I_K$, and since $P_t^{-1} \succeq X_t^\top R_t^{-1} X_t$ from (44), it follows that $\|P_t\|_{op} \leq (N\kappa)^{-1}$. Also on \mathcal{E}_N , $\|P_{t|t-1}^{-1}\|_{op} \leq (\underline{p})^{-1}$, and under the correctly specified Gaussian state model, $m_{t|t-1} - \theta_t$ is mean-zero with conditional covariance $P_{t|t-1}$, hence $\|m_{t|t-1} - \theta_t\| = O_{\mathbb{P}}(1)$ on \mathcal{E}_N . Therefore,

$$\sqrt{N} \|P_t P_{t|t-1}^{-1} (m_{t|t-1} - \theta_t)\| \leq \frac{1}{\sqrt{N} \kappa} \|P_{t|t-1}^{-1}\|_{op} \|m_{t|t-1} - \theta_t\| = o_{\mathbb{P}}(1).$$

For the noise term, conditional on \mathcal{F}_{t-1} we have $\varepsilon_t \sim \mathcal{N}_N(0, R_t)$, hence $\sqrt{N} P_t X_t^\top R_t^{-1} \varepsilon_t$ is Gaussian with mean 0 and covariance

$$\Sigma_N := N P_t X_t^\top R_t^{-1} X_t P_t = (NP_t) J (NP_t).$$

By part (i), $NP_t - J^{-1} \rightarrow 0$ in probability, and on \mathcal{E}_N we have uniform bounds on $\|J\|_{op}, \|J^{-1}\|_{op}, \|NP_t\|_{op}$. Thus

$$\|\Sigma_N - J^{-1}\|_{op} \leq \|NP_t - J^{-1}\|_{op} \|J\|_{op} \|NP_t\|_{op} + \|J^{-1}\|_{op} \|J\|_{op} \|NP_t - J^{-1}\|_{op} \rightarrow 0$$

in probability. If additionally $J_t^{(N)} \rightarrow J_t \succ 0$ in probability, then $J^{-1} \rightarrow J_t^{-1}$ and hence $\Sigma_N \rightarrow J_t^{-1}$ in probability.

Now, conditional on \mathcal{F}_{t-1} the vector $\sqrt{N}(m_t - \theta_t)$ is Gaussian with mean $\mu_N := \sqrt{N} P_t P_{t|t-1}^{-1} (m_{t|t-1} - \theta_t) = o_{\mathbb{P}}(1)$ and covariance Σ_N . For any fixed $u \in \mathbb{R}^K$,

$$\mathbb{E}^* \left[e^{iu^\top \sqrt{N}(m_t - \theta_t)} \right] = \mathbb{E}^* \left[\exp \left(iu^\top \mu_N - \frac{1}{2} u^\top \Sigma_N u \right) \right].$$

Since $(\mu_N, \Sigma_N) \rightarrow (0, J_t^{-1})$ in probability and the function $(\mu, \Sigma) \mapsto \exp(iu^\top \mu - \frac{1}{2} u^\top \Sigma u)$ is bounded and continuous, the bounded-continuity theorem yields convergence of characteristic functions to $\exp(-\frac{1}{2} u^\top J_t^{-1} u)$. Hence

$$\sqrt{N}(m_t - \theta_t) \Rightarrow \mathcal{N}_K(0, J_t^{-1}),$$

proving (ii).

(iii) Conditional frequentist coverage. Fix $j \in \{1, \dots, K\}$ and define the pivot

$$T_{N,j} := \frac{m_{j,t} - \theta_{j,t}}{\sqrt{(P_t)_{jj}}}.$$

Conditional on $(\theta_t, \mathcal{F}_{t-1})$, $T_{N,j}$ is univariate Gaussian since m_t is affine in Y_t and hence in ε_t . Using (46), its conditional mean equals

$$a_{N,j} := \frac{[\sqrt{N} P_t P_{t|t-1}^{-1} (m_{t|t-1} - \theta_t)]_j}{\sqrt{N(P_t)_{jj}}},$$

and its conditional variance is

$$v_{N,j} := \frac{N(P_t X_t^\top R_t^{-1} X_t P_t)_{jj}}{N(P_t)_{jj}} = \frac{(\Sigma_N)_{jj}}{(N P_t)_{jj}}.$$

From the negligibility bound above, $a_{N,j} = o_{\mathbb{P}}(1)$. By (i) and the convergence $\Sigma_N \rightarrow J^{-1}$ shown in (ii), we have $v_{N,j} \rightarrow 1$ in probability, and on \mathcal{E}_N the denominator $(N P_t)_{jj}$ is bounded away from 0. Therefore,

$$\mathbb{P}^* \left(\theta_{j,t} \in [m_{j,t} \pm z_{1-\alpha/2} \sqrt{(P_t)_{jj}}] \mid \theta_t, \mathcal{F}_{t-1} \right) = \mathbb{P}^* (|T_{N,j}| \leq z_{1-\alpha/2} \mid \theta_t, \mathcal{F}_{t-1}) \rightarrow 1 - \alpha,$$

since $T_{N,j} \mid (\theta_t, \mathcal{F}_{t-1}) \sim \mathcal{N}(a_{N,j}, v_{N,j})$ and the Gaussian cdf is continuous. This proves (iii). \square

Proof of 3.1

Proof of Theorem 3.1. Throughout, $\|\cdot\|$ denotes the Euclidean norm on vectors and the operator norm on matrices.

1. Well-posedness (explicit recursive construction). Work on a filtered probability space $(\Omega, \mathcal{F}, (\mathcal{F}_t)_{t \geq 0}, \mathbb{P})$ carrying:

- initial values (θ_0, η_0, Y_0) satisfying (A4);
- i.i.d. standard Gaussian sequences $(\xi_t)_{t \geq 1}$, $(\zeta_t)_{t \geq 1}$, $(\nu_t)_{t \geq 1}$ with

$$\xi_t \sim \mathcal{N}_K(0, I_K), \quad \zeta_t \sim \mathcal{N}_p(0, I_p), \quad \nu_t \sim \mathcal{N}_N(0, I_N);$$

- i.i.d. uniforms $(U_{ij,t})_{i \neq j, t \geq 1}$, independent of (ξ_t, ζ_t, ν_t) and of (θ_0, η_0, Y_0) .

Let (\mathcal{F}_t) be the filtration generated by the initial values and the innovations up to time t , together with the predictable sequences appearing in the model (in particular $Z_t, R_t, Q_t(s_t), S_t, x_{ij,t}$, which are \mathcal{F}_{t-1} -measurable by (A2)–(A3) and the theorem assumptions).

For $t \geq 1$, define

$$u_t := Q_t(s_t)^{1/2} \xi_t, \quad \omega_t := S_t^{1/2} \zeta_t, \quad \varepsilon_t := R_t^{1/2} \nu_t,$$

where $M^{1/2}$ denotes the (symmetric) positive semidefinite square root. Then $u_t \mid \mathcal{F}_{t-1} \sim \mathcal{N}_K(0, Q_t(s_t))$, $\omega_t \mid \mathcal{F}_{t-1} \sim \mathcal{N}_p(0, S_t)$, and $\varepsilon_t \mid \mathcal{F}_{t-1} \sim \mathcal{N}_N(0, R_t)$.

Given (θ_0, η_0, Y_0) , define recursively for $t \geq 1$:

$$\theta_t := \theta_{t-1} + u_t, \quad \eta_t := \eta_{t-1} + \omega_t.$$

Next define $A_t = (a_{ij,t})$ by

$$a_{ij,t} := \mathbf{1}\{U_{ij,t} \leq \text{logit}^{-1}(x'_{ij,t} \eta_t)\}, \quad i \neq j,$$

so that $a_{ij,t} \mid \eta_t \sim \text{Bernoulli}(p_{ij,t})$ with $\text{logit}(p_{ij,t}) = x'_{ij,t} \eta_t$. Define W_t from A_t via (A1) and then set

$$X_t := [1_N, W_t Y_{t-1}, Y_{t-1}, Z_t], \quad Y_t := X_t \theta_t + \varepsilon_t.$$

Each object at time t is \mathcal{F}_t -measurable and depends only on previously defined variables and time- t innovations. Hence $\{(\theta_t, \eta_t, Y_t, A_t) : t \geq 0\}$ exists and is uniquely defined pathwise by the recursion, i.e. the model is well-posed.

2. Finite second moments for the random-walk states. Since $\mathbb{E}(u_t \mid \mathcal{F}_{t-1}) = 0$,

$$\mathbb{E}(\theta'_{t-1} u_t) = \mathbb{E}[\mathbb{E}(\theta'_{t-1} u_t \mid \mathcal{F}_{t-1})] = \mathbb{E}[\theta'_{t-1} \mathbb{E}(u_t \mid \mathcal{F}_{t-1})] = 0.$$

Therefore,

$$\mathbb{E}\|\theta_t\|^2 = \mathbb{E}\|\theta_{t-1} + u_t\|^2 = \mathbb{E}\|\theta_{t-1}\|^2 + \mathbb{E}\|u_t\|^2.$$

Moreover, by conditional Gaussianity, $\mathbb{E}(\|u_t\|^2 \mid \mathcal{F}_{t-1}) = \text{tr}(Q_t(s_t))$, and hence

$$\mathbb{E}\|u_t\|^2 = \mathbb{E} \text{tr}(Q_t(s_t)) \leq K \mathbb{E}\|Q_t(s_t)\| \leq K C_Q,$$

using $\text{tr}(M) \leq K\|M\|$ for $K \times K$ positive semidefinite M and (A3). Iterating yields

$$\mathbb{E}\|\theta_t\|^2 \leq \mathbb{E}\|\theta_0\|^2 + t K C_Q < \infty,$$

since $\mathbb{E}\|\theta_0\|^2 < \infty$ by (A4).

Similarly, $\mathbb{E}(\omega_t \mid \mathcal{F}_{t-1}) = 0$ and $\mathbb{E}(\|\omega_t\|^2 \mid \mathcal{F}_{t-1}) = \text{tr}(S_t) \leq p\|S_t\| \leq pC_S$, so

$$\mathbb{E}\|\eta_t\|^2 = \mathbb{E}\|\eta_{t-1}\|^2 + \mathbb{E}\|\omega_t\|^2 \leq \mathbb{E}\|\eta_0\|^2 + tpC_S < \infty.$$

3. Auxiliary high-moment bound on (θ_t) (finite horizon). Fix an integer $m \geq 1$ and a time horizon $t \geq 1$. For each $s \leq t$, conditional on \mathcal{F}_{s-1} , $u_s = Q_s(s_s)^{1/2}\xi_s$ with $\xi_s \sim \mathcal{N}_K(0, I_K)$. Using $\|Q^{1/2}\xi\| \leq \|Q^{1/2}\| \|\xi\| = \|Q\|^{1/2}\|\xi\|$, we obtain

$$\|u_s\|^{2m} \leq \|Q_s(s_s)\|^m \|\xi_s\|^{2m}.$$

Taking conditional expectations yields

$$\mathbb{E}(\|u_s\|^{2m} \mid \mathcal{F}_{s-1}) \leq \|Q_s(s_s)\|^m \mathbb{E}\|\xi_s\|^{2m} =: C_{m,K} \|Q_s(s_s)\|^m,$$

where $C_{m,K} := \mathbb{E}\|\xi_s\|^{2m} < \infty$. By (A3),

$$\mathbb{E}\|u_s\|^{2m} \leq C_{m,K} C_Q^m < \infty.$$

Minkowski's inequality for L^{2m} gives

$$\|\theta_s\|_{L^{2m}} = \left(\mathbb{E}\|\theta_s\|^{2m} \right)^{1/(2m)} \leq \|\theta_0\|_{L^{2m}} + \sum_{r=1}^s \|u_r\|_{L^{2m}} < \infty,$$

using (A4) and the bound above. Hence, for every fixed t , all moments $\mathbb{E}\|\theta_s\|^{2m}$ needed below (with $s \leq t$ and m finite) are finite.

4. Finite second moments for (Y_t) . Write the NTVP–VAR recursion equivalently as

$$Y_t = B_t Y_{t-1} + c_t + \varepsilon_t, \quad B_t := \beta_{1,t} W_t + \beta_{2,t} I_N, \quad c_t := \beta_{0,t} 1_N + Z_t \gamma_t,$$

where $\theta_t = (\beta_{0,t}, \beta_{1,t}, \beta_{2,t}, \gamma_t')'$. For $1 \leq s \leq t$ define the random matrix products

$$\Phi_{t:s} := B_t B_{t-1} \cdots B_s, \quad \Phi_{t:t+1} := I_N.$$

Iterating yields the pathwise identity

$$Y_t = \Phi_{t:1} Y_0 + \sum_{s=1}^t \Phi_{t:s+1} (c_s + \varepsilon_s). \tag{47}$$

Using $\|\sum_{j=0}^t v_j\|^2 \leq (t+1) \sum_{j=0}^t \|v_j\|^2$, we obtain

$$\|Y_t\|^2 \leq (t+1) \left(\|\Phi_{t:1}\|^2 \|Y_0\|^2 + \sum_{s=1}^t \|\Phi_{t:s+1}\|^2 \|c_s + \varepsilon_s\|^2 \right). \tag{48}$$

We now show that each expectation on the right-hand side is finite. First, by (A1) and $|\beta_{j,r}| \leq \|\theta_r\|$,

$$\|B_r\| \leq |\beta_{1,r}| \|W_r\| + |\beta_{2,r}| \leq (C_W + 1) \|\theta_r\|.$$

Also, by (A2) and $|\beta_{0,r}| \leq \|\theta_r\|$, $\|\gamma_r\| \leq \|\theta_r\|$,

$$\|c_r\| \leq \|\beta_{0,r} 1_N\| + \|Z_r\| \|\gamma_r\| \leq (\sqrt{N} + C_Z) \|\theta_r\|.$$

Moreover, for $\varepsilon_r \mid \mathcal{F}_{r-1} \sim \mathcal{N}_N(0, R_r)$,

$$\mathbb{E}(\|\varepsilon_r\|^4 \mid \mathcal{F}_{r-1}) = \mathbb{E}((\varepsilon'_r \varepsilon_r)^2 \mid \mathcal{F}_{r-1}) = (\text{tr } R_r)^2 + 2 \text{tr}(R_r^2) \leq N(N+2) C_R^2,$$

since $\text{tr}(R_r) \leq N\|R_r\| \leq NC_R$ and $\text{tr}(R_r^2) \leq N\|R_r\|^2 \leq NC_R^2$. Hence $\sup_r \mathbb{E}\|\varepsilon_r\|^4 < \infty$.

Fix $t \geq 1$ and $1 \leq s \leq t$. By submultiplicativity,

$$\|\Phi_{t:s+1}\| \leq \prod_{r=s+1}^t \|B_r\|, \quad \text{hence} \quad \|\Phi_{t:s+1}\|^4 \leq \prod_{r=s+1}^t \|B_r\|^4.$$

Let $m := t - s$ (the number of factors). If $m = 0$ then $\Phi_{t:t+1} = I_N$ and $\|\Phi_{t:t+1}\|^4 = 1$. If $m \geq 1$, Hölder's inequality yields

$$\mathbb{E}\|\Phi_{t:s+1}\|^4 \leq \mathbb{E}\left[\prod_{r=s+1}^t \|B_r\|^4\right] \leq \prod_{r=s+1}^t \left(\mathbb{E}\|B_r\|^{4m}\right)^{1/m}.$$

Using $\|B_r\|^{4m} \leq (C_W + 1)^{4m} \|\theta_r\|^{4m}$ and Step 3 (applied with moment order $4m$), we have $\mathbb{E}\|B_r\|^{4m} < \infty$ for all $r \leq t$, hence $\mathbb{E}\|\Phi_{t:s+1}\|^4 < \infty$. The same argument with $s = 0$ shows $\mathbb{E}\|\Phi_{t:1}\|^4 < \infty$.

Next, using $\|a + b\|^4 \leq 8(\|a\|^4 + \|b\|^4)$,

$$\mathbb{E}\|c_s + \varepsilon_s\|^4 \leq 8\mathbb{E}\|c_s\|^4 + 8\mathbb{E}\|\varepsilon_s\|^4 < \infty,$$

since $\|c_s\|^4 \leq (\sqrt{N} + C_Z)^4 \|\theta_s\|^4$ and $\mathbb{E}\|\theta_s\|^4 < \infty$ by Step 3.

Finally, Cauchy–Schwarz gives, for each s ,

$$\mathbb{E}[\|\Phi_{t:s+1}\|^2 \|c_s + \varepsilon_s\|^2] \leq (\mathbb{E}\|\Phi_{t:s+1}\|^4)^{1/2} (\mathbb{E}\|c_s + \varepsilon_s\|^4)^{1/2} < \infty,$$

and similarly,

$$\mathbb{E}[\|\Phi_{t:1}\|^2 \|Y_0\|^2] \leq (\mathbb{E}\|\Phi_{t:1}\|^4)^{1/2} (\mathbb{E}\|Y_0\|^4)^{1/2} < \infty$$

by (A4). Since (48) has finitely many summands for fixed t , we conclude $\mathbb{E}\|Y_t\|^2 < \infty$.

We have shown well–posedness and $\mathbb{E}\|\theta_t\|^2 < \infty$, $\mathbb{E}\|\eta_t\|^2 < \infty$. The bound above gives $\mathbb{E}\|Y_t\|^2 < \infty$. This proves the theorem. \square

Remark B.1 (On the moment assumption in (A4)). *The proof controls products of random coefficient matrices along a finite horizon via Hölder and Cauchy–Schwarz. For a fixed horizon t , it suffices that (θ_0, Y_0) have sufficiently high finite moments (e.g. up to order $4t$ in the argument above). Assumption (A4) enforces these requirements uniformly over all horizons and is automatic under a Gaussian initialisation commonly used in linear–Gaussian state–space models.*

Proof of Theorem 3.2

Proof of Theorem 3.2. Fix $t \geq 1$. Pre-multiplying the NTVP–VAR(1) observation equation (10) by π' yields

$$\pi' Y_t = \beta_{0,t} \pi' \mathbf{1}_N + \beta_{1,t} \pi' W Y_{t-1} + \beta_{2,t} \pi' Y_{t-1} + (\pi' Z_t) \gamma_t + \pi' \varepsilon_t.$$

By the defining properties of the invariant probability vector π ,

$$\pi' \mathbf{1}_N = 1 \quad \text{and} \quad \pi' W = \pi',$$

hence

$$\pi' W Y_{t-1} = (\pi' W) Y_{t-1} = \pi' Y_{t-1}.$$

With the definitions $\bar{Y}_t^{(\pi)} := \pi' Y_t$ and $\bar{\varepsilon}_t^{(\pi)} := \pi' \varepsilon_t$, the preceding display becomes

$$\bar{Y}_t^{(\pi)} = \beta_{0,t} + (\beta_{1,t} + \beta_{2,t}) \bar{Y}_{t-1}^{(\pi)} + (\pi' Z_t) \gamma_t + \bar{\varepsilon}_t^{(\pi)},$$

which proves the claimed scalar recursion for every $t \geq 1$.

If, in addition, the covariates are π -centred so that $\pi' Z_t = 0$ for all t , then the covariate term vanishes and

$$\bar{Y}_t^{(\pi)} = \beta_{0,t} + (\beta_{1,t} + \beta_{2,t}) \bar{Y}_{t-1}^{(\pi)} + \bar{\varepsilon}_t^{(\pi)}.$$

Moreover, conditional on R_t , we have $\varepsilon_t | R_t \sim \mathcal{N}_N(0, R_t)$ by (10). Since $\bar{\varepsilon}_t^{(\pi)} = \pi' \varepsilon_t$ is a linear functional of a Gaussian vector, it is (conditionally) univariate Gaussian with mean and variance

$$\mathbb{E}[\bar{\varepsilon}_t^{(\pi)} | R_t] = \pi' \mathbb{E}(\varepsilon_t | R_t) = 0, \quad \text{Var}(\bar{\varepsilon}_t^{(\pi)} | R_t) = \pi' \text{Var}(\varepsilon_t | R_t) \pi = \pi' R_t \pi,$$

so $\bar{\varepsilon}_t^{(\pi)} | R_t \sim \mathcal{N}(0, \pi' R_t \pi)$.

Finally, suppose W is also column-stochastic, i.e. $\mathbf{1}'_N W = \mathbf{1}'_N$. Let $\pi_u := N^{-1} \mathbf{1}_N$. Then

$$\pi'_u \mathbf{1}_N = 1, \quad \pi'_u W = N^{-1} \mathbf{1}'_N W = N^{-1} \mathbf{1}'_N = \pi'_u,$$

so π_u is an invariant probability vector. Taking $\pi = \pi_u$ in the already-proved recursion and imposing the uniform centring condition $N^{-1} \mathbf{1}'_N Z_t = 0$ yields the same scalar TVP–AR(1) conclusion for the uniform mean $\bar{Y}_t := N^{-1} \mathbf{1}'_N Y_t$. \square

Proof of 3.3

Proof. We first show the equivalence between (19) and (20). From the definition of the community-averaging operator,

$$\Pi_{ci} = \frac{1}{|K_c|} \mathbf{1}\{i \in K_c\}.$$

Hence for any $c \leq C$ and any $j \leq N$,

$$(\Pi W_t)_{cj} = \sum_{i=1}^N \Pi_{ci} w_{ij,t} = \frac{1}{|K_c|} \sum_{i \in K_c} w_{ij,t}.$$

On the other hand,

$$(\Omega_t \Pi)_{cj} = \sum_{c''=1}^C \omega_{cc'',t} \Pi_{c''j}.$$

If $j \in K_{c'}$, then $\Pi_{c''j} = |K_{c''}|^{-1} \mathbf{1}\{j \in K_{c''}\}$ and the partition property implies $\Pi_{c''j} = 0$ for $c'' \neq c'$ and $\Pi_{c'j} = |K_{c'}|^{-1}$. Therefore,

$$(\Omega_t \Pi)_{cj} = \omega_{cc',t} \frac{1}{|K_{c'}|}.$$

Consequently, $(\Pi W_t)_{cj} = (\Omega_t \Pi)_{cj}$ for all c and all $j \in K_{c'}$ is exactly the balance condition (20), and since every j belongs to a unique community, this proves the equivalence of (19) and (20).

We now derive the reduced recursion. Left-multiply the NTVP–VAR(1) observation equation by Π . By linearity,

$$\Pi Y_t = \beta_{0,t} \Pi \mathbf{1}_N + \beta_{1,t} \Pi W_t Y_{t-1} + \beta_{2,t} \Pi Y_{t-1} + \Pi Z_t \gamma_t + \Pi \varepsilon_t.$$

By definition of Π , $\Pi \mathbf{1}_N = \mathbf{1}_C$. Introduce the aggregated quantities

$$\bar{Y}_t := \Pi Y_t, \quad \bar{Y}_{t-1} := \Pi Y_{t-1}, \quad \bar{Z}_t := \Pi Z_t, \quad \bar{\varepsilon}_t := \Pi \varepsilon_t.$$

Then

$$\bar{Y}_t = \beta_{0,t} \mathbf{1}_C + \beta_{1,t} (\Pi W_t) Y_{t-1} + \beta_{2,t} \bar{Y}_{t-1} + \bar{Z}_t \gamma_t + \bar{\varepsilon}_t.$$

Under the exact aggregation relation (19),

$$(\Pi W_t) Y_{t-1} = (\Omega_t \Pi) Y_{t-1} = \Omega_t (\Pi Y_{t-1}) = \Omega_t \bar{Y}_{t-1},$$

so the recursion closes as

$$\bar{Y}_t = \beta_{0,t} \mathbf{1}_C + \beta_{1,t} \Omega_t \bar{Y}_{t-1} + \beta_{2,t} \bar{Y}_{t-1} + \bar{Z}_t \gamma_t + \bar{\varepsilon}_t.$$

The coefficient state evolution is unchanged because only the observation equation is transformed by the deterministic linear map Π .

For the innovation distribution, if $\varepsilon_t \mid R_t \sim \mathcal{N}_N(0, R_t)$ then $\bar{\varepsilon}_t = \Pi \varepsilon_t \mid R_t$ is Gaussian with mean 0 and covariance

$$\text{Var}(\bar{\varepsilon}_t \mid R_t) = \Pi \text{Var}(\varepsilon_t \mid R_t) \Pi^\top = \Pi R_t \Pi^\top,$$

hence $\bar{\varepsilon}_t \mid R_t \sim \mathcal{N}_C(0, \Pi R_t \Pi^\top)$.

Finally, suppose $\|\Pi W_t - \Omega_t \Pi\|_{\text{op}} \leq \delta_t$ and define $\Delta_t := \Pi W_t - \Omega_t \Pi$. (Here $\|\cdot\|_{\text{op}}$ denotes the induced Euclidean operator norm.) Then for any $y \in \mathbb{R}^N$,

$$\|\Pi W_t y - \Omega_t \Pi y\|_2 = \|\Delta_t y\|_2 \leq \|\Delta_t\|_{\text{op}} \|y\|_2 \leq \delta_t \|y\|_2.$$

Moreover, adding and subtracting $\beta_{1,t} \Omega_t \Pi Y_{t-1}$ yields the exact decomposition

$$\bar{Y}_t = \beta_{0,t} \mathbf{1}_C + \beta_{1,t} \Omega_t \bar{Y}_{t-1} + \beta_{2,t} \bar{Y}_{t-1} + \bar{Z}_t \gamma_t + \bar{\varepsilon}_t + r_t, \quad r_t := \beta_{1,t} \Delta_t Y_{t-1}.$$

Applying the previous bound with $y = Y_{t-1}$ gives

$$\|r_t\|_2 \leq |\beta_{1,t}| \delta_t \|Y_{t-1}\|_2,$$

as claimed. \square

Proof of 3.4

Hop-by-hop spillover attribution and counterfactual impulse responses. Throughout, write $I := I_N$ and adopt the conventions $W^0 := I$ and that any empty matrix product equals I .

(a) Exact hop decomposition. For each $k \geq 1$,

$$B_{t+k} = \beta_{1,t+k}W + \beta_{2,t+k}I$$

belongs to the commutative algebra generated by $\{I, W\}$; hence $B_{t+k}B_{t+\ell} = B_{t+\ell}B_{t+k}$ for all k, ℓ . Therefore we may expand

$$\Phi_{t,h} = B_{t+h} \cdots B_{t+1} = \prod_{k=1}^h (\beta_{1,t+k}W + \beta_{2,t+k}I)$$

by selecting, for each $k \in \{1, \dots, h\}$, either the W -term or the I -term. For any subset $S \subseteq \{1, \dots, h\}$, picking the W -term exactly for indices in S yields the scalar coefficient

$$\left(\prod_{k \in S} \beta_{1,t+k} \right) \left(\prod_{k \notin S} \beta_{2,t+k} \right)$$

multiplying a product with exactly $|S|$ factors of W and the remaining factors equal to I . Since $IW = WI = W$, this product equals $W^{|S|}$, so

$$\Phi_{t,h} = \sum_{S \subseteq \{1, \dots, h\}} \left(\prod_{k \in S} \beta_{1,t+k} \right) \left(\prod_{k \notin S} \beta_{2,t+k} \right) W^{|S|}.$$

Grouping terms by $r := |S|$ gives

$$\Phi_{t,h} = \sum_{r=0}^h c_{t,h,r} W^r, \quad c_{t,h,r} = \sum_{\substack{S \subseteq \{1, \dots, h\} \\ |S|=r}} \left(\prod_{k \in S} \beta_{1,t+k} \right) \left(\prod_{k \notin S} \beta_{2,t+k} \right).$$

Finally, for a unit shock at node j (i.e. adding e_j to Y_t), the horizon- h effect equals $\Phi_{t,h}e_j$, hence

$$(\Phi_{t,h}e_j)_i = \sum_{r=0}^h c_{t,h,r} (W^r)_{ij},$$

which provides the hop-by-hop attribution.

(b) Macro impulse responses. If $\pi^\top W = \pi^\top$, then for each $k = 1, \dots, h$,

$$\pi^\top B_{t+k} = \beta_{1,t+k}\pi^\top W + \beta_{2,t+k}\pi^\top = (\beta_{1,t+k} + \beta_{2,t+k})\pi^\top.$$

Iterating over $k = 1, \dots, h$ yields

$$\pi^\top \Phi_{t,h} = \left\{ \prod_{k=1}^h (\beta_{1,t+k} + \beta_{2,t+k}) \right\} \pi^\top.$$

Multiplying by e_j gives $\pi^\top \Phi_{t,h}e_j = \pi_j \prod_{k=1}^h (\beta_{1,t+k} + \beta_{2,t+k})$.

(c) Counterfactual edge interventions. Let $A_k := B_{t+k}$ and $\tilde{A}_k := B_{t+k}^{\text{cf}}$. The standard telescoping identity for products gives

$$\Phi_{t,h} - \Phi_{t,h}^{\text{cf}} = \sum_{k=1}^h \left(A_h \cdots A_{k+1} (A_k - \tilde{A}_k) \tilde{A}_{k-1} \cdots \tilde{A}_1 \right),$$

with empty products interpreted as I . Here

$$A_k - \tilde{A}_k = \beta_{1,t+k} (W - W^{\text{cf}}).$$

By submultiplicativity,

$$\|\Phi_{t,h} - \Phi_{t,h}^{\text{cf}}\|_{\text{op}} \leq \sum_{k=1}^h \|A_h \cdots A_{k+1}\|_{\text{op}} |\beta_{1,t+k}| \|W - W^{\text{cf}}\|_{\text{op}} \|\tilde{A}_{k-1} \cdots \tilde{A}_1\|_{\text{op}}.$$

Moreover,

$$\|B_{t+k}\|_{\text{op}} \leq |\beta_{1,t+k}| \|W\|_{\text{op}} + |\beta_{2,t+k}| \leq |\beta_{1,t+k}| C_W + |\beta_{2,t+k}| \leq M_{t,h},$$

and similarly $\|B_{t+k}^{\text{cf}}\|_{\text{op}} \leq M_{t,h}$. Each summand contains exactly $h-1$ such factors, hence is bounded by $M_{t,h}^{h-1} |\beta_{1,t+k}| \|W - W^{\text{cf}}\|_{\text{op}}$. Summing over k yields

$$\|\Phi_{t,h} - \Phi_{t,h}^{\text{cf}}\|_{\text{op}} \leq M_{t,h}^{h-1} \left(\sum_{k=1}^h |\beta_{1,t+k}| \right) \|W - W^{\text{cf}}\|_{\text{op}}.$$

(d) Propagation of coefficient/network uncertainty. Apply the same telescoping identity with $\tilde{A}_k := \hat{B}_{t+k}$ to obtain

$$\hat{\Phi}_{t,h} - \Phi_{t,h} = \sum_{k=1}^h B_{t+h} \cdots B_{t+k+1} (\hat{B}_{t+k} - B_{t+k}) \hat{B}_{t+k-1} \cdots \hat{B}_{t+1}.$$

Using $\|B_{t+\ell}\|_{\text{op}} \leq M_{t,h}$ and $\|\hat{B}_{t+\ell}\|_{\text{op}} \leq \hat{M}_{t,h}$, each product of $h-1$ factors is bounded by $\max(M_{t,h}, \hat{M}_{t,h})^{h-1}$. Furthermore,

$$\hat{B}_{t+k} - B_{t+k} = (\hat{\beta}_{1,t+k} - \beta_{1,t+k}) W + (\hat{\beta}_{2,t+k} - \beta_{2,t+k}) I + \hat{\beta}_{1,t+k} (\hat{W} - W),$$

so

$$\|\hat{B}_{t+k} - B_{t+k}\|_{\text{op}} \leq C_W |\hat{\beta}_{1,t+k} - \beta_{1,t+k}| + |\hat{\beta}_{2,t+k} - \beta_{2,t+k}| + |\hat{\beta}_{1,t+k}| \|\hat{W} - W\|_{\text{op}}.$$

Summing over $k = 1, \dots, h$ yields the stated bound. \square

Proof of Theorem 3.5

Proof of Theorem 3.5. We prove that the joint model is linear–Gaussian in the dynamic linear model sense and that Kalman filtering/smoothing is exact. Let

$$\mathcal{F}_t := \sigma(a_{1:t}, Y_{1:t}, Z_{1:t}), \quad \mathcal{F}_t^{(e)} := \sigma(a_{1:t}, Y_{1:t-1}, Z_{1:t}),$$

so that $\mathcal{F}_t^{(e)} \subset \mathcal{F}_t$ and, by assumption, H_t is $\mathcal{F}_t^{(e)}$ -measurable.

(1) Joint state equation. From (21) and (22),

$$\theta_t = \theta_{t-1} + u_t, \quad \psi_t = \psi_{t-1} + w_t.$$

Stacking gives

$$\Xi_t = \begin{pmatrix} \theta_t \\ \psi_t \end{pmatrix} = \begin{pmatrix} \theta_{t-1} \\ \psi_{t-1} \end{pmatrix} + \begin{pmatrix} u_t \\ w_t \end{pmatrix} = \Xi_{t-1} + \omega_t,$$

where $\omega_t = (u_t^\top, w_t^\top)^\top$. By the mutual independence and Gaussianity of u_t and w_t , $\omega_t \sim \mathcal{N}(0, Q_t)$ with $Q_t = \text{blockdiag}(Q_t^{(n)}, Q_t^{(e)})$, and ω_t is independent of \mathcal{F}_{t-1} .

(2) Two linear–Gaussian observation blocks at time t . The edge observation equation (23) can be written in joint-state form as

$$a_t = L\psi_t + \zeta_t = H_t^{(e)}\Xi_t + \zeta_t, \quad H_t^{(e)} = \begin{pmatrix} 0_{M \times K_n} & L \end{pmatrix},$$

with $\zeta_t \sim \mathcal{N}(0, U_t)$ independent of $(\Xi_0, \{\omega_s\}_{s \geq 1})$ and independent across time.

Similarly, the node observation equation (24) can be written as

$$Y_t = H_t\theta_t + \varepsilon_t = H_t^{(n)}\Xi_t + \varepsilon_t, \quad H_t^{(n)} = \begin{pmatrix} H_t & 0_{N \times K_e} \end{pmatrix},$$

with $\varepsilon_t \sim \mathcal{N}(0, R_t)$ independent of $(\Xi_0, \{\omega_s\}_{s \geq 1}, \{\zeta_s\}_{s \geq 1})$ and independent across time. Because H_t is $\mathcal{F}_t^{(e)}$ -measurable, the matrix $H_t^{(n)}$ is known when conditioning on $\mathcal{F}_t^{(e)}$.

(3) Exact filtering by iterated Gaussian conditioning. We show by induction that $\Xi_t \mid \mathcal{F}_t$ is Gaussian with moments given by Kalman recursions (processing a_t then Y_t at each t). The base case is $\Xi_0 \sim \mathcal{N}(m_0, P_0)$.

Assume for some $t \geq 1$ that

$$\Xi_{t-1} \mid \mathcal{F}_{t-1} \sim \mathcal{N}(m_{t-1}, P_{t-1}).$$

Prediction. From $\Xi_t = \Xi_{t-1} + \omega_t$ with $\omega_t \sim \mathcal{N}(0, Q_t)$ independent of \mathcal{F}_{t-1} ,

$$\Xi_t \mid \mathcal{F}_{t-1} \sim \mathcal{N}(m_{t|t-1}, P_{t|t-1}), \quad m_{t|t-1} = m_{t-1}, \quad P_{t|t-1} = P_{t-1} + Q_t.$$

Edge update (using a_t). Conditional on Ξ_t , $a_t \sim \mathcal{N}(H_t^{(e)}\Xi_t, U_t)$. Hence $(\Xi_t, a_t) \mid \mathcal{F}_{t-1}$ is jointly Gaussian, and by the multivariate normal conditioning formula,

$$\Xi_t \mid \mathcal{F}_t^{(e)} \sim \mathcal{N}(m_t^{(e)}, P_t^{(e)}),$$

where (writing $v_t^{(e)} := a_t - H_t^{(e)}m_{t|t-1}$)

$$S_t^{(e)} := H_t^{(e)}P_{t|t-1}(H_t^{(e)})^\top + U_t, \quad K_t^{(e)} := P_{t|t-1}(H_t^{(e)})^\top(S_t^{(e)})^{-1},$$

$$m_t^{(e)} = m_{t|t-1} + K_t^{(e)}v_t^{(e)}, \quad P_t^{(e)} = P_{t|t-1} - K_t^{(e)}S_t^{(e)}(K_t^{(e)})^\top.$$

Since $U_t \succ 0$, we have $S_t^{(e)} \succ 0$ and $(S_t^{(e)})^{-1}$ exists.

Node update (using Y_t). Because H_t is $\mathcal{F}_t^{(e)}$ -measurable, the matrix $H_t^{(n)}$ is known conditional on $\mathcal{F}_t^{(e)}$. Conditional on Ξ_t and $\mathcal{F}_t^{(e)}$,

$$Y_t \sim \mathcal{N}(H_t^{(n)}\Xi_t, R_t),$$

and $(\Xi_t, Y_t) \mid \mathcal{F}_t^{(e)}$ is jointly Gaussian. Conditioning again yields

$$\Xi_t \mid \mathcal{F}_t \sim \mathcal{N}(m_t, P_t),$$

with (writing $v_t^{(n)} := Y_t - H_t^{(n)}m_t^{(e)}$)

$$\begin{aligned} S_t^{(n)} &:= H_t^{(n)}P_t^{(e)}(H_t^{(n)})^\top + R_t, & K_t^{(n)} &:= P_t^{(e)}(H_t^{(n)})^\top(S_t^{(n)})^{-1}, \\ m_t &= m_t^{(e)} + K_t^{(n)}v_t^{(n)}, & P_t &= P_t^{(e)} - K_t^{(n)}S_t^{(n)}(K_t^{(n)})^\top. \end{aligned}$$

Since $R_t \succ 0$, we have $S_t^{(n)} \succ 0$. This completes the induction and shows that Kalman filtering (with two observation updates per t) yields the exact filtering distributions.

(4) Exact smoothing (Rauch–Tung–Striebel recursion). We now derive the fixed-interval smoothing recursion for the joint state under the random-walk transition. Let $m_{t|t}, P_{t|t}$ denote the filtered moments m_t, P_t above, and let

$$m_{t+1|t} := m_{t|t}, \quad P_{t+1|t} := P_{t|t} + Q_{t+1}$$

be the one-step-ahead predictive moments under $\Xi_{t+1} = \Xi_t + \omega_{t+1}$.

Fix $t \in \{0, \dots, T-1\}$. Conditional on \mathcal{F}_t , the pair (Ξ_t, Ξ_{t+1}) is jointly Gaussian: indeed, $\Xi_t \mid \mathcal{F}_t \sim \mathcal{N}(m_{t|t}, P_{t|t})$ and $\Xi_{t+1} \mid (\Xi_t, \mathcal{F}_t) \sim \mathcal{N}(\Xi_t, Q_{t+1})$ with ω_{t+1} independent of \mathcal{F}_t . Therefore, by standard Gaussian regression,

$$\Xi_t \mid (\Xi_{t+1}, \mathcal{F}_t) \sim \mathcal{N}\left(m_{t|t} + J_t(\Xi_{t+1} - m_{t+1|t}), P_{t|t} - J_t P_{t+1|t} J_t^\top\right),$$

where the smoothing gain is

$$J_t := P_{t|t}(P_{t+1|t})^{-1}.$$

Now take conditional expectations with respect to the smoothing distribution of Ξ_{t+1} given \mathcal{F}_T . Writing $m_{t|T} := \mathbb{E}[\Xi_t \mid \mathcal{F}_T]$ and $P_{t|T} := \text{Var}(\Xi_t \mid \mathcal{F}_T)$, the tower property yields the recursion

$$m_{t|T} = m_{t|t} + J_t(m_{t+1|T} - m_{t+1|t}),$$

and a standard variance decomposition gives

$$P_{t|T} = P_{t|t} + J_t(P_{t+1|T} - P_{t+1|t})J_t^\top.$$

With terminal condition $m_{T|T} = m_{T|T}$ and $P_{T|T} = P_{T|T}$, this is exactly the Rauch–Tung–Striebel smoother for the random-walk transition.

Since $\Xi_t = (\theta_t^\top, \psi_t^\top)^\top$, the filtered and smoothed distributions obtained above are the exact joint posteriors for node states and edge states. \square

Proof of 3.6

Low-rank tensor network TVP-VAR (CP factor state). We prove (i)–(iv).

1. CP decomposition implies a rank- R slice expansion. By (26), for each r and indices (i, j, ℓ) ,

$$(b_{r,t}^{(1)} \otimes b_{r,t}^{(2)} \otimes b_{r,t}^{(3)})_{i,j,\ell} = b_{r,t}^{(1)}(i) b_{r,t}^{(2)}(j) b_{r,t}^{(3)}(\ell).$$

Hence for each fixed lag $\ell \in \{1, \dots, p\}$,

$$(B_{\ell,t})_{i,j} = (\mathcal{B}_t)_{i,j,\ell} = \sum_{r=1}^R b_{r,t}^{(1)}(i) b_{r,t}^{(2)}(j) b_{r,t}^{(3)}(\ell),$$

which is equivalently the matrix identity

$$B_{\ell,t} = \sum_{r=1}^R b_{r,t}^{(3)}(\ell) b_{r,t}^{(1)}(b_{r,t}^{(2)})^\top. \quad (49)$$

2. Dimension count (proves (i)). By (28), each component r contributes N coordinates from $b_{r,t}^{(1)}$, N coordinates from $b_{r,t}^{(2)}$, and p coordinates from $b_{r,t}^{(3)}$, for a total of $2N+p$. Therefore $\dim(\xi_t) = R(2N+p)$. For comparison, an unrestricted $\mathcal{B}_t \in \mathbb{R}^{N \times N \times p}$ has N^2p entries.

3. Observation equation and tri-linearity (first part of (ii)). Substituting (49) into (25) gives, for $t \geq p+1$,

$$\begin{aligned} Y_t &= \sum_{\ell=1}^p \left(\sum_{r=1}^R b_{r,t}^{(3)}(\ell) b_{r,t}^{(1)}(b_{r,t}^{(2)})^\top \right) Y_{t-\ell} + \varepsilon_t \\ &= \sum_{r=1}^R b_{r,t}^{(1)}(b_{r,t}^{(2)})^\top \left(\sum_{\ell=1}^p b_{r,t}^{(3)}(\ell) Y_{t-\ell} \right) + \varepsilon_t. \end{aligned} \quad (50)$$

Define the lag-weighted regressor vector

$$s_{r,t} := \sum_{\ell=1}^p b_{r,t}^{(3)}(\ell) Y_{t-\ell} \in \mathbb{R}^N. \quad (51)$$

Then (50) becomes

$$Y_t = \sum_{r=1}^R b_{r,t}^{(1)}(b_{r,t}^{(2)})^\top s_{r,t} + \varepsilon_t. \quad (52)$$

The conditional mean map is therefore

$$g_t(\xi_t; Y_{t-1}, \dots, Y_{t-p}) = \sum_{r=1}^R b_{r,t}^{(1)}(b_{r,t}^{(2)})^\top s_{r,t},$$

which equals (29). It is tri-linear (multi-affine) in the three factor blocks: $s_{r,t}$ is linear in $b_{r,t}^{(3)}$ by (51), and for fixed $s_{r,t}$ the map $(b_{r,t}^{(1)}, b_{r,t}^{(2)}) \mapsto b_{r,t}^{(1)}(b_{r,t}^{(2)})^\top s_{r,t}$ is bilinear. This proves the first part of (ii).

4. Blockwise conditional linearity (second part of (ii)). Fix t and condition on $(Y_{t-1}, \dots, Y_{t-p})$.

Linearity in $b_t^{(1)}$ given $b_{1:R,t}^{(2)}, b_{1:R,t}^{(3)}$. Condition on $\{b_{r,t}^{(2)}\}_{r=1}^R$ and $\{b_{r,t}^{(3)}\}_{r=1}^R$ and define the scalars

$$\alpha_{r,t} := (b_{r,t}^{(2)})^\top s_{r,t} = \sum_{\ell=1}^p b_{r,t}^{(3)}(\ell) (b_{r,t}^{(2)})^\top Y_{t-\ell} \in \mathbb{R}. \quad (53)$$

Then (52) becomes

$$Y_t = \sum_{r=1}^R \alpha_{r,t} b_{r,t}^{(1)} + \varepsilon_t. \quad (54)$$

Let $b_t^{(1)} := ((b_{1,t}^{(1)})^\top, \dots, (b_{R,t}^{(1)})^\top)^\top \in \mathbb{R}^{RN}$ and define

$$H_t^{(1)} := [\alpha_{1,t} I_N \ \alpha_{2,t} I_N \ \dots \ \alpha_{R,t} I_N] \in \mathbb{R}^{N \times RN}. \quad (55)$$

Then $Y_t = H_t^{(1)} b_t^{(1)} + \varepsilon_t$, which is linear–Gaussian in $b_t^{(1)}$.

Linearity in $b_t^{(2)}$ given $b_{1:R,t}^{(1)}, b_{1:R,t}^{(3)}$. Condition on $\{b_{r,t}^{(1)}\}_{r=1}^R$ and $\{b_{r,t}^{(3)}\}_{r=1}^R$, so $s_{r,t}$ in (51) is known. Using (52),

$$Y_t = \sum_{r=1}^R b_{r,t}^{(1)} s_{r,t}^\top b_{r,t}^{(2)} + \varepsilon_t = \sum_{r=1}^R (b_{r,t}^{(1)} s_{r,t}^\top) b_{r,t}^{(2)} + \varepsilon_t.$$

Let $b_t^{(2)} := ((b_{1,t}^{(2)})^\top, \dots, (b_{R,t}^{(2)})^\top)^\top \in \mathbb{R}^{RN}$ and define

$$H_t^{(2)} := [b_{1,t}^{(1)} s_{1,t}^\top \ b_{2,t}^{(1)} s_{2,t}^\top \ \dots \ b_{R,t}^{(1)} s_{R,t}^\top] \in \mathbb{R}^{N \times RN}. \quad (56)$$

Then $Y_t = H_t^{(2)} b_t^{(2)} + \varepsilon_t$, which is linear–Gaussian in $b_t^{(2)}$.

Linearity in $b_t^{(3)}$ given $b_{1:R,t}^{(1)}, b_{1:R,t}^{(2)}$. Condition on $\{b_{r,t}^{(1)}\}_{r=1}^R$ and $\{b_{r,t}^{(2)}\}_{r=1}^R$. Define, for each r ,

$$m_{r,t} := ((b_{r,t}^{(2)})^\top Y_{t-1}, (b_{r,t}^{(2)})^\top Y_{t-2}, \dots, (b_{r,t}^{(2)})^\top Y_{t-p})^\top \in \mathbb{R}^p. \quad (57)$$

Then (53) can be written $\alpha_{r,t} = (b_{r,t}^{(3)})^\top m_{r,t}$, and (54) gives

$$Y_t = \sum_{r=1}^R b_{r,t}^{(1)} m_{r,t}^\top b_{r,t}^{(3)} + \varepsilon_t = \sum_{r=1}^R (b_{r,t}^{(1)} m_{r,t}^\top) b_{r,t}^{(3)} + \varepsilon_t.$$

Let $b_t^{(3)} := ((b_{1,t}^{(3)})^\top, \dots, (b_{R,t}^{(3)})^\top)^\top \in \mathbb{R}^{Rp}$ and define

$$H_t^{(3)} := [b_{1,t}^{(1)} m_{1,t}^\top \ b_{2,t}^{(1)} m_{2,t}^\top \ \dots \ b_{R,t}^{(1)} m_{R,t}^\top] \in \mathbb{R}^{N \times Rp}. \quad (58)$$

Then $Y_t = H_t^{(3)} b_t^{(3)} + \varepsilon_t$, which is linear–Gaussian in $b_t^{(3)}$. This completes (ii).

5. Stacked random–walk evolution (proves (iii)). Stacking (27) over r and k yields

$$\xi_t = \xi_{t-1} + u_t,$$

where u_t is the stacked innovation vector. Since the innovations in (27) are Gaussian and independent over t , u_t is Gaussian with covariance matrix $Q_t := \text{Var}(u_t) \succ 0$. Thus the state evolution is linear–Gaussian, proving (iii).

6. Block–tridiagonal precision of the state path prior (proves (iv)). Let $\Xi_{0:T} := (\xi_0^\top, \dots, \xi_T^\top)^\top$. Under $\xi_0 \sim \mathcal{N}(m_0, P_0)$ and the random–walk transitions $\xi_t | \xi_{t-1} \sim \mathcal{N}(\xi_{t-1}, Q_t)$, the joint density satisfies

$$p(\Xi_{0:T}) \propto \exp \left\{ -\frac{1}{2}(\xi_0 - m_0)^\top P_0^{-1}(\xi_0 - m_0) - \frac{1}{2} \sum_{t=1}^T (\xi_t - \xi_{t-1})^\top Q_t^{-1}(\xi_t - \xi_{t-1}) \right\}.$$

For each $t \geq 1$,

$$(\xi_t - \xi_{t-1})^\top Q_t^{-1}(\xi_t - \xi_{t-1}) = \xi_t^\top Q_t^{-1} \xi_t - 2\xi_t^\top Q_t^{-1} \xi_{t-1} + \xi_{t-1}^\top Q_t^{-1} \xi_{t-1}.$$

Summing over t and collecting coefficients of the quadratic form in (ξ_0, \dots, ξ_T) yields a precision matrix $J_{0:T}$ for $\Xi_{0:T}$ with nonzero blocks only on the main diagonal and first off–diagonals:

$$J_{00} = P_0^{-1} + Q_1^{-1}, \quad J_{tt} = Q_t^{-1} + Q_{t+1}^{-1} \quad (1 \leq t \leq T-1), \quad J_{TT} = Q_T^{-1},$$

and

$$J_{t,t-1} = J_{t-1,t}^\top = -Q_t^{-1} \quad (1 \leq t \leq T),$$

with all other blocks equal to zero. Hence $J_{0:T}$ is block tridiagonal in time, proving (iv). \square

Proof of Theorem 3.7

Proof. All neighbourhoods and open sets below are understood in the *subspace topology* on Ξ .

Step 1 (The restricted prior has full support on Ξ). We show that $\Pi(U) > 0$ for every nonempty open set $U \subset \Xi$. Fix j and condition on any $\kappa^2 > 0$. The Gamma density in (33) is strictly positive on $(0, \infty)$, and for each $\xi_j^2 > 0$ the normal density of $\alpha_j | \xi_j^2$ is strictly positive on \mathbb{R} . Therefore the conditional marginal density

$$f_{\alpha_j | \kappa^2}(\alpha) = \int_0^\infty \varphi(\alpha; 0, \xi^2) g(\xi^2 | \kappa^2) d\xi^2$$

is strictly positive for all $\alpha \in \mathbb{R}$, and hence the unconditional marginal density $f_{\alpha_j}(\alpha) = \int f_{\alpha_j | \kappa^2}(\alpha) \Pi_\kappa(d\kappa^2)$ is strictly positive for all $\alpha \in \mathbb{R}$.

Let $\vartheta_0 \in (0, \bar{\vartheta}]$ and $\epsilon > 0$. Define

$$\delta(\epsilon, \vartheta_0) := \min \left\{ 1, \frac{\epsilon}{2\sqrt{\vartheta_0} + 1} \right\}.$$

If $|\alpha_j - \sqrt{\vartheta_0}| < \delta(\epsilon, \vartheta_0)$, then $|\alpha_j + \sqrt{\vartheta_0}| \leq 2\sqrt{\vartheta_0} + 1$, so

$$|\alpha_j^2 - \vartheta_0| = |\alpha_j - \sqrt{\vartheta_0}| \cdot |\alpha_j + \sqrt{\vartheta_0}| < \delta(\epsilon, \vartheta_0) (2\sqrt{\vartheta_0} + 1) \leq \epsilon.$$

Hence

$$\Pi^0(|\vartheta_j - \vartheta_0| < \epsilon) \geq \Pi^0(|\alpha_j - \sqrt{\vartheta_0}| < \delta(\epsilon, \vartheta_0)) > 0,$$

because f_{α_j} is strictly positive.

For $\vartheta_0 = 0$, $\{|\alpha_j| < \sqrt{\epsilon}\} \subset \{\alpha_j^2 < \epsilon\}$, so

$$\Pi^0(\vartheta_j < \epsilon) \geq \Pi^0(|\alpha_j| < \sqrt{\epsilon}) > 0.$$

Thus Π^0 assigns positive mass to every neighbourhood of every $\vartheta_0 \in [0, \bar{\vartheta}]$ for each coordinate j . Since Π_η assigns positive mass to every neighbourhood of η^* in \mathcal{H} , the product structure in (33) implies that Π^0 assigns positive mass to every nonempty basic open set in $[0, \bar{\vartheta}]^K \times \mathcal{H}$, hence to every nonempty open $U \subset \Xi$. Finally, because Π is the restriction/renormalisation of Π^0 to Ξ and $\Pi^0(\Xi) > 0$, we have $\Pi(U) = \Pi^0(U)/\Pi^0(\Xi) > 0$ for every nonempty open $U \subset \Xi$.

Step 2 (Posterior concentration lemma under uniform likelihood separation). We use the following standard lemma.

Lemma B.2. *Let Ξ be compact and let Π be a prior on Ξ with $\Pi(U) > 0$ for every nonempty open $U \subset \Xi$. Suppose there exists a continuous function $h : \Xi \rightarrow [0, \infty)$ with a unique zero at $\xi^* \in \Xi$ such that*

$$\sup_{\xi \in \Xi} \left| \frac{1}{T} \log \frac{p_\xi(Y_{1:T})}{p_{\xi^*}(Y_{1:T})} + h(\xi) \right| \xrightarrow[T \rightarrow \infty]{} 0 \quad \text{in } \mathbb{P}_{\xi^*}\text{-probability.}$$

Then for every open neighbourhood U of ξ^* in Ξ ,

$$\Pi(U^c \mid Y_{1:T}) \xrightarrow[T \rightarrow \infty]{} 0 \quad \text{in } \mathbb{P}_{\xi^*}\text{-probability.}$$

Proof. Fix an open neighbourhood U of ξ^* . By continuity of h , compactness of Ξ , and uniqueness of the zero at ξ^* ,

$$h_U := \inf_{\xi \in U^c} h(\xi) > 0.$$

Choose $\varepsilon > 0$ so small that $\varepsilon < h_U/4$ and such that the open set

$$V_\varepsilon := \{\xi \in \Xi : h(\xi) < \varepsilon\}$$

satisfies $V_\varepsilon \subset U$ (possible since $h(\xi^*) = 0$ and h is continuous). By the assumed uniform convergence, $\mathbb{P}_{\xi^*}(E_T) \rightarrow 1$ where

$$E_T := \left\{ \sup_{\xi \in \Xi} \left| \frac{1}{T} \log \frac{p_\xi(Y_{1:T})}{p_{\xi^*}(Y_{1:T})} + h(\xi) \right| \leq \varepsilon \right\}.$$

On E_T , for all $\xi \in U^c$,

$$\frac{1}{T} \log \frac{p_\xi(Y_{1:T})}{p_{\xi^*}(Y_{1:T})} \leq -h(\xi) + \varepsilon \leq -h_U + \varepsilon \leq -3\varepsilon,$$

and for all $\xi \in V_\varepsilon$,

$$\frac{1}{T} \log \frac{p_\xi(Y_{1:T})}{p_{\xi^*}(Y_{1:T})} \geq -h(\xi) - \varepsilon \geq -2\varepsilon.$$

Therefore, on E_T ,

$$\begin{aligned}\Pi(U^c \mid Y_{1:T}) &= \frac{\int_{U^c} \exp\left(\log \frac{p_\xi(Y_{1:T})}{p_{\xi^*}(Y_{1:T})}\right) \Pi(d\xi)}{\int_{\Xi} \exp\left(\log \frac{p_\xi(Y_{1:T})}{p_{\xi^*}(Y_{1:T})}\right) \Pi(d\xi)} \\ &\leq \frac{\int_{U^c} e^{-3\varepsilon T} \Pi(d\xi)}{\int_{V_\varepsilon} e^{-2\varepsilon T} \Pi(d\xi)} = \frac{\Pi(U^c)}{\Pi(V_\varepsilon)} e^{-\varepsilon T} \xrightarrow[T \rightarrow \infty]{} 0,\end{aligned}$$

because $\Pi(V_\varepsilon) > 0$. Since $\mathbb{P}_{\xi^*}(E_T) \rightarrow 1$, the convergence holds in \mathbb{P}_{ξ^*} -probability. \square

Step 3 (Posterior consistency for $\xi = (\vartheta, \eta)$). In Theorem 3.7 the parameter is $\xi = (\vartheta, \eta) \in \Xi$. By Step 1, the restricted prior Π assigns positive mass to every nonempty open set in Ξ . By the assumption (34) and the stated properties of h , Lemma B.2 applies. Hence for every open neighbourhood U of ξ^* in Ξ ,

$$\Pi(U^c \mid Y_{1:T}) \xrightarrow[T \rightarrow \infty]{} 0 \quad \text{in } \mathbb{P}_{\xi^*}\text{-probability.}$$

Step 4 (Coordinate-wise separation for ϑ_j). Fix j .

(i) *Constant case.* If $\vartheta_j^* = 0$, fix $\delta > 0$ and define the closed set

$$B_{j,\delta} := \{\xi = (\vartheta, \eta) \in \Xi : \vartheta_j \geq \delta\}.$$

Since $\xi^* \notin B_{j,\delta}$ and Ξ is a metric space, there exists an open neighbourhood U of ξ^* in Ξ such that $U \cap B_{j,\delta} = \emptyset$, i.e. $B_{j,\delta} \subset U^c$. Therefore,

$$\Pi(\vartheta_j \geq \delta \mid Y_{1:T}) = \Pi(B_{j,\delta} \mid Y_{1:T}) \leq \Pi(U^c \mid Y_{1:T}) \xrightarrow[T \rightarrow \infty]{} 0 \quad \text{in } \mathbb{P}_{\xi^*}\text{-probability.}$$

(ii) *Time-varying case.* If $\vartheta_j^* > 0$, fix $\delta \in (0, \vartheta_j^*)$ and define the closed set

$$C_{j,\delta} := \{\xi = (\vartheta, \eta) \in \Xi : \vartheta_j \leq \delta\}.$$

Again $\xi^* \notin C_{j,\delta}$, so there exists an open neighbourhood U of ξ^* in Ξ with $U \cap C_{j,\delta} = \emptyset$, hence $C_{j,\delta} \subset U^c$. Thus,

$$\Pi(\vartheta_j \leq \delta \mid Y_{1:T}) = \Pi(C_{j,\delta} \mid Y_{1:T}) \leq \Pi(U^c \mid Y_{1:T}) \xrightarrow[T \rightarrow \infty]{} 0 \quad \text{in } \mathbb{P}_{\xi^*}\text{-probability.}$$

If $\min_{j \in S_0} \vartheta_j^* \geq \underline{\vartheta} > 0$ and $\delta \in (0, \underline{\vartheta})$, then

$$C_\delta := \bigcup_{j \in S_0} \{\xi \in \Xi : \vartheta_j \leq \delta\}$$

is closed (finite union) and does not contain ξ^* . The same argument yields $\Pi(C_\delta \mid Y_{1:T}) \rightarrow 0$, and therefore

$$\sup_{j \in S_0} \Pi(\vartheta_j \leq \delta \mid Y_{1:T}) \leq \Pi(C_\delta \mid Y_{1:T}) \xrightarrow[T \rightarrow \infty]{} 0.$$

This establishes the stated uniformity and completes the proof. \square

Proof of Theorem 3.8

Proof of Theorem 3.8. Fix a component j .

Step 0 (threshold below jump size). Since $d_{j,T} \rightarrow 0$ and $\kappa_j > 0$, there exists $T_0 < \infty$ such that for all $T \geq T_0$,

$$d_{j,T} < \kappa_j/2. \quad (59)$$

Step 1 (define increments and a high-probability event). For $t \geq 2$ define the one-step increments

$$\Delta\hat{\theta}_{j,t-1} := \hat{\theta}_{j,t-1} - \hat{\theta}_{j,t-2}, \quad \Delta\theta_{j,t-1}^* := \theta_{j,t-1}^* - \theta_{j,t-2}^*.$$

Define the event

$$E_T := \left\{ \max_{2 \leq t \leq T} |\Delta\hat{\theta}_{j,t-1} - \Delta\theta_{j,t-1}^*| \leq \frac{d_{j,T}}{2} \right\}.$$

Step 2 ($\mathbb{P}(E_T) \rightarrow 1$). Let $\varepsilon > 0$ be arbitrary. By (35), there exist $M < \infty$ and $T_1 < \infty$ such that for all $T \geq T_1$,

$$\mathbb{P}\left(\max_{2 \leq t \leq T} |\Delta\hat{\theta}_{j,t-1} - \Delta\theta_{j,t-1}^*| > M\sqrt{\frac{\log T}{T}}\right) < \varepsilon.$$

Since $\sqrt{T/\log T} d_{j,T} \rightarrow \infty$, there exists $T_2 < \infty$ such that for all $T \geq T_2$,

$$M\sqrt{\frac{\log T}{T}} \leq \frac{d_{j,T}}{2}.$$

Hence for all $T \geq \max\{T_1, T_2\}$,

$$\left\{ \max_{2 \leq t \leq T} |\Delta\hat{\theta}_{j,t-1} - \Delta\theta_{j,t-1}^*| > \frac{d_{j,T}}{2} \right\} \subseteq \left\{ \max_{2 \leq t \leq T} |\Delta\hat{\theta}_{j,t-1} - \Delta\theta_{j,t-1}^*| > M\sqrt{\frac{\log T}{T}} \right\}.$$

Therefore $\mathbb{P}(E_T) \geq 1 - \varepsilon$ for all sufficiently large T . Since ε was arbitrary, $\mathbb{P}(E_T) \rightarrow 1$.

Step 3 (on E_T , the plug-in indicator matches the true jump indicator). Fix $T \geq T_0$ and any $t \in \{2, \dots, T\}$. On E_T we consider two cases.

Case 1: no jump. If $t-1 \notin \mathcal{J}_{j,T}^*$, then $\theta_{j,t-1}^* = \theta_{j,t-2}^*$ and hence $\Delta\theta_{j,t-1}^* = 0$. Therefore, on E_T ,

$$|\Delta\hat{\theta}_{j,t-1}| = |\Delta\hat{\theta}_{j,t-1} - \Delta\theta_{j,t-1}^*| \leq \frac{d_{j,T}}{2} < d_{j,T},$$

so $\hat{s}_{j,t} = 0$.

Case 2: a jump. If $t-1 \in \mathcal{J}_{j,T}^*$, then $|\Delta\theta_{j,t-1}^*| \geq \kappa_j$. By the reverse triangle inequality and the definition of E_T ,

$$|\Delta\hat{\theta}_{j,t-1}| \geq |\Delta\theta_{j,t-1}^*| - |\Delta\hat{\theta}_{j,t-1} - \Delta\theta_{j,t-1}^*| \geq \kappa_j - \frac{d_{j,T}}{2}.$$

Using (59), for $T \geq T_0$ we have $d_{j,T}/2 < \kappa_j/4$, hence

$$\kappa_j - \frac{d_{j,T}}{2} > \kappa_j - \frac{\kappa_j}{4} = \frac{3}{4}\kappa_j > d_{j,T},$$

so $\hat{s}_{j,t} = 1$.

Thus, on E_T , for every $t = 2, \dots, T$,

$$\hat{s}_{j,t} = I(t-1 \in \mathcal{J}_{j,T}^*) = I(\theta_{j,t-1}^* \neq \theta_{j,t-2}^*).$$

Step 4 (conclusion (i)). On E_T ,

$$\sum_{t=2}^T \hat{s}_{j,t} = \sum_{t=2}^T I(t-1 \in \mathcal{J}_{j,T}^*) = |\mathcal{J}_{j,T}^* \cap \{1, \dots, T-1\}| \leq J_{j,T}^* \leq J^*.$$

Since $\mathbb{P}(E_T) \rightarrow 1$, the indicator identity and the above bound hold with probability tending to one.

Step 5 (conclusion (ii)). By definition $F_{j,T} \geq 0$, and on E_T we have $\hat{s}_{j,t} = 0$ whenever $\theta_{j,t-1}^* = \theta_{j,t-2}^*$, hence $F_{j,T} = 0$ on E_T . Therefore,

$$0 \leq \frac{F_{j,T}}{T} \leq I(E_T^c).$$

Because $\mathbb{P}(E_T^c) \rightarrow 0$, it follows that $F_{j,T}/T \rightarrow 0$ in probability (and in fact $F_{j,T} = 0$ with probability tending to one).

This proves (i) and (ii) for the fixed component j . Since j was arbitrary, the result holds componentwise. \square

Proof of 3.9

Proof. Write $\mathcal{X}_T := \sigma(A_{1:T}, Y_{1:T-1}) = \mathcal{F}_{T-1}$. Throughout the proof we work conditionally on \mathcal{X}_T , so that the regression design is nonrandom, and then conclude by integrating over \mathcal{X}_T and using $P^*(\mathcal{E}_T) \rightarrow 1$.

1. Stacked regression in the increment parameter b . From (37) we have $\theta_t = \theta_0 + \sum_{r=1}^t u_r$. Hence,

$$m_t(\theta_t) = X_t \theta_t = X_t \theta_0 + \sum_{r=1}^t X_t u_r.$$

Define the stacked observation vector and noise

$$Y := (Y_1^\top, \dots, Y_T^\top)^\top \in \mathbb{R}^n, \quad \varepsilon := (\varepsilon_1^\top, \dots, \varepsilon_T^\top)^\top \in \mathbb{R}^n,$$

where $\varepsilon_t := Y_t - X_t \theta_t$. By assumption, $\varepsilon_t \mid \mathcal{X}_T$ are independent and $\varepsilon_t \mid \mathcal{X}_T \sim N_N(0, R_t)$.

Let $\mathbb{X} \in \mathbb{R}^{n \times p_T}$ be the (deterministic given \mathcal{X}_T) block lower-triangular matrix implementing the above mapping $b \mapsto (X_t \theta_t)_{t \leq T}$: its t -th block row equals

$$[X_t \ X_t \ \cdots \ X_t \ 0 \ \cdots \ 0],$$

with X_t repeated in the columns corresponding to $(\theta_0, u_1, \dots, u_t)$ and zeros thereafter. Then the model can be written as

$$Y = \mathbb{X}b + \varepsilon, \quad \varepsilon \mid \mathcal{X}_T \sim N_n(0, \mathbb{R}), \quad \mathbb{R} := \text{blockdiag}(R_1, \dots, R_T). \quad (60)$$

2. Whitening and the contraction metric. By (A1), \mathbb{R} is invertible and $\underline{r}I_n \preceq \mathbb{R} \preceq \bar{r}I_n$. Define the whitened quantities

$$\tilde{Y} := \mathbb{R}^{-1/2}Y, \quad \tilde{\mathbb{X}} := \mathbb{R}^{-1/2}\mathbb{X}, \quad Z := \mathbb{R}^{-1/2}\varepsilon.$$

Then (60) becomes, conditionally on \mathcal{X}_T ,

$$\tilde{Y} = \tilde{\mathbb{X}}b + Z, \quad Z \mid \mathcal{X}_T \sim N_n(0, I_n). \quad (61)$$

For $b, b' \in \mathbb{R}^{p_T}$ define the prediction (semi)metric

$$d(b, b') := \frac{1}{\sqrt{n}} \|\tilde{\mathbb{X}}(b - b')\|_2.$$

In the Gaussian experiment (61), the Kullback–Leibler divergence between P_{b^*} and P_b satisfies

$$\text{KL}(b^*, b) = \frac{1}{2} \|\tilde{\mathbb{X}}(b - b^*)\|_2^2 = \frac{n}{2} d(b, b^*)^2, \quad \text{Var}_{b^*} \left(\log \frac{dP_{b^*}}{dP_b} \right) = n d(b, b^*)^2. \quad (62)$$

Finally, note the identity (by construction of \mathbb{X})

$$\frac{1}{n} \|\mathbb{X}(b - b^*)\|_2^2 = \frac{1}{T} \sum_{t=1}^T \frac{1}{N} \|X_t(\theta_t - \theta_t^*)\|_2^2. \quad (63)$$

Since $\underline{r}I_n \preceq \mathbb{R} \preceq \bar{r}I_n$,

$$\frac{1}{\bar{r}} \frac{1}{n} \|\mathbb{X}(b - b^*)\|_2^2 \leq d(b, b^*)^2 \leq \frac{1}{\underline{r}} \frac{1}{n} \|\mathbb{X}(b - b^*)\|_2^2. \quad (64)$$

Therefore it suffices to prove contraction in $d(\cdot, \cdot)$.

3. Tests with exponentially small errors. Fix $\epsilon > 0$. For any fixed b , the Neyman–Pearson test between $N(\tilde{\mathbb{X}}b^*, I_n)$ and $N(\tilde{\mathbb{X}}b, I_n)$ satisfies (conditionally on \mathcal{X}_T)

$$P_{b^*}(\phi_b) \vee P_b(1 - \phi_b) \leq \exp \left(-\frac{1}{8} \|\tilde{\mathbb{X}}(b - b^*)\|_2^2 \right) = \exp \left(-\frac{n}{8} d(b, b^*)^2 \right). \quad (65)$$

Let \mathcal{B} be a sieve (defined in Step 4 below) and consider the alternative set

$$\mathcal{A}_\epsilon := \{b \in \mathcal{B} : d(b, b^*) > \epsilon\}.$$

Let $\{b^{(1)}, \dots, b^{(J)}\}$ be an $\epsilon/2$ -net of \mathcal{A}_ϵ in the metric d . Define $\phi := \max_{1 \leq j \leq J} \phi_{b^{(j)}}$. By a union bound and (65),

$$P_{b^*}(\phi) \leq \sum_{j=1}^J P_{b^*}(\phi_{b^{(j)}}) \leq J \exp \left(-\frac{n}{32} \epsilon^2 \right), \quad (66)$$

$$\sup_{b \in \mathcal{A}_\epsilon} P_b(1 - \phi) \leq \exp \left(-\frac{n}{32} \epsilon^2 \right), \quad (67)$$

where the second bound follows since for every $b \in \mathcal{A}_\epsilon$ there exists $b^{(j)}$ with $d(b, b^{(j)}) \leq \epsilon/2$, hence $d(b^{(j)}, b^*) \geq \epsilon/2$ by the triangle inequality.

Thus the tests are exponentially powerful provided $\log J \lesssim n\epsilon^2$, which we verify next.

4. Sieve and entropy. Let $L > 1$ be fixed (large enough; chosen at the end) and define

$$\mathcal{B} := \left\{ b \in \mathbb{R}^{p_T} : \|b\|_0 \leq Ls, \|b\|_\infty \leq M_n \right\}, \quad M_n := \frac{(aL + 10)}{c_2} s \log(p_T n). \quad (68)$$

(Here c_2 is from the slab tail bound in (40).)

On the event \mathcal{E}_T in (A2) we bound the Lipschitz constant of d with respect to $\|\cdot\|_2$. Write $\mathbb{X} = \mathbb{D}\mathbb{S}$, where $\mathbb{D} = \text{blockdiag}(X_1, \dots, X_T)$ and \mathbb{S} is the block ‘‘cumulative sum’’ operator $(v_0, \dots, v_T) \mapsto (\sum_{r=0}^1 v_r, \dots, \sum_{r=0}^T v_r)$. A direct Cauchy–Schwarz bound gives $\|\mathbb{S}\|_{op} \leq T + 1$. Therefore, on \mathcal{E}_T ,

$$\|\tilde{\mathbb{X}}\|_{op} \leq \|\text{blockdiag}(R_1^{-1/2}X_1, \dots, R_T^{-1/2}X_T)\|_{op} \|\mathbb{S}\|_{op} \leq (T+1) \max_t \|R_t^{-1/2}X_t\|_{op} \leq (T+1)\sqrt{C_X N}.$$

Hence, on \mathcal{E}_T ,

$$d(b, b') \leq \frac{\|\tilde{\mathbb{X}}\|_{op}}{\sqrt{n}} \|b - b'\|_2 \leq \Lambda_T \|b - b'\|_2, \quad \Lambda_T := \sqrt{C_X} \frac{T+1}{\sqrt{T}} \leq 2\sqrt{C_X} \sqrt{T}. \quad (69)$$

Let $\eta := \epsilon/(2\Lambda_T)$. Then any η –net in $\|\cdot\|_2$ is an $\epsilon/2$ –net in d . A standard sparse covering-number bound yields, for a universal constant $C > 0$,

$$\log N(\eta, \mathcal{B}, \|\cdot\|_2) \leq Ls \log\left(\frac{C p_T M_n}{\eta}\right).$$

Using $\eta = \epsilon/(2\Lambda_T)$, we obtain on \mathcal{E}_T ,

$$\log N(\epsilon/2, \mathcal{B}, d) \leq Ls \log\left(\frac{C' p_T M_n \Lambda_T}{\epsilon}\right) \lesssim s \log(p_T n), \quad (70)$$

because M_n is polynomial in $p_T n$, Λ_T is polynomial in T and hence polynomial in $p_T n$, and ϵ^2 will be chosen of order $s \log(p_T n)/n$. Thus $\log J \lesssim n\epsilon^2$ as required for (66)–(67).

5. Prior mass in a KL neighbourhood. Let $\epsilon_{N,T}^2 := s \log(p_T n)/n$ and set $\epsilon := \epsilon_{N,T}$. By (62), the KL ball $\{\text{KL}(b^*, b) \leq n\epsilon^2\}$ contains $\{d(b, b^*) \leq \sqrt{2}\epsilon\}$.

Let $S^* := \{j : b_j^* \neq 0\}$ with $|S^*| = s^* \leq s$. On \mathcal{E}_T , by (69), the Euclidean ball $\{\|b - b^*\|_2 \leq \epsilon/\Lambda_T\}$ is contained in $\{d(b, b^*) \leq \epsilon\}$. Therefore

$$\Pi(d(b, b^*) \leq \epsilon) \geq \Pi(\xi = S^*) \cdot \Pi(\|b_{S^*} - b_{S^*}^*\|_2 \leq \epsilon/\Lambda_T \mid \xi = S^*).$$

For the model prior (39), using $\binom{p_T}{s^*} \leq (ep_T/s^*)^{s^*}$, we have for some constant $c_0 > 0$,

$$\Pi(\xi = S^*) = \pi(K = s^*) \cdot \binom{p_T}{s^*}^{-1} \geq c_0 (p_T n)^{-as^*} (ep_T/s^*)^{-s^*} \geq \exp\{-C_0 s \log(p_T n)\}$$

for a constant $C_0 > 0$ (using $s^* \leq s$ and $s \log(p_T n) = o(n)$). Next, conditional on $\xi = S^*$, the coordinates are i.i.d. with density g . Since $\|b^*\|_\infty \leq B$ and g is bounded below on $[-B-1, B+1]$, for $r := \epsilon/(\Lambda_T \sqrt{s^*})$ and n large enough (so $r \leq 1$),

$$\Pi\left(\|b_{S^*} - b_{S^*}^*\|_2 \leq \epsilon/\Lambda_T \mid \xi = S^*\right) \geq \prod_{j \in S^*} \Pi(|b_j - b_j^*| \leq r) \geq (2c_g r)^{s^*} \geq \exp\{-C_1 s \log(p_T n)\}$$

for some constant $C_1 > 0$, since $\epsilon^2 = s \log(p_T n)/n$ and Λ_T is polynomial in $p_T n$. Combining the last two displays yields

$$\Pi(d(b, b^*) \leq \epsilon) \geq \exp\{-C n\epsilon^2\} \quad \text{for some constant } C > 0. \quad (71)$$

By (62), this also lower bounds the prior mass of a KL neighbourhood of radius $n\epsilon^2$.

6. Prior mass outside the sieve. Recall the sieve \mathcal{B} in (68). First, by the size prior (39),

$$\Pi(\|b\|_0 > Ls) = \Pi(K > Ls) \leq \sum_{k > Ls} c(p_T n)^{-ak} \leq c'(p_T n)^{-aLs} \leq \exp\{-(aL/2)s \log(p_T n)\}$$

for n large enough. Second, conditional on $K \leq Ls$, by the slab tail bound in (40) and the choice of M_n ,

$$\Pi(\|b\|_\infty > M_n, K \leq Ls) \leq \mathbb{E}[K \Pi_g(|X| > M_n); K \leq Ls] \leq Ls \cdot c_1 e^{-c_2 M_n} \leq \exp\{-5s \log(p_T n)\}.$$

Hence, for L large enough,

$$\Pi(\mathcal{B}^c) \leq \exp\{-(C+4)n\epsilon^2\} \quad (72)$$

for the same constant C as in (71).

7. Apply a general posterior contraction theorem (conditionally on \mathcal{X}_T). Fix $\epsilon = \epsilon_{N,T}$. On \mathcal{E}_T , we have: (i) tests with errors (66)–(67) and with $\log J \lesssim n\epsilon^2$ by (70); (ii) KL neighbourhood prior mass (71); and (iii) sieve complement bound (72). Therefore, by a standard posterior contraction theorem for i.i.d. observations (e.g. Ghosal–Ghosh–van der Vaart, 2000, applied to the Gaussian regression (61)), there exists $M > 0$ such that, on \mathcal{E}_T ,

$$\Pi(d(b, b^*)^2 > M\epsilon_{N,T}^2 \mid \tilde{Y}, \mathcal{X}_T) \rightarrow 0 \quad \text{in } P^*(\cdot \mid \mathcal{X}_T)\text{-probability.}$$

Since $P^*(\mathcal{E}_T) \rightarrow 1$, this implies the same convergence in P^* -probability.

8. Translate to the loss in (41). By (64) and (63),

$$d(b, b^*)^2 \geq \frac{1}{\bar{r}} \cdot \frac{1}{T} \sum_{t=1}^T \frac{1}{N} \|X_t(\theta_t - \theta_t^*)\|_2^2,$$

so contraction in $d(\cdot, \cdot)$ implies contraction of the average prediction loss. This proves (41). Finally, $\epsilon_{N,T} \rightarrow 0$ follows from (A5). \square

Proof of 3.10

Network stability and local stationarity. Throughout, $\|\cdot\|$ denotes the Euclidean norm on \mathbb{R}^N and $\|\cdot\|_{op}$ the induced (operator) norm on $\mathbb{R}^{N \times N}$. For a random vector $X \in \mathbb{R}^N$ we write $\|X\|_{L^2} := (\mathbb{E}\|X\|^2)^{1/2}$.

Part (i). Exponential stability of the conditional mean. Fix a deterministic path $(\theta_t, W_t, Z_t)_{t \geq 1}$ such that

$$(S1) \quad \sup_{t \geq 1} \|B_t\|_{op} \leq \delta < 1, \quad (S2) \quad \sup_{t \geq 1} \|c_t\| \leq C_c < \infty,$$

where

$$Y_t = B_t Y_{t-1} + c_t + \varepsilon_t, \quad B_t := \beta_{1,t} W_t + \beta_{2,t} I_N, \quad c_t := \beta_{0,t} \mathbf{1}_N + Z_t \gamma_t.$$

Let

$$m_t := \mathbb{E}(Y_t \mid Y_0, \theta_{1:t}, W_{1:t}, Z_{1:t}).$$

Assume the innovation is mean-zero conditional on the past (e.g. $\mathbb{E}(\varepsilon_t | \mathcal{F}_{t-1}) = 0$) and that under a deterministic path the regressors (B_t, c_t) are measurable with respect to the conditioning σ -field. Taking conditional expectations yields the deterministic affine recursion

$$m_t = B_t m_{t-1} + c_t, \quad t \geq 1, \quad m_0 = Y_0. \quad (73)$$

For integers $1 \leq s \leq t$, define

$$\Phi_{t:s} := B_t B_{t-1} \cdots B_s, \quad \Phi_{t:t+1} := I_N.$$

Iterating (73) gives

$$m_t = \Phi_{t:1} Y_0 + \sum_{s=1}^t \Phi_{t:s+1} c_s. \quad (74)$$

By submultiplicativity and (S1),

$$\|\Phi_{t:s}\|_{op} \leq \prod_{r=s}^t \|B_r\|_{op} \leq \delta^{t-s+1}, \quad 1 \leq s \leq t.$$

Taking norms in (74) and using (S2) gives

$$\|m_t\| \leq \|\Phi_{t:1}\|_{op} \|Y_0\| + \sum_{s=1}^t \|\Phi_{t:s+1}\|_{op} \|c_s\| \leq \delta^t \|Y_0\| + C_c \sum_{s=1}^t \delta^{t-s}.$$

Since $\sum_{s=1}^t \delta^{t-s} = \sum_{j=0}^{t-1} \delta^j \leq (1-\delta)^{-1}$, we obtain

$$\|m_t\| \leq \frac{C_c}{1-\delta} + \delta^t \|Y_0\|, \quad t \geq 1,$$

which proves (i) with $C = C_c/(1-\delta)$ and $\kappa = \delta$.

Part (ii). Network local stationarity. Work with the triangular array $\{Y_{t,T}\}_{t=0}^T$ satisfying

$$Y_{t,T} = B(t/T) Y_{t-1,T} + c(t/T) + R(t/T)^{1/2} \nu_t, \quad t = 1, \dots, T, \quad (75)$$

where $\{\nu_t\}_{t \in \mathbb{Z}}$ is i.i.d. with $\mathbb{E} \nu_t = 0$ and $\mathbb{E} \|\nu_t\|^2 < \infty$. Assume that $\beta_j(\cdot)$, $\gamma(\cdot)$, $W(\cdot)$, $Z(\cdot)$, and $R(\cdot)^{1/2}$ are Lipschitz on $[0, 1]$, and that

$$\sup_{u \in [0,1]} \|B(u)\|_{op} \leq \delta < 1, \quad \text{where } B(u) := \beta_1(u)W(u) + \beta_2(u)I_N, \quad (76)$$

and $c(u) := \beta_0(u)\mathbf{1}_N + Z(u)\gamma(u)$. Fix $\tau \in (0, 1)$ and write $B_\tau := B(\tau)$, $c_\tau := c(\tau)$, $R_\tau := R(\tau)$.

Step 1: existence of the stationary frozen process. Define $\{Y_t^{(\tau)}\}_{t \in \mathbb{Z}}$ by the moving-average expansion

$$Y_t^{(\tau)} := \sum_{k=0}^{\infty} B_\tau^k (c_\tau + R_\tau^{1/2} \nu_{t-k}), \quad t \in \mathbb{Z}. \quad (77)$$

Let $X_{t,k} := B_\tau^k (c_\tau + R_\tau^{1/2} \nu_{t-k})$. Then

$$\|X_{t,k}\|_{L^2} \leq \|B_\tau^k\|_{op} \|c_\tau + R_\tau^{1/2} \nu_0\|_{L^2} \leq \delta^k M_\tau, \quad M_\tau := \|c_\tau + R_\tau^{1/2} \nu_0\|_{L^2} < \infty,$$

so by Minkowski,

$$\left\| \sum_{k=m}^n X_{t,k} \right\|_{L^2} \leq \sum_{k=m}^n \|X_{t,k}\|_{L^2} \leq M_\tau \sum_{k=m}^n \delta^k \xrightarrow[m,n \rightarrow \infty]{} 0.$$

Hence (77) converges in L^2 . The process is strictly stationary because it is a measurable shift-invariant function of the i.i.d. sequence $\{\nu_t\}$, and it satisfies the recursion

$$Y_t^{(\tau)} = B_\tau Y_{t-1}^{(\tau)} + c_\tau + R_\tau^{1/2} \nu_t.$$

Uniqueness of the strictly stationary L^2 solution follows from the contraction $\|B_\tau\|_{op} \leq \delta < 1$.

Step 2: a uniform bound on $\|Y_t^{(\tau)}\|_{L^2}$. From (77) and Minkowski,

$$\sup_{t \in \mathbb{Z}} \|Y_t^{(\tau)}\|_{L^2} \leq \sum_{k=0}^{\infty} \|B_\tau^k (c_\tau + R_\tau^{1/2} \nu_0)\|_{L^2} \leq \frac{\|c_\tau\| + \|R_\tau^{1/2} \nu_0\|_{L^2}}{1 - \delta} < \infty. \quad (78)$$

Step 3: difference recursion under a coupling. Couple $\{Y_{t,T}\}$ and $\{Y_t^{(\tau)}\}$ using the same $\{\nu_t\}_{t \in \mathbb{Z}}$ and define $D_{t,T} := Y_{t,T} - Y_t^{(\tau)}$. Subtracting the frozen recursion from (75) gives

$$D_{t,T} = B(t/T) D_{t-1,T} + r_{t,T}, \quad t \geq 1, \quad (79)$$

where

$$r_{t,T} := (B(t/T) - B_\tau) Y_{t-1}^{(\tau)} + (c(t/T) - c_\tau) + (R(t/T)^{1/2} - R_\tau^{1/2}) \nu_t.$$

Step 4: geometric propagation of errors. For $1 \leq s \leq t$ define $\Phi_{t:s}^{(T)} := B(t/T) B((t-1)/T) \cdots B(s/T)$ and $\Phi_{t:t+1}^{(T)} := I_N$. Iterating (79) gives

$$D_{t,T} = \Phi_{t:1}^{(T)} D_{0,T} + \sum_{s=1}^t \Phi_{t:s+1}^{(T)} r_{s,T}.$$

By (76) and submultiplicativity,

$$\|\Phi_{t:s}^{(T)}\|_{op} \leq \prod_{j=s}^t \|B(j/T)\|_{op} \leq \delta^{t-s+1}.$$

Hence, by Minkowski,

$$\|D_{t,T}\|_{L^2} \leq \delta^t \|D_{0,T}\|_{L^2} + \sum_{s=1}^t \delta^{t-s} \|r_{s,T}\|_{L^2}. \quad (80)$$

Step 5: Lipschitz control of $\|r_{s,T}\|_{L^2}$. Since $B(\cdot)$, $c(\cdot)$ and $R(\cdot)^{1/2}$ are Lipschitz on $[0, 1]$, there exists $L < \infty$ such that for all $u \in [0, 1]$,

$$\|B(u) - B_\tau\|_{op} \leq L|u - \tau|, \quad \|c(u) - c_\tau\| \leq L|u - \tau|, \quad \|R(u)^{1/2} - R_\tau^{1/2}\|_{op} \leq L|u - \tau|.$$

Using (78) and $\|\nu_s\|_{L^2} < \infty$, we obtain for all $s \geq 1$,

$$\|r_{s,T}\|_{L^2} \leq \|B(s/T) - B_\tau\|_{op} \|Y_{s-1}^{(\tau)}\|_{L^2} + \|c(s/T) - c_\tau\| + \|R(s/T)^{1/2} - R_\tau^{1/2}\|_{op} \|\nu_s\|_{L^2} \leq C |s/T - \tau|,$$

for some constant $C < \infty$ (depending on τ but not on s, t, T).

Step 6: conclude $\|D_{t,T}\|_{L^2} \rightarrow 0$ for $t/T \rightarrow \tau$. Let $t = t_T$ be any integer sequence with $t_T/T \rightarrow \tau$ and assume $\sup_T \|D_{0,T}\|_{L^2} < \infty$. Using Step 5 in (80),

$$\|D_{t_T,T}\|_{L^2} \leq \delta^{t_T} \|D_{0,T}\|_{L^2} + C \sum_{s=1}^{t_T} \delta^{t_T-s} |s/T - \tau|.$$

The first term vanishes since $\delta^{t_T} \rightarrow 0$ as $t_T \rightarrow \infty$. For the second term, set $k = t_T - s$:

$$\sum_{s=1}^{t_T} \delta^{t_T-s} |s/T - \tau| = \sum_{k=0}^{t_T-1} \delta^k \left| \frac{t_T-k}{T} - \tau \right| \leq \sum_{k=0}^{t_T-1} \delta^k \left(\left| \frac{t_T}{T} - \tau \right| + \frac{k}{T} \right).$$

Since $\sum_{k \geq 0} \delta^k = (1-\delta)^{-1}$ and $\sum_{k \geq 0} k\delta^k = \delta(1-\delta)^{-2}$,

$$\sum_{s=1}^{t_T} \delta^{t_T-s} |s/T - \tau| \leq \frac{1}{1-\delta} \left| \frac{t_T}{T} - \tau \right| + \frac{\delta}{(1-\delta)^2} \cdot \frac{1}{T} \xrightarrow{T \rightarrow \infty} 0.$$

Therefore $\|D_{t_T,T}\|_{L^2} \rightarrow 0$. The same argument applies to $t_T + h$ for any fixed integer h (and all large T such that $t_T + h \in \{0, \dots, T\}$), yielding

$$\|Y_{t_T+h,T} - Y_{t_T+h,T}^{(\tau)}\|_{L^2} = \|D_{t_T+h,T}\|_{L^2} \rightarrow 0,$$

which proves the claimed local stationarity. \square

Proof of 3.11

Proof of Theorem 3.11. Fix $t \geq 1$. By construction of \mathcal{F}_{t-1} , the quantities $\mathbf{1}_N$, Y_{t-1} , Z_t , W_t and \widetilde{W}_t are \mathcal{F}_{t-1} -measurable, and $\mathbb{E}[\varepsilon_t | \mathcal{F}_{t-1}] = 0$. Taking conditional expectations in (42) yields

$$\widehat{Y}_{t|t-1} = \mathbb{E}[\beta_{0,t} | \mathcal{F}_{t-1}] \mathbf{1}_N + \mathbb{E}[\beta_{1,t} | \mathcal{F}_{t-1}] W_t Y_{t-1} + \mathbb{E}[\beta_{2,t} | \mathcal{F}_{t-1}] Y_{t-1} + Z_t \mathbb{E}[\gamma_t | \mathcal{F}_{t-1}],$$

where we used linearity of conditional expectation and the fact that \mathcal{F}_{t-1} -measurable regressors can be pulled out of the conditional expectation.

By definition of $\widetilde{Y}_{t|t-1}$,

$$\widetilde{Y}_{t|t-1} = \mathbb{E}[\beta_{0,t} | \mathcal{F}_{t-1}] \mathbf{1}_N + \mathbb{E}[\beta_{1,t} | \mathcal{F}_{t-1}] \widetilde{W}_t Y_{t-1} + \mathbb{E}[\beta_{2,t} | \mathcal{F}_{t-1}] Y_{t-1} + Z_t \mathbb{E}[\gamma_t | \mathcal{F}_{t-1}].$$

Subtracting the two displays gives the identity

$$\widehat{Y}_{t|t-1} - \widetilde{Y}_{t|t-1} = \mathbb{E}[\beta_{1,t} | \mathcal{F}_{t-1}] (W_t - \widetilde{W}_t) Y_{t-1}.$$

Hence, by submultiplicativity of the operator norm,

$$\|\widehat{Y}_{t|t-1} - \widetilde{Y}_{t|t-1}\| \leq |\mathbb{E}[\beta_{1,t} | \mathcal{F}_{t-1}]| \|W_t - \widetilde{W}_t\|_{\text{op}} \|Y_{t-1}\|.$$

Squaring,

$$\|\widehat{Y}_{t|t-1} - \widetilde{Y}_{t|t-1}\|^2 \leq |\mathbb{E}[\beta_{1,t} | \mathcal{F}_{t-1}]|^2 \|W_t - \widetilde{W}_t\|_{\text{op}}^2 \|Y_{t-1}\|^2.$$

By conditional Cauchy–Schwarz,

$$\left| \mathbb{E}[\beta_{1,t} \mid \mathcal{F}_{t-1}] \right|^2 \leq \mathbb{E}[\beta_{1,t}^2 \mid \mathcal{F}_{t-1}] \leq B_1^2 \quad \text{a.s.},$$

and by (43) we also have $\|W_t - \widetilde{W}_t\|_{\text{op}} \leq \Delta_W$ almost surely. Therefore,

$$\|\widehat{Y}_{t|t-1} - \widetilde{Y}_{t|t-1}\|^2 \leq B_1^2 \Delta_W^2 \|Y_{t-1}\|^2 \quad \text{a.s.}$$

Taking expectations gives

$$\|\widehat{Y}_{t|t-1} - \widetilde{Y}_{t|t-1}\|_{\mathbb{L}^2}^2 = \mathbb{E}\|\widehat{Y}_{t|t-1} - \widetilde{Y}_{t|t-1}\|^2 \leq B_1^2 \Delta_W^2 \mathbb{E}\|Y_{t-1}\|^2 = B_1^2 \Delta_W^2 \|Y_{t-1}\|_{\mathbb{L}^2}^2.$$

Taking $\sup_{1 \leq t \leq T}$ yields

$$\sup_{1 \leq t \leq T} \|\widehat{Y}_{t|t-1} - \widetilde{Y}_{t|t-1}\|_{\mathbb{L}^2}^2 \leq B_1^2 \Delta_W^2 \max_{0 \leq s \leq T-1} \|Y_s\|_{\mathbb{L}^2}^2.$$

If additionally $\sup_{s \geq 0} \|Y_s\|_{\mathbb{L}^2}^2 \leq C_Y$, the displayed bound reduces to $B_1^2 C_Y \Delta_W^2$, completing the proof. \square